Natural Resources Canada | Ressources naturelles Canada

GEOLOGICAL SURVEY OF CANADA
OPEN FILE 7871

Geology, mineralogy, and geochemistry of the Cu-PGE (DJ/DB) zone of the Turnagain Alaskan-type intrusion, north-central British Columbia: Supporting databases for the convergent-margin Ni-Cu-PGE study

S. Jackson-Brown, J.S. Scoates, G.T. Nixon, and D.E. Ames

2015

Canada

GEOLOGICAL SURVEY OF CANADA
OPEN FILE 7871

Geology, mineralogy, and geochemistry of the Cu-PGE (DJ/DB) zone of the Turnagain Alaskan-type intrusion, north-central British Columbia: Supporting databases for the convergent-margin Ni-Cu-PGE study

S. Jackson-Brown[1], J.S. Scoates[1], G.T. Nixon[2], and D.E. Ames[3]

[1]Department of Earth, Ocean, and Atmospheric Sciences, University of British Columbia, Vancouver, British Columbia
[2]British Columbia Geological Survey, Victoria, British Columbia
[3]Geological Survey of Canada, Ottawa, Ontario

2015

doi:10.4095/297472

This publication is available for free download through GEOSCAN (http://geoscan.nrcan.gc.ca/)

Recommended citation

Jackson-Brown, S., Scoates, J.S., Nixon, G.T., and Ames, D.E., 2015. Geology, mineralogy, and geochemistry of the Cu-PGE (DJ/DB) zone of the Turnagain Alaskan-type intrusion, north-central British Columbia: Supporting databases for the convergent-margin Ni-Cu-PGE study; Geological Survey of Canada, Open File 7871, 1 zip file. doi:10.4095/297472

Publications in this series have not been edited; they are released as submitted by the author.

Contribution to the Geological Survey of Canada's Targeted Geoscience Initiative 4 (TGI-4) Program (2010-2015)

TABLE OF CONTENTS

Figures

Tables

Geology, mineralogy, and geochemistry of the Cu-PGE (DJ/DB) zone of the Turnagain Alaskan-type intrusion, north-central British Columbia: Supporting databases for the convergent-margin Ni-Cu-PGE study

S. Jackson-Brown[1], J.S. Scoates[1], G.T. Nixon[2], and D.E. Ames[3]

[1]Department of Earth, Ocean and Atmospheric Sciences, 2020 - 2207 Main Mall, University of British Columbia, Vancouver, British Columbia V6T 1Z4
[2]British Columbia Geological Survey, Ministry of Energy and Mines, P.O. Box 9333 Stn Prov Gov't, Victoria, British Columbia V8W 9N3
[3]Geological Survey of Canada, 601 Booth Street, Ottawa, Ontario K1A 0E8

ABSTRACT

Convergent margins are becoming increasingly viable tectonic settings for the discovery of mafic-ultramafic intrusion hosted nickel-copper-platinum group element (PGE) mineralization. The ca. 190 Ma Turnagain intrusion in the Northern Cordillera of British Columbia is a mineralized Alaskan-type ultramafic-mafic intrusion. A substantial Ni-Co resource (1842 million tonnes at 0.21% per tonne Ni and 0.013% per tonne Co) has been delineated in what is known as the Horsetrail zone, with additional Cu-PGE potential identified in the DJ/DB zone, which is located 2.5 km northwest of the Ni-sulphide mineralization. This report presents geochemical and mineralogical databases that are the results of work undertaken to characterize the Cu-PGE mineralization at the DJ/DB zone in order to improve exploration models for base metal and PGE deposits. Included are observations of the mineralogy as well as the textures of the mineralization and host rocks in the DJ/DB zone for comparison with those of the Horsetrail zone with the aim to develop exploration criteria for the base- and precious-metal-rich mineralization. Extensive geochemical databases compiled herein include whole rock major element oxide, trace element, and PGE analyses, electron microprobe data for clinopyroxene, amphibole, biotite, Mg-silicate, oxide, sulphide, and platinum group minerals (PGM), in-situ laser ablation ICP-MS analyses of sulphides, and sulphur isotope analyses of sulphides.

INTRODUCTION AND OBJECTIVES

Ni-Cu-PGE deposits in convergent-margin settings

Mafic-ultramafic intrusions host most of the largest nickel, copper, and platinum group element (PGE) deposits worldwide (e.g. Bushveld Complex, South Africa: McDonald and Holwell, 2011; Noril'sk, Russia: Lightfoot and Keays, 2005; Stillwater Complex, Montana, USA: Zientek and Parks, 2014). These intrusions generally form in extensional tectonic settings that may, under favourable conditions, be host to high-tonnage deposits (Ripley, 2010). Conventionally, convergent-margin settings have not been considered prospective targets for Ni-Cu-PGE mineral exploration due to an apparent lack of sulphide-rich ultramafic bodies (Ripley, 2010). However, there are an increasing number of economically viable magmatic sulphide deposits that have been discovered in ultramafic intrusions within convergent-margin settings (e.g. Aguablanca, Spain: Piña et al., 2008; Xiarihamu, China: Li et al., 2015). These ultramafic-mafic intrusions are typically formed by the emplacement and differentiation of relatively small quantities of hydrous mafic magmas that have been generated in the mantle wedge above subduction zones (e.g. Himmelberg and Loney, 1995). These intrusions are classified into two broad petrological categories, based on the presence or absence of orthopyroxene (Nixon et al., 2015): 1) intrusions that do not contain orthopyroxene, known as Ural-Alaskan-type or Alaskan-type, and 2) orthopyroxene-rich Giant-Mascot types (Nixon et al., 2015). Alaskan-type intrusions commonly host chromitite-related PGE mineralization (Nixon and Hammack, 1991), but generally lack (i.e. are devoid of) base metal sulphide mineralization, with the exception of a few Alaskan-type intrusions in the North American Cordillera and the Ural Mountains of Russia (Johan, 2002).

The Turnagain Alaskan-type intrusion in the Yukon-Tanana terrane is host to a very large Ni-Co resource: 1842 Mt at 0.21% per tonne Ni and 0.013% per tonne Co (Riles et al., 2011; Mudd and Jowitt, 2014). Previous studies have focused on the Ni-Co-rich mineralization in the Horsetrail zone (Clark, 1975, 1980; Scheel, 2007), however, the Cu-PGE-bearing DJ/DB zone has received little attention. This report presents the results of a graduate thesis project undertaken by the first author (S. Jackson-Brown, MSc. thesis, in prep.) as a contribution to the TGI-4 Ni-Cu-PGE-Cr project of the Geological Survey of Canada.

Purpose of study

The purpose of this study is to 1) define the textures and compositions of Cu-PGE mineralization in the DJ/DB zone; 2) determine the controls on mineralization with the aim of establishing exploration criteria for these base- and precious-metal-rich zones in similar Alaskan-type intrusions; and 3) compare Turnagain to mineralized Alaskan-type intrusions elsewhere (e.g. Duke Island, Alaska, USA: Thakurta et al., 2014; Salt Chuck, Alaska, USA: Loney and Himmelberg, 1992), as well as to other mafic-ultramafic intrusions in convergent-margin settings (e.g. Giant Mascot, B.C.: Manor, 2014; Aguablanca, Spain: Piña et al., 2008). Observations of the sulphide mineralization in the Horsetrail zone by Scheel (2007) are combined with those from this study on PGE mineralization in the DJ/DB zone to characterize the anomalously sulphide-rich Turnagain intrusion. Key criteria will then be presented that can be used to explore for base metal sulphide + PGE mineralization in Alaskan-type intrusions in other convergent-margin settings in Canada and worldwide.

GEOLOGICAL SETTING OF THE TURNAGAIN INTRUSION AND STUDY AREA

The Turnagain intrusion is a 25 km^2 Alaskan-type ultramafic-mafic intrusion in north-central British Columbia, located 70 km east of Dease Lake (Fig. 1, inset). Clark (1980) recognized the presence of olivine-clinopyroxene-hornblende cumulates in the Turnagain intrusion with no orthopyroxene, a defining characteristic of Alaskan-type intrusions (e.g. Irvine, 1974; Nixon et al., 1997). The intrusion lies within the metasedimentary-metavolcanic Yukon-Tanana terrane, northeast of the Kutcho Fault (Fig. 1). The northern and eastern margins of the intrusion are in fault contact with pyritic and graphitic phyllite and slate. The southern and western margins are intrusive contacts with hornfels metasedimentary and metavolcanic rocks that have been observed both in outcrop, at an inlier at the western extremity of the intrusion, and in drillcore (Clark, 1975; Scheel, 2007).

The Turnagain intrusion is divided into four distinct phases based on intrusive contacts observed on surface and in drillcore (Clark, 1980; Scheel, 2007; Jackson-Brown et al., 2014) (Fig. 1). The earliest intrusive phase (Phase 1) comprises steeply dipping, layered wehrlite and clinopyroxenite along the northern part of the intrusion (Clark, 1975). A large dunite body (Phase 2) that forms the core of the intrusion cuts Phase 1 wehrlite and clinopyroxenite. The dunite body grades to the south into wehrlite and clinopyroxenite that host the Ni-Co-rich Horsetrail zone (Clark, 1980; Scheel et al., 2005). Hornblendite and clinopyroxenite (Phase 3) in the western portion of the intrusion host the DJ/DB zone Cu-PGE mineralization. Clinopyroxenite locally contains xenoliths of dunite near the southern margin of the Phase 3 intrusion (see Appendix D; Jackson-Brown et al., 2014). Lastly, a central body of melanocratic to leucocratic diorite (Phase 4) intrudes the contacts between dunite and Phase 3 clinopyroxenite and hornblendite that host the DJ/DB zone (Clark, 1980; Scheel et al., 2005).

Soil surveys completed in 2004 by Hard Creek Nickel Corporation identified anomalously high Cu, Pt, and Pd concentrations in the DJ/DB zone (>1200 ppm Cu, >600 ppb Pt+Pd), and subsequent drilling revealed several PGE-rich bedrock areas (Riles et al., 2011). Both clinopyroxenite and hornblendite in the DJ/DB zone are sulphide-bearing and variably mineralized, although the controls on mineralization are poorly understood.

METHODS

Sampling

A total of 114 drillcore samples from 19 diamond drillholes (Table 1) and 17 surface samples were collected during two field visits to the Turnagain intrusion in 2011 and 2013 by Dr. Graham Nixon and Sarah Jackson-Brown, respectively (see Appendix A for full list of samples and analyses completed on each, see Appendix B for field photographs). Drillcore sampling focussed on areas with high Pt+Pd concentrations (>500 ppb over 4 m) in assay data from Hard Creek Nickel Corporation (Appendix C). Samples of representative rock types, unmineralized rocks, and characteristic rock textures were also sampled. Most surface samples were taken from large boulders as exposure is poor. Transport of boulders is considered to be minimal (<1 km) due to the large size (>1 m) and angularity, and are composed of rock types observed in nearby drillholes.

Polished petrographic thin sections of 95 samples were studied. An additional eight standard thin sections were also prepared, two of which were stained to check for the presence of K-feldspar. All thin sections were examined using both plane-polarized and cross-polarized transmitted light to determine silicate and accessory mineralogy. The polished thin sections were additionally examined under reflected light to determine the predominant sulphide and oxide minerals present in the samples.

Scanning electron microscopy

Thirteen polished petrographic thin sections were carbon coated at the Electron Microbeam/X-Ray Diffraction Facility at the University of British Columbia (UBC), Vancouver, and the SEM Facility at

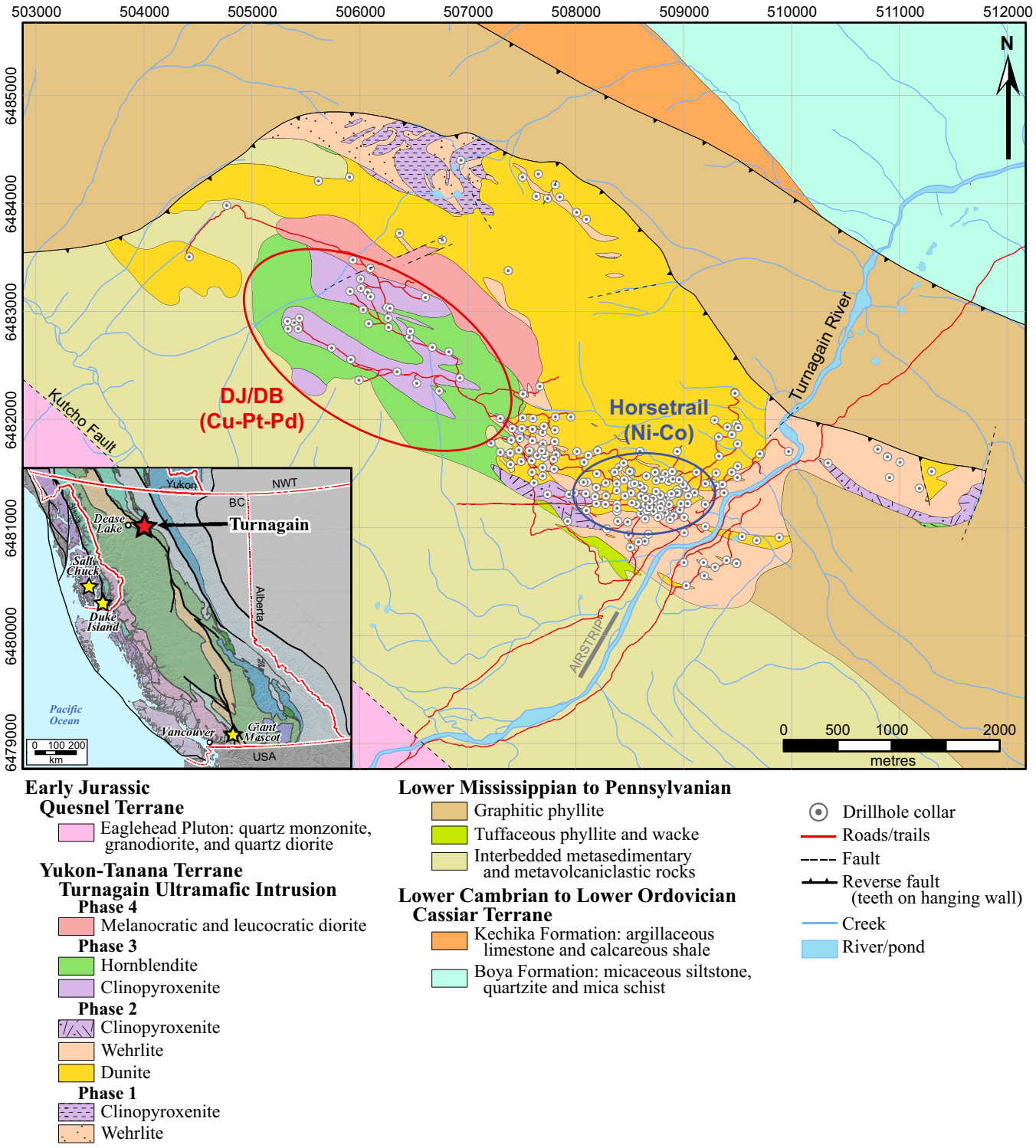

Figure 1. Geology of the Turnagain ultramafic intrusion and host rocks showing the location of the Cu-PGE-enriched DJ/DB zone and the major Ni-Co mineralized Horsetrail zone (modified from Nixon et al., 2012; projection is NAD83, UTM Zone 9). Inset: Map of the tectono-stratigraphic configuration of the Canadian Cordillera with locations of major convergent-margin Ni-Cu-PGE mineralized mafic-ultramafic intrusions, including the Turnagain intrusion (map modified from Colpron and Nelson, 2011). Major terranes (from left to right): Wrangellia (light purple), Alexander (dark purple), Coast Plutonic Complex (pink), Stikinia (green), Cache Creek (tan), Quesnellia (grey-green), Slide Mountain (dark green), Ancestral North America (light/dark blue).

the Geological Survey of Canada (GSC), Ottawa. At UBC, back-scattered electron (BSE) imaging and qualitative energy-dispersive spectrometry (EDS) were carried out on a Philips XL-30 scanning electron microscope (SEM) equipped with a Bruker Quanta 200 energy-dispersion X-ray microanalysis system. An

Table 1. Location and orientation information for diamond drillholes sampled in the Cu-PGE (DJ/DB) zone, Turnagain intrusion.

Drillhole ID	Easting	Northing	Elevation (masl)	Azimuth (degrees)	Dip (degrees)	EOH (m)
DDH03-07	508583.25	6480856.29	1036.14	169.45	-47.07	434
DDH04-43	506826.18	6482617.08	1401.58	0.00	-90.00	159
DDH04-46	506468.86	6482806.91	1436.26	0.00	-90.00	145
DDH04-48	506254.41	6483031.55	1459.44	0.00	-90.00	167
DDH04-49	506254.44	6483032.55	1459.56	180.00	-50.00	75
DDH04-55	506280.84	6483021.70	1462.38	0.00	-90.00	60
DDH04-58	506010.28	6483207.20	1454.88	35.00	-80.00	111
DDH04-59	506006.85	6483289.47	1462.93	0.00	-80.00	111
DDH05-83	506528.86	6482326.02	1352.83	224.50	-52.00	172
DDH05-88	505395.46	6482884.27	1336.38	40.55	-50.50	172
DDH05-89	505925.46	6482544.45	1356.58	40.77	-50.75	166
DDH05-101	505395.46	6482884.28	1336.75	40.83	-65.00	185
DDH05-102	506345.95	6482434.50	1366.17	219.30	-51.40	337
DDH06-143	504769.64	6483975.36	1402.34	31.98	-50.00	340
DDH06-149	505911.96	6483180.07	1435.80	41.88	-49.50	315
DDH06-150	506032.27	6483009.63	1428.63	44.70	-49.80	258
DDH06-161	505431.81	6482833.59	1338.16	41.41	-48.50	285
DDH07-207	505919.14	6482546.35	1357.22	189.34	-49.90	312
DDH07-211	505337.42	6482829.35	1323.36	45.75	-68.30	276

All geographical data is in NAD83, Zone 9
masl = metres above sea level
EOH = end of hole

operating voltage of 15 kV was used with a spot diameter of 6 μm and peak count time of 30 s. At the GSC, BSE imaging and EDS analyses were acquired using a Zeiss EVO 50 series SEM with extended pressure capability (up to 3000 Pascals) and equipped with a backscattered electron detector (BSD), Everhart-Thornley secondary electron detector (SE), and variable pressure secondary electron detector (VPSE). The Oxford EDS system includes the X-MAX 150 Silicon Drift Detector, INCA Energy 450 software, and Aztec microanalysis software. An operating voltage (EHT) of 20 kV was used, with a probe current of 400 pA to 1 nA, and peak count time of 30 s.

Electron microprobe analyses

Quantitative mineral analyses of silicates, sulphides and platinum group minerals were determined on carbon-coated, polished petrographic thin sections (n=17) using an automated four-spectrometer Cameca Camebax MBX electron microprobe by wavelength-dispersive X-ray analysis at the Department of Earth Sciences, Carleton University, Ottawa. Raw X-ray data were converted to elemental weight percent by the Cameca PAP matrix correction program. Silicates were analyzed using a 20 kV accelerating voltage, 25 nA beam current, 2 μm diameter beam, and counting time of 20 s or 40,000 accumulated counts. Sulphides and precious metal minerals were analyzed using a 20 keV accelerating voltage, 35 nA beam current, 2 μm diameter beam, and counting time of 10 s or 40,000 accumulated counts. Mineral formula calculations were done according to the procedures outlined in the appendix of Deer et al. (1996), with the exception of iron oxide formulas, which were calculated following the method by Droop (1987).

Whole rock major and trace element geochemical analyses

Major element oxide and trace element concentrations of 21 whole rock samples and three duplicates were analyzed at Activation Laboratories Ltd. (Actlabs) in Ancaster, Ontario. Samples were submitted as either whole rocks or rock chips (at least 50 g in weight) and processed by Actlabs. Samples were crushed to a nominal minus 10 mesh (1.7 mm) and split to obtain a representative sample, then pulverized to at least 95% minus 150 mesh (106 microns) with Cr- and Ni-free mild steel mills. For the major elements, a 1 g sample was mixed with a flux of lithium metaborate and lithium tetraborate and then fused in an induction furnace. The molten mixture was then poured into a solution of 5% HNO_3 and mixed continuously for 30 minutes until completely dissolved. The samples were analyzed for major element oxides (excluding FeO) and select trace elements using a simultaneous/sequential Thermo Jarrell-Ash ENVIRO II inductively coupled plasma optical emission spectrometer (ICP-OES). Additional trace elements were determined by diluting and analyzing the previously fused samples using the inductively coupled plasma mass spectrometry (ICP-MS) method. FeO was obtained through the titration method, using cold acid digestion of ammonium metavanadate and hydrofluoric acid. Chalcophile elements (Co, Cu, Ni, Cd, Li, Mn, Pb, and Zn) were obtained through the total digestion method in which a 0.25 g sample was digested in HF, followed by a mixture of nitric and perchloric acids, then heated and taken to dryness. The samples were brought back into solution with HCl and nitric acid and analyzed using a Perkin Elmer Sciex ELAN ICP-MS. Gold, platinum, and palladium values were measured via fire assay of 5-50 g samples. The samples were mixed with fluxes and Ag (collecting agent) and heated in a fire clay crucible to 1060°C (~60 minutes). The crucibles were removed from the oven and the slag was poured into a mould, each crucible leaving a lead button containing PGE and precious metals. Each button was placed in a preheated cupel to absorb the lead, leaving an Ag bead+Au, Pt, and Pd. The bead was digested in hot HNO_3 and HCl and analyzed using an ICP-MS. Semi-metals (As, Bi, Sb, and Te) were determined via nitric peroxide digestion and ICP-MS analyses. Volatiles (B, C, S, Cl, and F) were measured using the following methods: gamma ray emission detection (B), irradiation energy (C, S), neutron activation analysis (Cl), and ion-selective electrode (F). Internal calibration was achieved using a variety of international reference materials and independent control samples.

Chalcophile, platinum group element, and sulphur geochemical analyses

The concentrations of platinum group elements (Ir, Ru, Rh, Pt, and Pd) and Au in 27 whole rock samples and three duplicates were measured by nickel-sulphide fire-assay (NiS-FA) ICP-MS and the chalcophile elements (Ni, Cu, and Co) were analyzed by atomic absorption spectroscopy techniques at Geoscience Laboratories in Sudbury, Ontario, Canada. Samples were crushed to 74 µm (200 mesh) using a high-chrome steel mill to avoid contamination of precious metals.

Nickel sulphide fire-assay techniques at Geolabs are detailed by Richardson and Burnham (2002), following procedures from Shazali et al. (1987) and Jackson et al. (1990). Nickel, sulphur, sodium carbonate, and sodium tetraborate were added to a 15 g aliquot of sample powder, and fused for 1.5 hours in a fire-clay crucible at 1050°C. Following cooling, the crucible was broken to recover a nickel sulphide button. This button was dissolved with HCl in a closed Teflon™ vessel to remove any NiS matrix. The co-precipitation of the NiS button with tellurium produced a concentrate containing all Au and PGE lost during button dissolution. Concentrates were then vacuum-filtered, re-dissolved in aqua regia, and brought to volume with deionized water prior to analysis by a Perkin-Elmer ELAN 5000 inductively coupled plasma mass spectrometer (ICP-MS). Osmium was not reported due to the potential loss as a volatile oxide during the aqua regia re-dissolution stage. Reference materials used were CANMET-certified TDB-1, WPR-1, WGB-1, and WMG-1, and an in-house komatiite sample OKUM.

The remaining <74 µm pulps from the same crush as the NiS-FA method were mixed with a three-acid (hydrofluoric, nitric, and perchloric) mix in an open Teflon™ digestion vessel and heated until dry. A solution was produced by adding a second acid mixture, transferred to a 50 mL volumetric container and diluted with 10% HNO_3 respective to the volume of sample. Chalcophile element (Ni, Cu, Co, Cd, Zn, Li, and Pb) concentrations were measured by atomic absorption methods with a Varian Atomic Absorption Spectrometer AA280FS Series.

Sulphur and carbon determination techniques are outlined in Amirault and Burnham (2013). Sample material was taken from a 0.2 g pre-measured aliquot and combusted from radio-frequency inductive heating with a constant stream of purified oxygen. Gases (CO_2 and SO_2) were produced and detected by non-dispersive infrared (NDIR) cells. Concentrations were then measured by a LECO CS844 carbon and sulphur analyzer.

Laser ablation ICP-MS analysis of sulphide minerals

Laser ablation inductively-coupled plasma mass spectrometry (LA-ICP-MS) analyses of the four major sulphides (i.e. pyrrhotite, chalcopyrite, pyrite, and pentlandite) were completed on 12 polished thin sections at the LA-ICP-MS laboratory at the GSC (Ottawa) (e.g. Lawley et al., 2015). Single spot analyses were completed using a Photon-Machines Analyte 193 excimer laser ablation system (λ = 193 nm) with Helex ablation cell and an Agilent 7700x quadrupole ICP-MS. Ablation was performed in a He environment, mixed with Ar gas for ICP-MS analysis. Laser pulse energy was set to 40% of 4 mJ. Two calibration standards were utilized for this study, Po726, a homogeneous synthetic pyrrhotite (prepared by J.H.G. Laflamme at CANMET) for the platinum group elements (Ru, Rh, Pd, Os, Ir, Pt, and Au), and GSE-1G, a USGS reference glass of basaltic composition doped with over 50 trace elements (Guillong et al., 2005) for the remaining chalcophile and lithophile elements. The MASS-1 (previously PS-1) Fe-Cu-Zn-S pressed pellet reference material (Wilson et al., 2002) was used with the standards to test the accuracy and precision of the analyses. Standards were analyzed throughout the sequence, two analyses of each standard and one analysis of MASS-1 for every 10 unknowns to ensure accuracy and correct for instrumental drift. Analysis of standards was completed using a laser pulse rate frequency of 10 Hz and a spot size of 43 µm. For the analysis of samples, laser frequency was set to 6 Hz, with spot sizes ranging from 7 to 30 µm, depending on the size of the sulphide being analyzed. Data collection lasted for approximately 100 seconds, with 40 seconds of gas blank followed by 60 seconds of ablated sample measurement. Data collection and correction was done using GLITTER data reduction software (Griffin et al., 2008), developed by the ARC National Key Centre for Geochemical Evolution and Metallogeny of Continents (GEMOC) and CSIRO Exploration and Mining. Final concentrations were determined by subtracting the background (gas blank) signal from each of the analyzed isotopes, and normalizing to either Po726 (for PGE) or GSE-1G (for the remaining isotopes). Microinclusions of accessory minerals were encountered during analysis and were excluded from the time-resolved spectrum before calculation of the average signal.

Measured isotopes were ^{29}Si, ^{34}S, ^{42}Ca, ^{51}V, ^{53}Cr, ^{57}Fe, ^{59}Co, ^{61}Ni, ^{65}Cu, ^{66}Zn, ^{75}As, ^{77}Se, ^{88}Sr, ^{89}Y, ^{90}Zr, $^{101,102}Ru$, ^{103}Rh, $^{105,106,108}Pd$, $^{107,109}Ag$, ^{111}Cd, ^{118}Sn, ^{121}Sb, ^{125}Te, ^{181}Ta, ^{185}Re, ^{189}Os, ^{193}Ir, ^{195}Pt, ^{197}Au, ^{202}Hg, ^{205}Tl, $^{206,208}Pb$ and ^{209}Bi. Due to the thinness of the samples being ablated (i.e. 30 µm thick thin sections), silicon and calcium were monitored to determine if the laser ablated completely through the sample and into the glass during the run. The S, Cu, and Ni values were used to monitor the mineral phase during ablation. Analyses with greater than 750 ppm Si or Ca were not reported due to low reliability of the

analyses for sulphide samples. Isotopic interference from ^{65}Cu on ^{101}Ru, ^{103}Rh, and ^{105}Pd meant that these isotopes were unusable when analyzing chalcopyrite or grains with greater than 100 ppm Cu. Interference from ^{61}Ni on ^{101}Ru meant that this isotope could not be used. In samples with >10000 ppm Ni, interference on ^{106}Pd from ^{111}Cd was corrected by Dr. Zhaoping Yang at the GSC using LAMTRACE software.

Sulphur isotope analyses

Three sulphide minerals (e.g. pyrrhotite, chalcopyrite, and pyrite) were extracted from sulphide-bearing samples (n=32) using a Dremel 400 Series XPR hand-held drill with a 1/32" drill bit. The relative proportion of different sulphide minerals being extracted was recorded to estimate the percentage of S in the sample for approximately 3 mg of sulphide powder. All powders (n=36), including three blind duplicates, were analyzed at the G.G. Hatch Stable Isotope Laboratory at the University of Ottawa, Canada. Samples were weighed into tin capsules with at least twice the sample weight of tungstic oxide (WO_3) for inorganic or organic sulphur. Calibrated internal standards were prepared with every batch of samples for normalization of the data. Each analysis required 100 µg of S. Samples were loaded into an Elementar Vario Micro Cube elemental analyzer and flash combusted at 1800°C. Released gases (N_2, CO_2, H_2O, and SO_2) were carried by ultra-pure helium through the elemental analyzer to be cleaned, then gas chromatograph separation removed SO_2 by moving gases through a series of adsorption traps (i.e. "trap and purge"). Isotopic compositions of organic sulphur (SO_2) were measured by a ThermoFinnigan Delta XP isotope ratio mass spectrometer coupled with a ConFlo IV. The measured isotope for sulphur was ^{34}S assuming mass-dependent fractionation. Values are reported relative to the Vienna Canyon Diablo Troilite (VCDT) and analytical precision for $\delta^{34}S$ is 0.2‰.

RESULTS

Mineralogy and textures of major rock types in the DJ/DB zone

Clinopyroxenite and hornblendite form the two major rock types in the DJ/DB, Cu-PGE zone of the Turnagain intrusion (Fig. 2, Appendix D).

Clinopyroxenite is the dominant rock type in the DJ/DB zone, which, based on petrography, can be separated into four distinct units: hornblende clinopyroxenite, clinopyroxenite, magnetite clinopyroxenite, and olivine clinopyroxenite (Appendices E, F1,2). Clinopyroxene compositions are diopsidic in all units (Appendix F3). Hornblende clinopyroxenite is composed of fine- to medium-grained, pale green-grey diopside with interstitial to interlayered dark green amphibole (5–44%), biotite (<15%), magnetite (<5%), and disseminated to net-textured and locally layered sulphide (6–31%). Hornblende clinopyroxenite is weakly to moderately altered to chlorite (<15%, after biotite), tremolite (<15%, after clinopyroxene), and minor calcite. Clinopyroxenite comprises fine- to coarse-grained diopside with interstitial biotite (<35%, up to 5% of which may be an alteration product of amphibole), interstitial hornblende (<8%), blebby magnetite (<5%), and disseminated to massive sulphide (<53%) that exhibits localized banding. Alteration ranges from very weak to very strong, and is composed of up to 28% tremolite, <25% chlorite, and minor serpentine and calcite, with local areas of talc alteration (<28%). Magnetite clinopyroxene contains fine- to coarse-grained diopside with subhedral to euhedral magnetite (<20%), disseminated to blebby sulphides (<14%), and minor interstitial biotite and hornblende. Weak to moderate alteration is present as minor chlorite and/or biotite (after amphibole), with trace tremolite and calcite. Olivine clinopyroxenite, referred to as olivine-(serpentinite-magnetite) clinopyroxenite, is composed of diopside and olivine (Fo_{79}) that is pseudomorphed by serpentine and magnetite. Original olivine contents ranged from 2 to 28% (with localized clots of olivine), and there may be up to 20% relict olivine with thin veinlets of replacement magnetite (<10%) and fine-grained radial serpentine (<45%). Interstitial biotite (<12%), interstitial amphibole (<7%), and sulphide (<37%) also occur. Alteration consists of <10% chlorite, with minor calcite and trace tremolite. Sulphides in all clinopyroxene-rich rocks are present as disseminated to massive (with localized layering). Pyrrhotite is the most common sulphide (<50%) in clinopyroxenites, and forms the majority of layered, net-textured, and semi-massive to massive sulphide occurrences. Chalcopyrite is the second most common sulphide (<35%) and generally forms as disseminated to blebby textures with localized veins. Other sulphides include pyrite (<10%), minor pentlandite, and a variety of trace sulphide, antimonide, and platinum group minerals that all form disseminated grains associated with either pyrrhotite or chalcopyrite.

Hornblendite is dominated by fine-grained to pegmatitic, dark-green amphibole and up to 10 vol.% fine- to medium-grained clinopyroxene, <7% biotite, <11% fine-grained subhedral to euhedral magnetite, 1–15% disseminated sulphide (up to 40% as net-textured sulphide), and is locally feldspathic (<10%). Minor alteration (<5%) is present as chlorite and trace tremolite. Amphibole compositions are predominantly magnesio-hastingsite to potassic-magnesio-hastingsite (see Appendix F3 for mineral analyses). Rare blue-green subcalcic sodio-magnesio-hastingsite occurs as alteration rims on amphiboles in some altered samples (e.g.

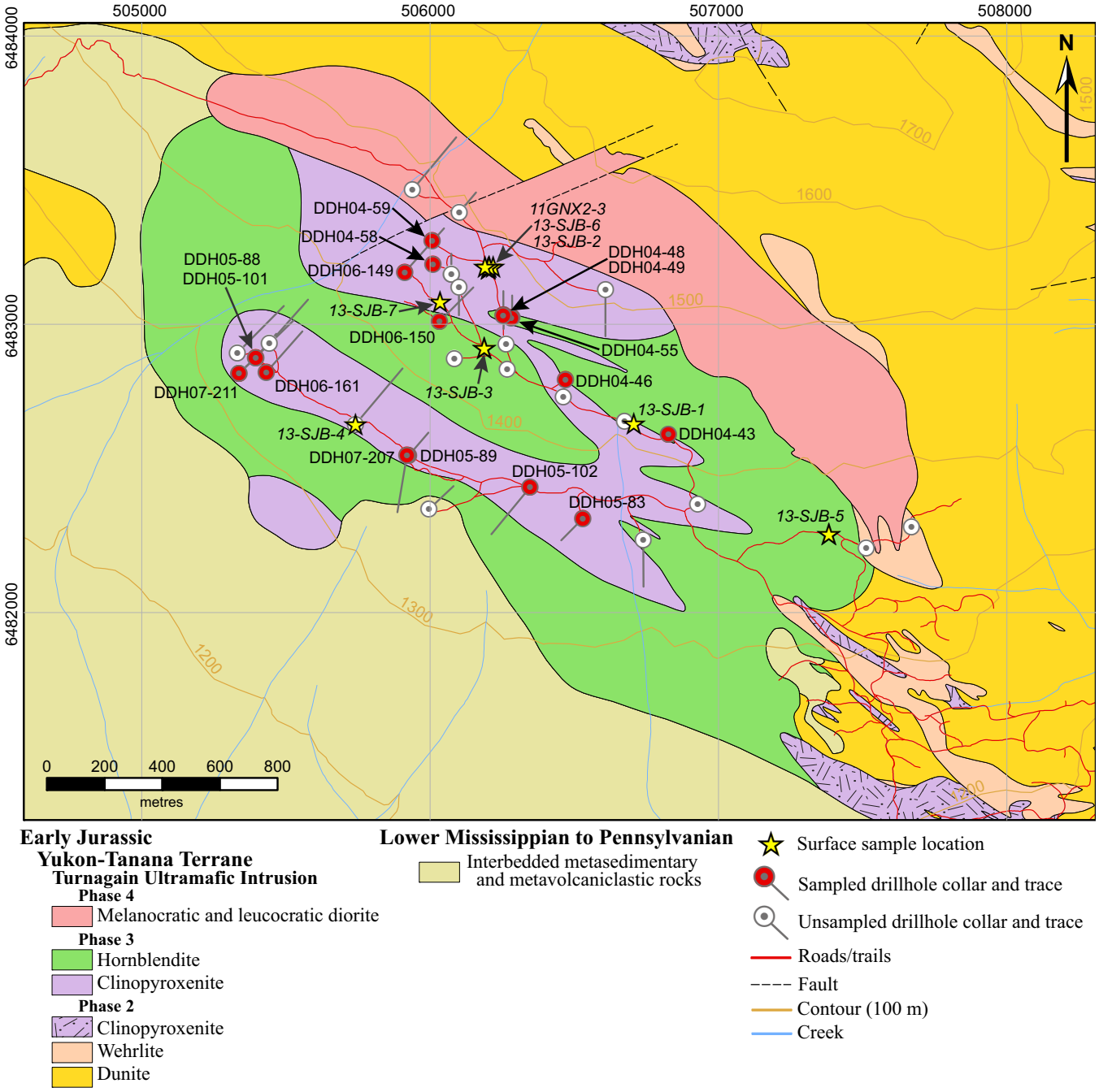

Figure 2. Geological map of the DJ/DB zone of the Turnagain intrusion and immediate surroundings, showing surface sample and drill collar locations (modified from Nixon et al., 2012; projection is NAD83, UTM Zone 9; contour interval is 100 m).

DDH05-88-106, DDH05-101-4, see sample description of DDH05-88-104 in Appendix F2). Most hornblendite samples contain randomly oriented amphibole, with local zones (1–100 cm wide) of moderately to strongly oriented crystals. Oriented amphiboles typically occur in the coarser grained and pegmatitic units, and they can exhibit both gradational and sharp contacts with surrounding rocks; they also occur at contacts between two hornblendite units of different grain size or along contacts with clinopyroxenite. Hornblendite commonly grades into clinopyroxenite; localized veins of hornblendite cut earlier clinopyroxenite and hornblendite. Sulphide mineralization in hornblendite consists primarily of pyrrhotite (<12%) and chalcopyrite (1–5%), with minor pyrite and pentlandite, and trace sphalerite. Sulphides are typically interstitial to amphibole, but can also occur as individual blebs and as secondary crosscutting veins.

Sulphide and platinum group minerals in the DJ/DB zone

Base metal sulphides in the DJ/DB zone are composed

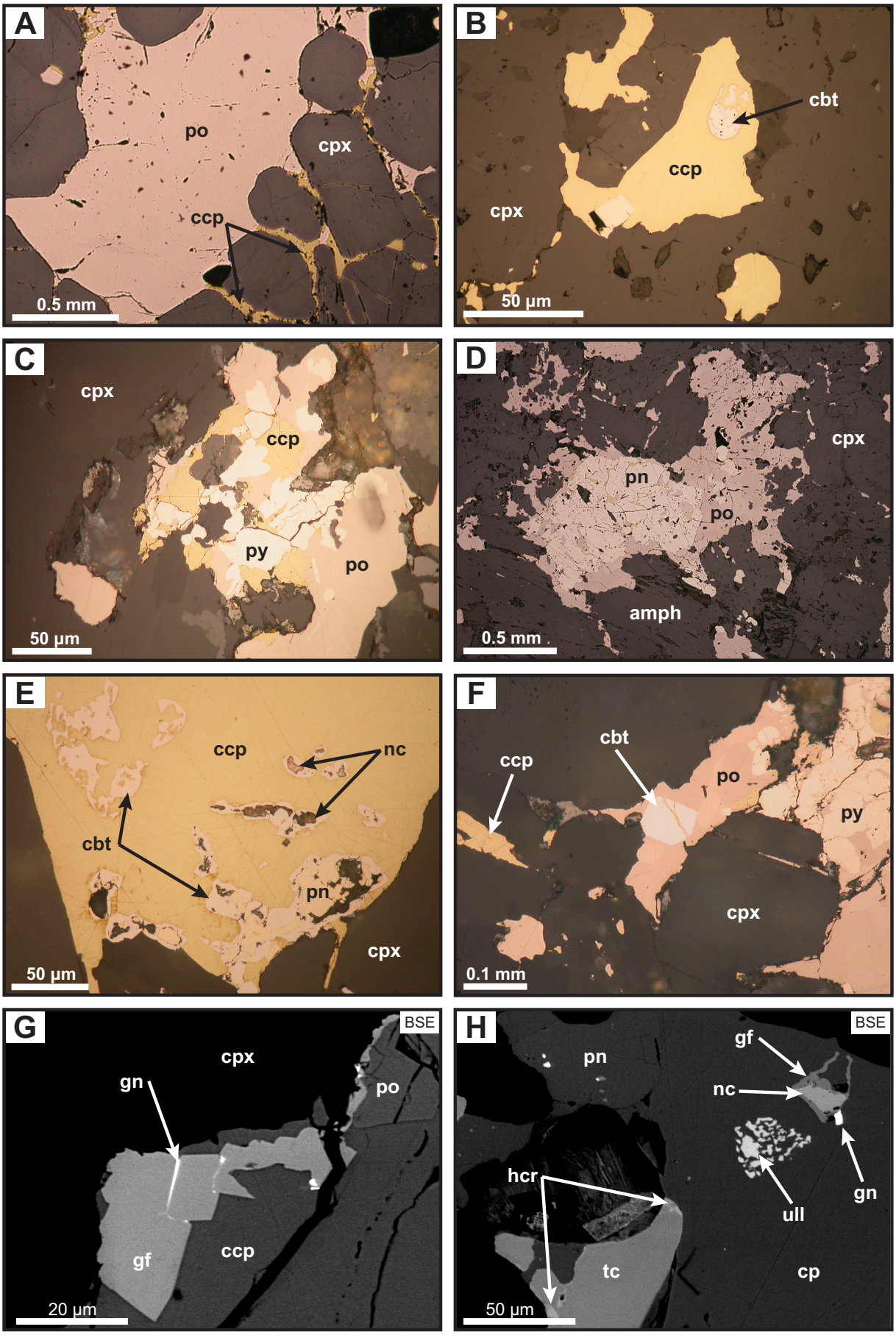
A
po
cpx
ccp
0.5 mm
B
cbt
ccp
cpx
50 µm
C
cpx
ccp
py
po
50 µm
D
cpx
pn
po
amph
0.5 mm
E
ccp
nc
cbt
pn
cpx
50 µm
F
cbt
ccp
po
py
cpx
0.1 mm
G
BSE
cpx
gn
po
gf
ccp
20 µm
H
BSE
pn
gf
nc
hcr
ull
gn
tc
cp
50 µm

Figure 3 (opposite page). Photomicrographs in reflected light (a-f) and backscattered electron (BSE) images (g-h) of base metal sulphide, arsenide, sulpharsenide, and sulphantimonide minerals in clinopyroxenite from the DJ/DB zone. **a)** Sample DDH07-211-5: coarse-grained interstitial pyrrhotite bleb with peripheral chalcopyrite along grain boundaries of surrounding clinopyroxene grains. **b)** Sample DDH07-211-4: chalcopyrite bleb in clinopyroxene containing grains of subhedral cobaltite. **c)** Sample DDH07-211-4: an aggregate of subhedral pyrite in a composite bleb of pyrrhotite and chalcopyrite. **d)** Sample DDH05-88-102: blocky pentlandite in pyrrhotite. **e)** Sample DDH07-211-1: chalcopyrite bleb containing subhedral to anhedral cobaltite. Anhedral crystals of pentlandite and nickeline are enclosed in cobaltite. **f)** Sample DDH07-211-5: fractured, euhedral grain of cobaltite in pyrrhotite. Pyrrhotite also contains pyrite and chalcopyrite. **g)** Sample DDH07-211-1: subhedral, cobalt-rich gersdorffite within chalcopyrite with galena in fractures. **h)** Sample DDH07-211-1: chalcopyrite containing blebs of pentlandite, galena, gersdorffite, ullmannite, and tucekite. Nickeline is enclosed in gersdorffite and tucekite is partly rimmed by hauchecornite. Mineral abbreviations: amph = amphibole; cbt = cobaltite; ccp = chalcopyrite; cpx = clinopyroxene; gf = gersdorffite; gn = galena; hcr = hauchecornite; nc = nickeline; pn = pentlandite; po = pyrrhotite; py = pyrite; tc = tucekite; ull = ullmannite.

primarily of pyrrhotite (<50 modal %), chalcopyrite (<35%), pyrite (<10%), and minor pentlandite (<1%). Trace and accessory sulphide phases include millerite (NiS), sphalerite (ZnS), bornite (Cu_5FeS_4), siegenite [$(Ni,Co)_3S_4$], marcasite (FeS_2), galena (PbS), and molybdenite (MoS_2). Pyrrhotite is the dominant sulphide, forming sub-millimetre to 3 mm diameter grains both interstitial to silicates and as blebs within silicates (Fig. 3a,c,d,f). Pyrrhotite compositions (n= 45) range from $Fe_{58.7}S_{39.5}$ to $Fe_{61.6}S_{38.9}$ (average= $Fe_{60.3}Ni_{0.29}S_{39.3}$), with a maximum Ni content of 1 wt% (Fig. 4, Appendix F3). Chalcopyrite is commonly intergrown with pyrrhotite and forms either interstitial to silicates or as blebs within silicates (Fig. 3b,c,e). Chalcopyrite compositions are stoichiometric (average=$Cu_{1.01}Fe_{0.99}S_2$, n=42). Pyrite is observed as either aggregates of subhedral to euhedral grains within pyrrhotite and chalcopyrite (Fig. 3c,f), or as anhedral grains in veinlets that crosscut silicates. Pyrite compositions are stoichiometric ($Fe_{0.99}S_2$, n=29, Fig. 4) although some grains contain up to 3.4 wt% Co. Pentlandite forms both as subhedral, sub-millimeter grains in pyrrhotite and chalcopyrite (Fig. 3d), and as exsolution flames within pyrrhotite. Pentlandite (n=20) has an average composition of $(Ni_{4.60}Fe_{3.81}Co_{0.54})S_8$, but is characterized by lower Ni and higher Co contents when present as inclusions and flames within pyrrhotite, and in strongly altered samples [average= $(Fe_{3.91}Ni_{3.72}Co_{1.39})S_8$, Fig. 4].

The DJ/DB zone contains a wide variety of arsenic- and antimony-bearing accessory minerals. Nickeline (NiAs), present as anhedral grains enclosed within cobaltite and gersdorffite, has approximately stoichiometric compositions [average=$(Ni_{0.96}Fe_{0.01})(As_{0.96}Sb_{0.03}S_{0.02})$, n=4, Fig. 5]. Sulpharsenide and sulphantimonide minerals include cobaltite (CoAsS), gersdorffite (NiAsS), ullmannite (NiSbS), tucekite ($Ni_9Sb_2S_8$), and hauchecornite ($Ni_9Bi(Sb,Bi)S_8$). Cobaltite is observed in two forms: 1) equant, euhedral grains (~50 µm) associated with chalcopyrite, pyrrhotite, and magnetite (Fig. 3b,f); or 2) anhedral grains or grain aggregates within chalcopyrite, rarely enclosing grains of nickeline and pentlandite (Fig. 3e). The average cobaltite composition (n=8) is $(Co_{0.86}Fe_{0.07}Ni_{0.07})$

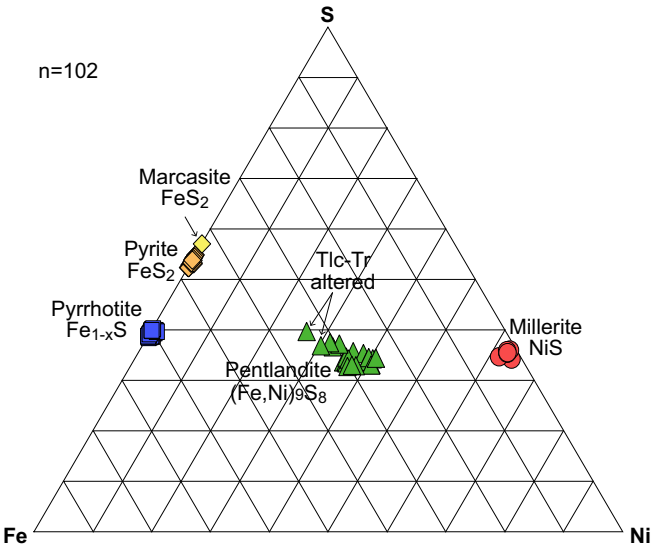

Figure 4. Ternary diagram showing the compositions of Ni-, Fe-, and S-bearing base metal sulphides in the DJ/DB zone of the Turnagain intrusion (pyrrhotite, chalcopyrite, pyrite, marcasite, pentlandite, and millerite). Note the decrease in Ni in pentlandite within talc-tremolite (Tlc-Tr) altered samples. Analyses are EPMA results in weight percent normalized to 100%.

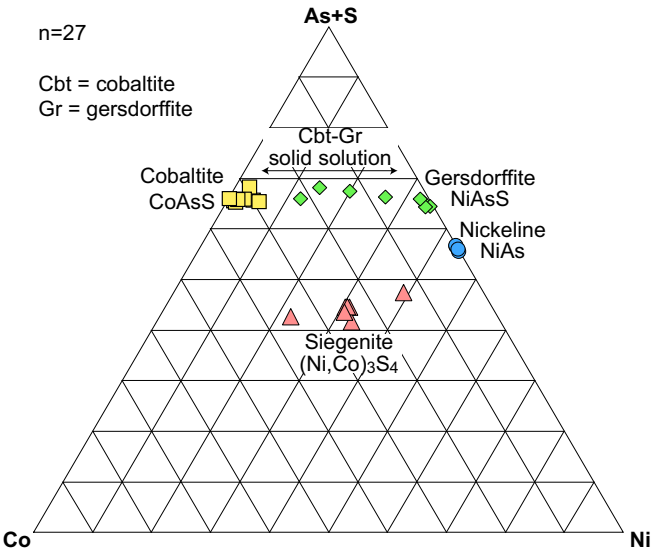

Figure 5. Ternary diagram showing the compositions of Ni-, Co-, and As-/S-bearing base metal sulphides in the DJ/DB zone of the Turnagain intrusion (cobaltite, gersdorffite, siegenite, and nickeline). Note the range of gersdorffite compositions, trending towards cobaltite. Analyses are EPMA results in weight percent normalized to 100%.

Table 2. Summary of platinum group minerals from microprobe and SEM analysis of samples from the Cu-PGE (DJ/DB) zone of the Turnagain intrusion.

Sample	Rock type	Sperrylite ($PtAs_2$)	Sudburyite (PdSb)	Other Platinum Group Minerals
DDH04-59-1	Ol (Srp-Mag) clinopyroxenite	X	X	
DDH05-83-1*	clinopyroxenite			Pd-melonite [$(Ni,Pd)Te_2$]
DDH05-88-1*	clinopyroxenite	X	X	PdAgSbTe
DDH05-89-2*	Ol (Srp-Mag) clinopyroxenite		X	ungavaite (Pd_4Sb_3)
DDH05-101-1*	Ol (Srp-Mag) clinopyroxenite	X		
DDH05-101-5*	Cal-Chl vein in clinopyroxenite	X		
DDH05-102-5	clinopyroxenite	X	X	
DDH05-102-7*	clinopyroxenite		X	genkinite? [$(Pt,Pd)_4Sb_3$]
DDH06-149-2*	Ol (Srp-Mag) clinopyroxenite	X		
DDH06-161-1	clinopyroxenite/hornblendite contact	X	X	
DDH06-161-3*	Tr-Tlc altd clinopyroxenite	X	X	testibiopalladite? [PdTe(Sb,Te)]
DDH07-211-4*	hornblendite	X		
DDH07-211-5	clinopyroxenite	X		
DDH07-211-10	clinopyroxenite		X	
DDH07-211-11	Ol (Srp-Mag) clinopyroxenite	X		
DDH07-211-110	Ol (Srp-Mag) clinopyroxenite		X	

*Petrography, SEM, and microprobe analysis completed by Ingrid Kjarsgaard at Carleton University (Ottawa, ON)
Mineral abbreviations: Cal = calcite, Chl = chlorite, Mag = magnetite, Ol = olivine, Srp = serpentine, Tlc = talc, Tr = tremolite

$As_{0.97}S_{1.02}$ (Fig. 5) with some grains containing up to 1.3 wt% Pt and 0.5 wt% Pd. Gersdorffite commonly occurs as subhedral to anhedral grains within chalcopyrite, rarely enclosing nickeline (Fig. 3g,h). Gersdorffite and cobaltite form a solid-solution series with gersdorffite compositions (n=8) ranging from nickel-rich $(Ni_{0.98}Co_{0.02}Fe_{0.02})AsS$ to cobalt-rich $(Co_{0.60}Ni_{0.34}Fe_{0.04})AsS$ (Fig. 5), with no appreciable Pt or Pd. Ullmanite, tucekite, and hauchecornite are only observed in a single chalcopyrite bleb in one sample (DDH07-211-1). Ullmannite is found as submicron to 10 μm grains, whereas tucekite is observed as 20 to 50 μm grains with 1–5 μm thick rims of hauchecornite (Fig. 3h).

Platinum- and palladium-bearing PGM have been identified in samples from the DJ/DB zone. The two dominant phases are sperrylite ($PtAs_2$) and sudburyite (PdSb), with rare occurrences of Pd-melonite [$(Ni,Pd)Te_2$], ungavaite (Pd_4Sb_3), testibiopalladite [PdTe(Sb,Te)], and genkinite [$(Pt,Pd)_4Sb_3$] (Table 2, Appendix F3). All varieties of PGM commonly form equant to lath-shaped grains that range in size from submicron to 40 μm grains (Fig. 6a–f). They are observed included within and along grain boundaries between chalcopyrite, pyrrhotite, cobaltite, magnetite, chlorite, and clinopyroxene. Sperrylite and sudburyite are commonly intergrown with one another, and are more rarely observed as 1 to 10 μm partial rims around chalcopyrite and pyrrhotite (Fig. 6g,h).

Sulphur isotope geochemistry

Sulphur isotopic compositions ($\delta^{34}S$) of sulphide mineral separates span a wide range from -14.1‰ to +4.2‰ VCDT in ultramafic rocks of the DJ/DB zone (n=33) (Fig. 7). These values slightly overlap with hornfels phyllite and distal phyllite that is unaffected by contact metamorphism and are characteristically lighter (-20.1‰ to -11.6‰ VCDT) (Fig. 7). The S-isotope composition of the DJ/DB zone overlaps with 26 sulphur isotope values determined by Scheel (2007) from the Horsetrail zone and wallrock phyllite. Ultramafic rocks in the Turnagain intrusion display values considerably lighter than the range of values that typically characterize mid ocean ridge basalt (MORB) or arc mantle sources (Fig. 7). These light isotopic signatures indicate that significant crustal sulphur was assimilated during emplacement of the ultramafic magma(s). The heavier isotopic values of the hornblende-rich rocks indicate that the late magma pulses that led to the formation of the DJ/DB zone may have experienced lower degrees of crustal contamination during ascent and emplacement.

Figure 6 (opposite page). Backscattered electron (BSE) images of platinum group minerals from the DJ/DB zone. a) Sample DDH07-211-5: sperrylite inclusions in chalcopyrite with minor pyrrhotite. b) Sample DDH06-161-3: sudburyite grain enclosed in pyrrhotite. c) Sample DDH05-88-1: sudburyite on the periphery of a chalcopyrite bleb in contact with clinopyroxene. d) Sample DDH04-59-1: sudburyite and sperrylite grains in chlorite near magnetite. e) Sample DDH07-211-11: sperrylite in secondary chlorite around clinopyroxene. f) Sample DDH05-88-1: satellite grain of sperrylite in clinopyroxene and adjacent to a chalcopyrite bleb. g) Sample DDH05-102-5: sperrylite and sudburyite rims and fracture-controlled veinlets along a composite grain of chalcopyrite and pyrrhotite. h) Sample DDH05-88-1: pyrrhotite bleb with a partial rim and veinlets of sperrylite. Mineral abbreviations as in Figure 3, in addition to: chl = chlorite; mag = magnetite; sd = sudburyite; spy = sperrylite; tr = tremolite.

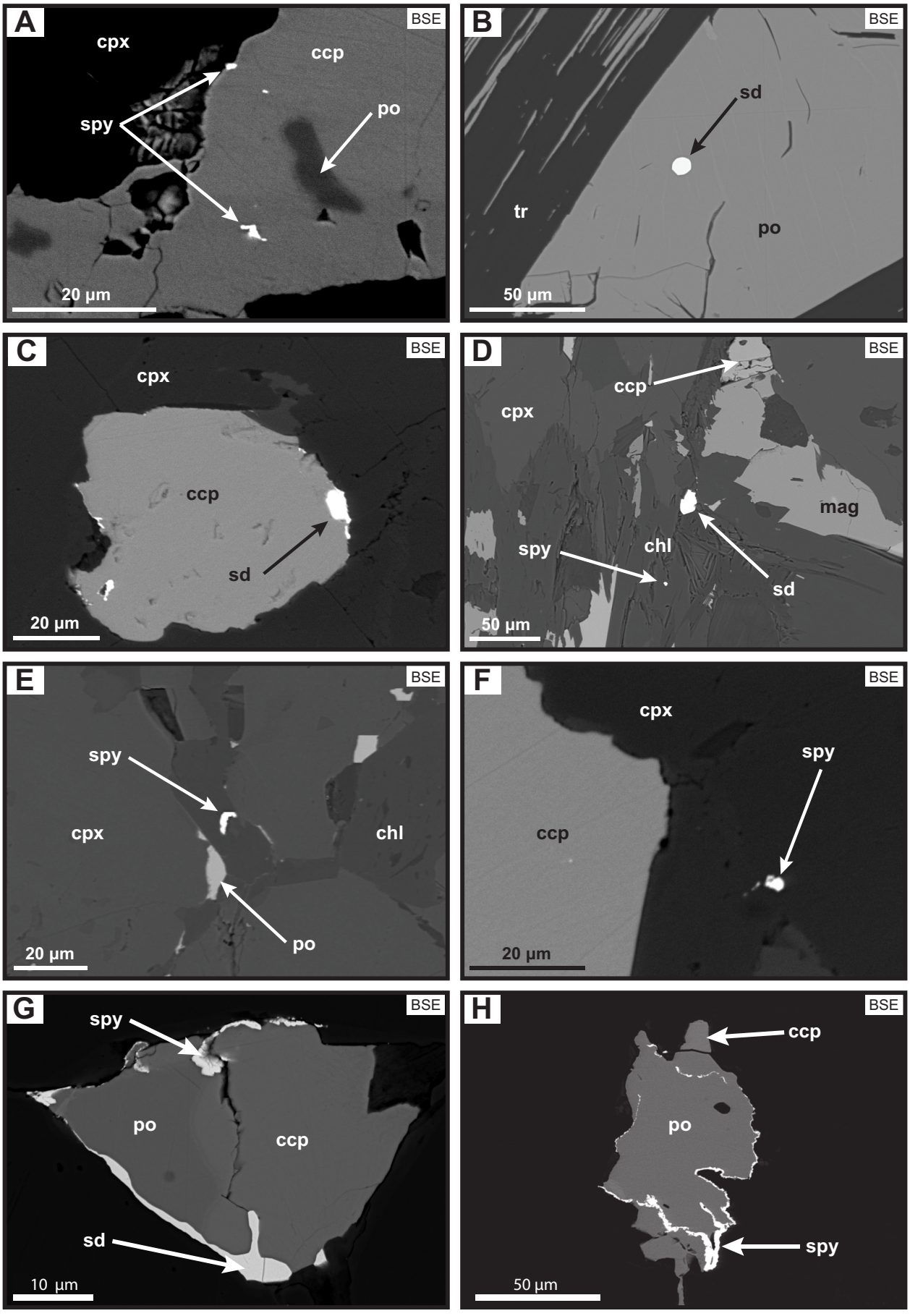
A
BSE
cpx
ccp
spy
po
20 µm
B
BSE
sd
tr
po
50 µm
C
BSE
cpx
ccp
sd
20 µm
D
BSE
ccp
cpx
mag
spy
chl
sd
50 µm
E
BSE
spy
cpx
chl
po
20 µm
F
BSE
cpx
spy
ccp
20 µm
G
BSE
spy
po
ccp
sd
10 µm
H
BSE
ccp
po
spy
50 µm

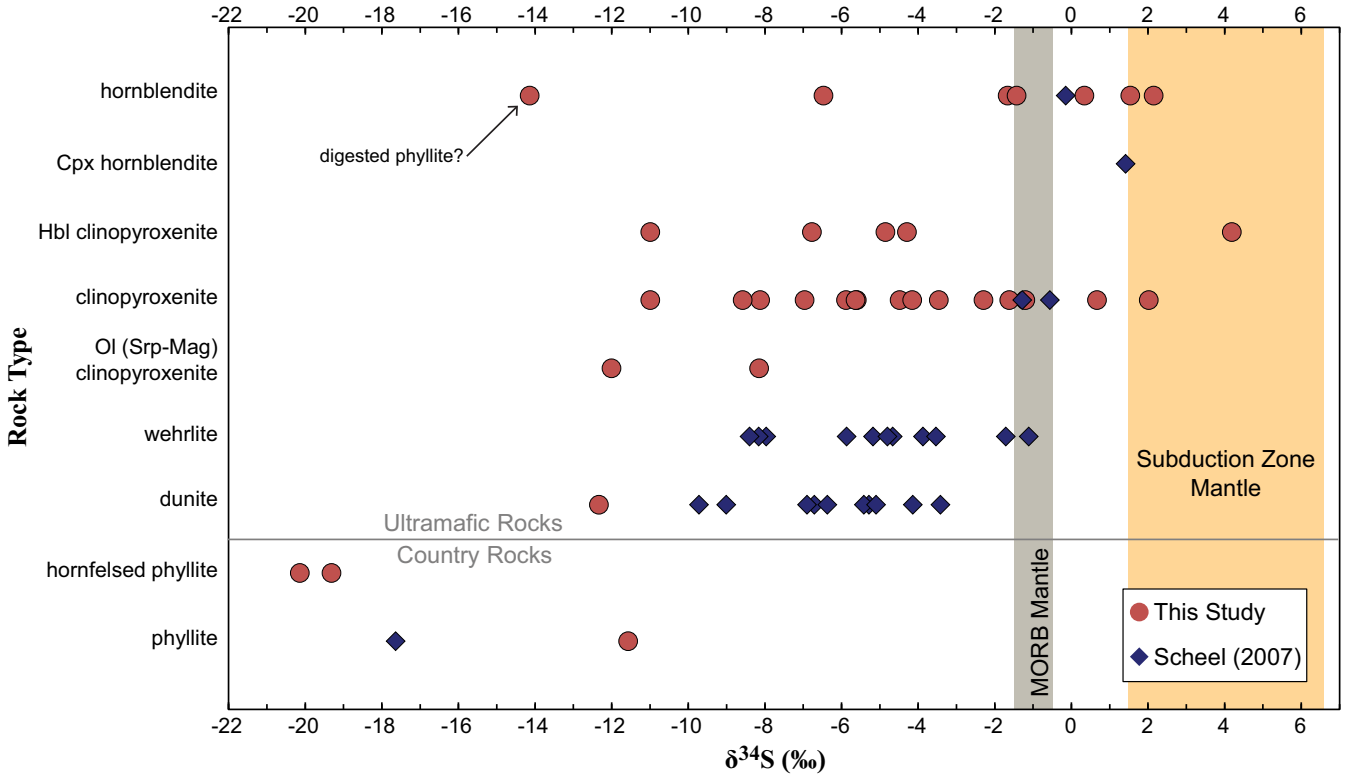

Figure 7. Sulphur isotope compositions of sulphide minerals from sulphide-rich rocks in and adjacent to the DJ/DB zone (this study) and the Horsetrail zone of the Turnagain intrusion (Scheel, 2007). The orange field covers a range of $\delta^{34}S$ compositions from volcanic arcs (compiled by Manor, 2014), which is taken to represent $\delta^{34}S$ values of the mantle wedge (range = +1.4 to +6.5‰). The grey field indicates the initial range of $\delta^{34}S$ compositions (-0.91 ±0.5‰) from mid-ocean ridge basalt (MORB) glass, which represents MORB mantle values (Labidi et al., 2012). Mineral abbreviations: Cpx = clinopyroxenite; Hbl = hornblende; Mag = magnetite; Ol = olivine, Srp = serpentine.

SUMMARY

The host rocks to Cu-PGE mineralization in the DJ/DB zone of the Turnagain intrusion are Phase 3 clinopyroxenite and hornblendite, in contrast to the host dunite and wehrlite (Phase 2) that dominate the Ni-Co resource of the Horsetrail zone. Clinopyroxenite was subdivided into hornblende clinopyroxenite, clinopyroxenite, magnetite clinopyroxenite, and olivine clinopyroxenite. Both major rock types host a variety of base metal sulphides (<53%), arsenic- and antimony-bearing minerals, and platinum group minerals. Base metal sulphides include pyrrhotite, chalcopyrite, and pyrite, with minor pentlandite and trace millerite, sphalerite, bornite, siegenite, marcasite, galena, and molybdenite. Arsenic and antimony phases present are cobaltite, gersdorffite, ullmannite, tucekite, and hauchecornite. Platinum group minerals are either Pt-bearing (sperrylite) or Pd-bearing (sudburyite, with rare occurrences of Pd-melonite, ungavaite, testibiopalladite, and genkinite). Sulphur isotope compositions of sulphides from the DJ/DB zone span a wide range of $\delta^{34}S$ values, and indicate that crustal sulphur from the surrounding phyllite was assimilated by parental magma during emplacement. The TGI-4 databases of geochemistry (whole rock, stable isotope, and platinum group elements) and mineral chemistry (electron microprobe, laser ablation ICP-MS) generated in this study and presented herein will be augmented by geochronology in a forthcoming publication.

ACKNOWLEDGEMENTS

We thank Tony Hitchins and Mark Jarvis of Hard Creek Nickel Corporation for assistance with field work and access to Turnagain materials and data. Thanks to Dr. Mati Raudsepp, Jenny Lai, and Elisabetta Pani of the Electron Microbeam/X-ray Diffraction Facility at UBC for their help and guidance on the SEM. Thanks to Dr. Ingrid Kjarsgaard in Ottawa for additional detailed petrographic descriptions and all EMPA analyses and stoichiometric calculations. Thanks also to Pat Hunt at the GSC, Ottawa, for assistance with SEM mapping of PGM. Thanks to Drs. Zhaoping Yang and Simon Jackson at the GSC for training and use of the GSC LA-ICP-MS Facility in Ottawa, and their invaluable assistance with data collection and reduction. Funding for this project is provided by the Geological Survey of Canada Targeted Geoscience Initiative 4 (TGI-4) Ni-Cu-PGE-Cr project, the Government of Canada Research Affiliate Program, a SEG Canadian Foundation Graduate

Student Research Grant awarded to Sarah Jackson-Brown in 2013, and an NSERC Discovery Grant to Dr. James Scoates.

REFERENCES

Amirault, F. and Burnham, O.M., 2013. Carbon and sulphur analysis in geological samples by combustion–infrared: Verifying method capabilities on new instrumentation, *In:* Summary of Fieldwork and Other Activities 2013; Ontario Geological Survey, Open File Report 6290, p. 43-1 to 43-5.

Clark, T., 1975. Geology of an ultramafic complex on the Turnagain River, northwestern B.C.; Ph.D. thesis, Queens University, Kingston, Ontario, 454 p.

Clark, T., 1980. Petrology of the Turnagain ultramafic complex, northwestern British Columbia; Canadian Journal of Earth Sciences, v. 17, p. 744–757.

Colpron, M. and Nelson, J.L., 2011. A digital atlas of terranes for the Northern Cordillera; British Columbia Ministry of Energy and Mines, British Columbia Geological Survey GeoFile 2011-11.

Deer, W.A., Howie, R.A., and Zussman, J., 1996. An Introduction to the Rock-Forming Minerals, 2nd Edition; Harlow, England, Pearson Education Ltd, 712 p.

Droop, G.T.R., 1987. A general equation for estimating Fe^{3+} concentrations in ferro-magnesian silicates and oxides from microprobe analyses, using stoichiometric criteria; Mineralogical Magazine v. 51, p. 431–435.

Griffin, W.L., Powell, W.J., Pearson, N.J., and O'Reilly, S.Y., 2008. GLITTER: Data reduction software for laser ablation ICP-MS, *In:* Laser Ablation ICP–MS in the Earth Sciences: Current Practices and Outstanding Issues, (ed.) P. Sylvester; Mineralogical Association of Canada, Short Course Series, v. 40, p. 308–311.

Guillong, M., Hametner, K., Reusser, E., Wilson, S.A., and Günther, D., 2005. Preliminary characterization of new glass reference materials (GSA-1G, GSC-1G, GSD-1G and GSE-1G) by laser ablation-inductively coupled plasma-mass spectrometry using 193 nm, 213 nm and 266 nm wavelengths; Geostandards & Geoanalytical Research, v. 29, p. 315–331.

Himmelberg, G.R. and Loney, R.A., 1995. Characteristics and petrogenesis of Alaskan-type ultramafic-mafic intrusions, southeastern Alaska; U.S. Geological Survey, Professional Paper 1564, p. 47.

Irvine, T.N., 1974. Petrology of the Duke Island Ultramafic Complex Southeastern Alaska; Geological Society of America, GSA Memoirs 138, 244 p.

Jackson, S.E., Fryer, B.J., Gosse, W., Healey, D.C., Longerich, H.P., and Strong, D.F., 1990. Determination of the precious metals in geological materials by inductively coupled plasma-mass spectrometry (ICP-MS) with nickel sulphide fire-assay collection and tellurium coprecipitation; Chemical Geology, v. 83, p. 119–132.

Jackson-Brown, S., Scoates, J.S., Nixon, G.T., and Ames, D.E., 2014, Mineralogy of sulphide, arsenide, and platinum group minerals from the DJ/DB Zone of the Turnagain Alaskan-type ultramafic intrusion, north-central British Columbia, *In:* Geological Fieldwork 2013; British Columbia Geological Survey, Paper 2014-1, p. 157–168.

Johan, Z., 2002. Alaskan-type complexes and their platinum-group element mineralization, *In:* Geology, Geochemistry, Mineralogy and Mineral Beneficiation of Platinum-group Elements; Canadian Institute of Mining and Metallurgy, Special Volume 54, p. 669–719.

Labidi, J., Cartigny, P., Birck, J.L., Assayag, N., and Bourrand, J.J., 2012. Determination of multiple sulphur isotopes in glasses: A reappraisal of the MORB $\delta^{34}S$; Chemical Geology, v. 334, p. 189–198.

Lawley, C., Creaser, R.A., Jackson, S.E., Yang, Z., Davis, B., Pehrsson, S., Dubé, B., Mercier-Langevin, P., and Vaillancourt, D., 2015. Unravelling the western Churchill Province Paleoproterozoic gold metallotect: Constraints from Re-Os arsenopyrite and U-Pb xenotime geochronology and LA-ICPMS arsenopyrite trace element chemistry at the BIF-hosted Meliadine Gold District, Nunavut, Canada: Economic Geology, v. 110, p. 1425–1454.

Li, C., Zhang, Z., Li, W., Wang, Y., Sun, T., and Ripley, E.M., 2015. Geochronology, petrology and Hf–S isotope geochemistry of the newly-discovered Xiarihamu magmatic Ni–Cu sulphide deposit in the Qinghai–Tibet plateau, western China; Lithos, v. 216-217, p. 224–240.

Lightfoot, P.C. and Keays, R.R., 2005. Siderophile and chalcophile metal variations in flood basalts from the Siberian trap, Noril'sk region: Implications for the origin of the Ni-Cu-PGE sulphide ores; Economic Geology, v. 100, p. 439–462.

Loney, R.A. and Himmelberg, G.R., 1992. Petrogenesis of the Pd-rich intrusion at Salt Chuck, Prince of Wales Island: An Early Paleozoic Alaskan-type ultramafic body; Canadian Mineralogist, v. 30, p. 1005–1022.

Manor, M.J., 2014. Convergent margin Ni-Cu-PGE deposits: Geology, geochronology, and geochemistry of the Giant Mascot magmatic sulphide deposit, Hope, British Columbia; M.Sc. thesis, University of British Columbia, Vancouver, British Columbia, 387 p.

McDonald, I. and Holwell, D.A., 2011. Geology of the Northern Bushveld Complex and the setting and genesis of the Platreef Ni-Cu-PGE deposit; Reviews in Economic Geology, v. 17, p. 297–327.

Mudd, G.M. and Jowitt, S.M., 2014. A detailed assessment of global Cu reserve and resource trends and worldwide Cu endowments; Economic Geology, v. 109, p. 1813–1841.

Nixon, G.T. and Hammack, J.L., 1991. Metallogeny of ultramafic-mafic rocks in British Columbia with emphasis on the platinum-group elements, *In:* Ore Deposits, Tectonics and Metallogeny in the Canadian Cordillera; British Columbia Geological Survey, Paper 1991-4, p. 125–161.

Nixon, G.T., Hammack, J.L., Ash, C.H., Cabri, L.J., Case, G., Connelly, J.N., Heaman, L., Laflamme, J.H.G., Nuttall, C., Paterson, W.P.E., and Wong, R.H., 1997. Geology and platinum-group-element mineralization of Alaskan-type ultramafic-mafic complexes in British Columbia;: British Columbia Geological Survey, Bulletin 93, 141 p.

Nixon, G.T., Hitchins, A.C., and Ross, G.P., compilers, 2012. Geology of the Turnagain Ultramafic Intrusion, northern British Columbia; British Columbia Geological Survey, Open File 2012-05, map 1:10 000 scale.

Nixon, G.T., Manor, M.J., Jackson-Brown, S., Scoates, J.S., and Ames, D.E., 2015. Magmatic Ni-Cu-PGE deposits at convergent margins, *In:* Targeted Geoscience Initiative 4: Canadian Nickel-Copper-Platinum Group Elements-Chromium Ore Systems - Fertility, Pathfinders, New and Revised Models, (ed.) D.E. Ames and M.G. Houle; Geological Survey of Canada, Open File 7856, p. 17–34.

Piña, R., Gervilla, F., Ortega, L., and Lunar, R., 2008. Mineralogy and geochemistry of platinum-group elements in the Aguablanca Ni-Cu deposit (SW Spain); Mineralogy and Petrology, v. 92, p. 259–282.

Richardson, T. and Burnham, O.M., 2002, Precious metal analysis at the Geoscience Laboratories: Results from the new low-level analytical facility In: Summary of Fieldwork and Other Activities 2013; Ontario Geological Survey, Open File Report 6100, p. 35-1 to 35-5.

Riles, A., Molavi, M., Simpson, R., Fong, B., Reid, J., McTavish, G., and Friedman, D., 2011. Turnagain project Hard Creek Nickel Corporation, preliminary economic assessment, 151 p.

Ripley, E.M., 2010. A new perspective on exploration for magmatic sulphide-rich Ni-Cu-(PGE) deposits, Chapter 24 *In:* The Challenge of Finding New Mineral Resources: Global Metallogeny, Innovative Exploration, and New Discoveries: Volume II Zinc-Lead, Nickel-Copper-PGE, and Uranium, (ed.) R.J. Goldfarb, E.E. Marsh, and T. Monecke; Society of Economic Geologists, Special Publication 15, p. 437–450.

Scheel, J.E., 2007. Age and origin of the Turnagain Alaskan-type intrusion and associated Ni-sulphide mineralization, North-Central British Columbia, Canada; M.Sc. thesis, University of British Columbia, Vancouver, British Columbia, 210 p.

Scheel, J.E., Nixon, G.T., and Scoates, J.S., 2005. New observations on the geology of the Turnagain Alaskan-Type ultramafic intrusive suite and associated Ni-Cu-PGE mineralization, British Columbia, *In:* Geological Fieldwork 2004; British Columbia Geological Survey, Paper 2005-1, p. 167–176.

Shazali, I., Van't Dack, L., and Gijbels, R., 1987. Determination of precious metals in ores and rocks by thermal neutron activation spectrometry after preconcentration by nickel sulphide fire assay and coprecipitation with tellurium; Analytica Chimica Acta, v. 196, p. 49–58.

Thakurta, J., Ripley, E.M., and Li, C., 2014. Platinum group element geochemistry of sulphide-rich horizons in the Ural-Alaskan-type ultramafic complex of Duke Island, southeastern Alaska; Economic Geology, v. 109, p. 643–659.

Wilson, S.A., Ridley, W.I., and Koenig, A.E., 2002. Development of sulfide calibration standards for the laser ablation inductively-coupled plasma mass spectrometry technique; Journal of Analytical Atomic Spectrometry, v. 17, p. 406–409.

Zientek, M.L. and Parks, H.L., 2014. A geologic and mineral exploration spatial database for the Stillwater Complex, Montana; U.S. Geological Survey, Scientific Investigations Report 2014-5183, 28 p.

Appendix C. Visual logs and assay results for sampled drillholes from the DJ/DB zone

Appendix C contains downhole cross-sections for all sampled drillholes. Location information indicates the location of each drillhole collar (NAD83 UTM Zone 9). Sections were cut parallel to the downhole orientation of the hole. The geology down each drillhole is represented by a colour-coded centerline. Each side of the trace shows a histogram and colour-coded assay values for copper (left) and combined platinum + palladium (right) concentrations from assay data provided by Hard Creek Nickel Corporation. Samples are indicated on the right-hand side of the drillhole trace, with a line leading to the sample location. The thickness of the histogram bars is representative of downhole assay sample lengths. Abbreviations: Az = azimuth of the drillhole, Dip = dip of the drillhole at the collar, EOH = end of hole (in metres). Mineral abbreviations: ep = epidote, fsp = feldspar, hbl = hornblende.

Representative orientation data are plotted on drillhole traces for measured fabrics: oriented hornblende (green, W=weak, M=moderate, S=strong), magnetite banding (B=blebby, C=continuous), sulphide banding (D=discontinuous band; L=coherent band), and bedding in phyllite.

Appendix C continued.

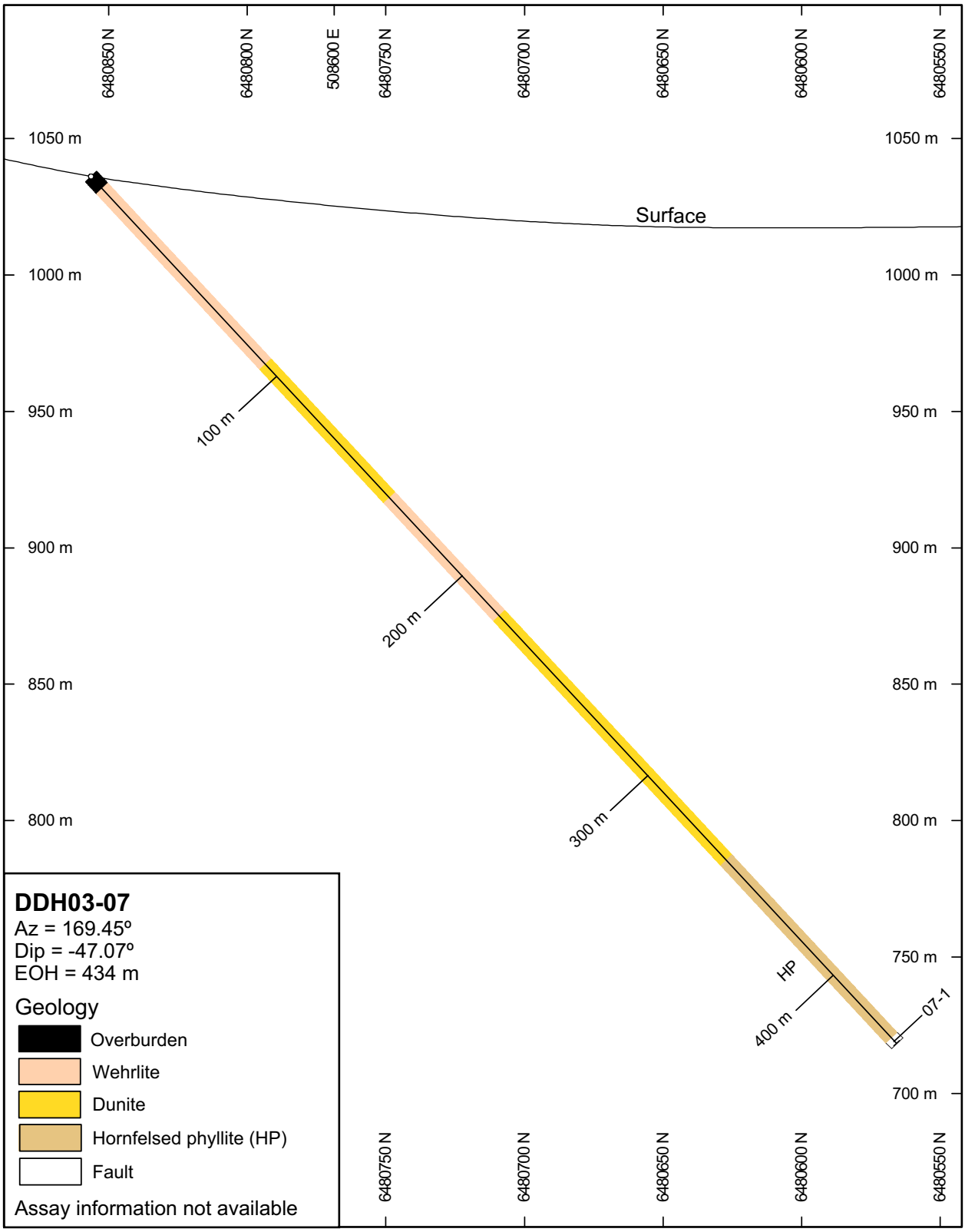

Appendix C continued.

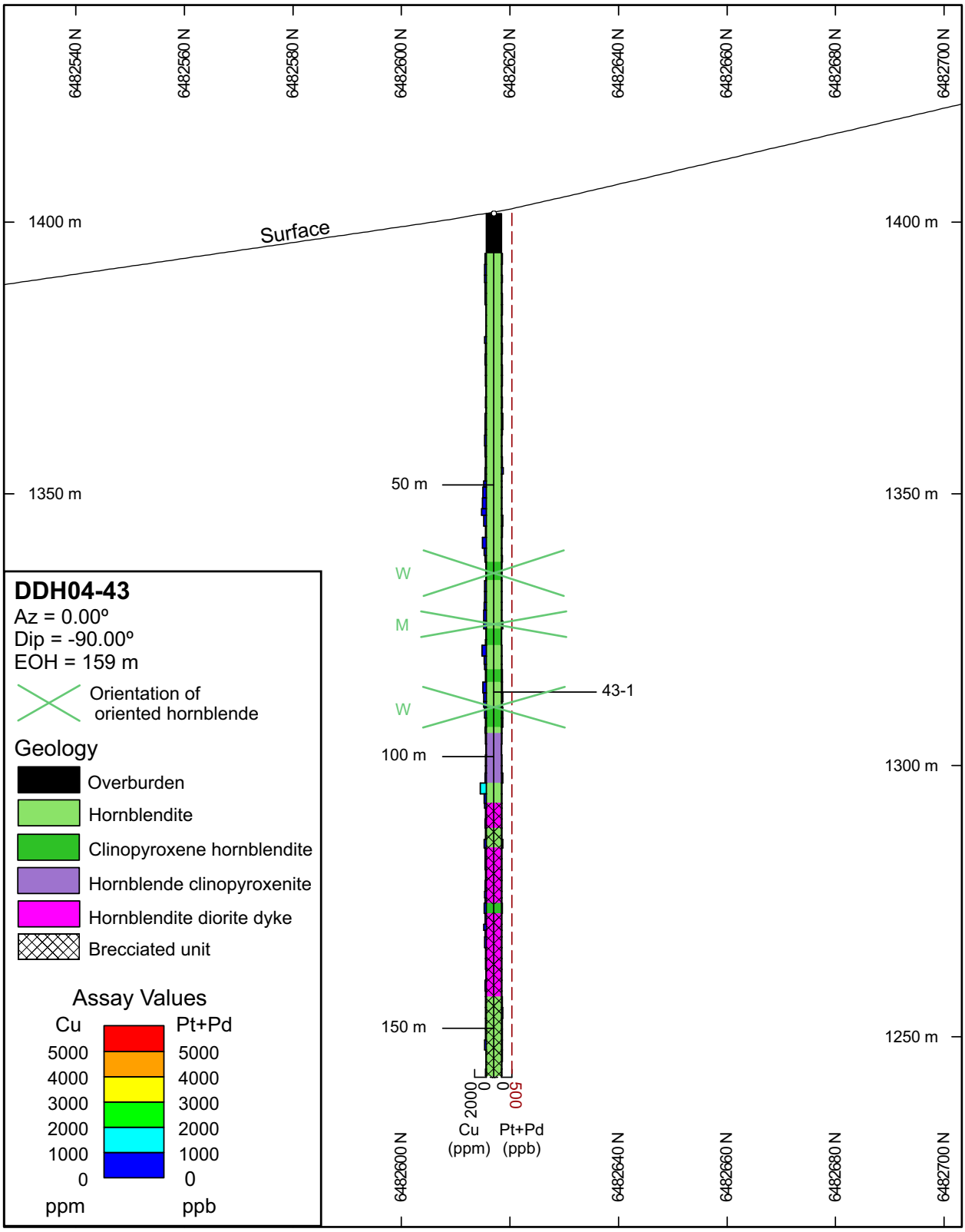

Appendix C continued.

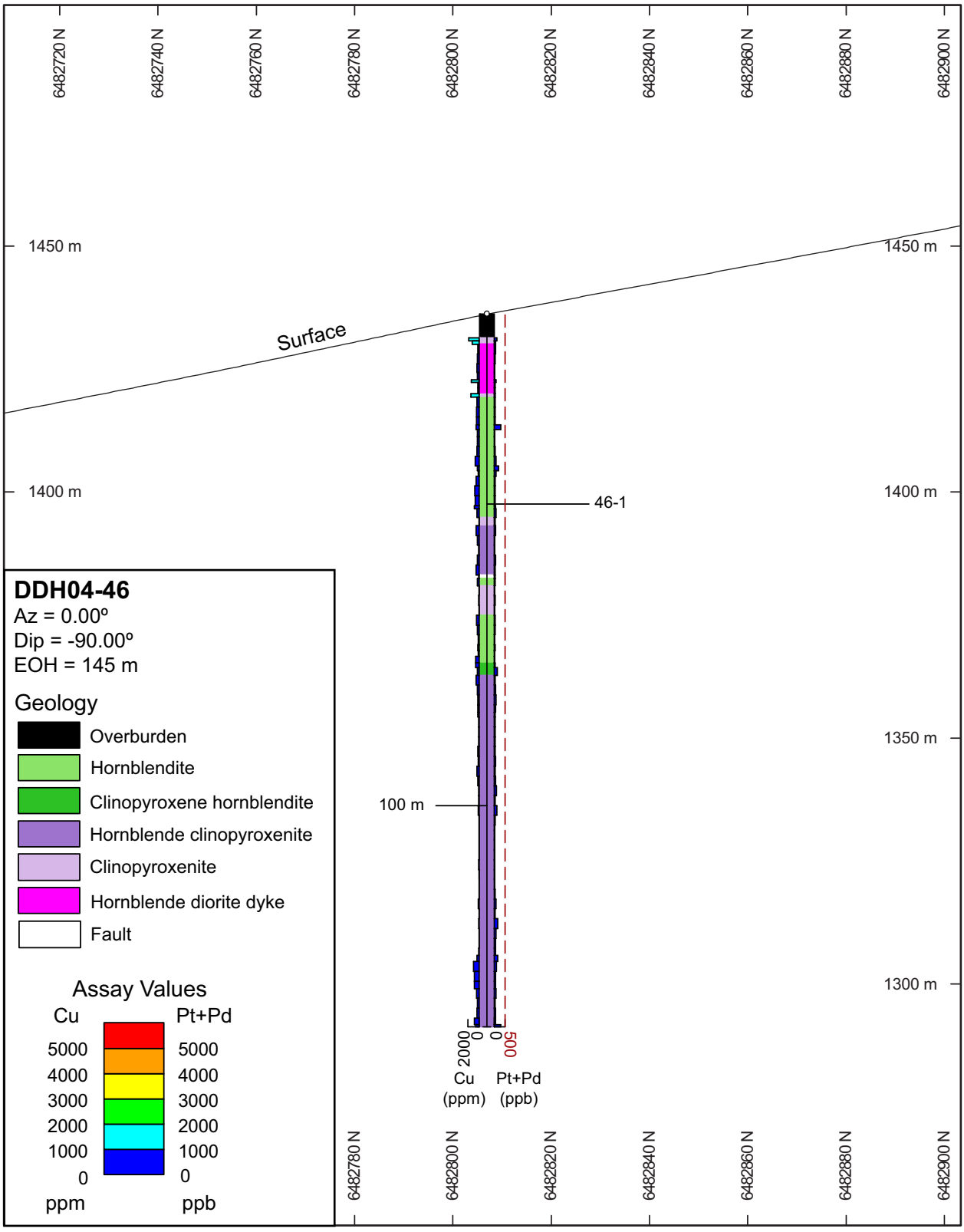

Appendix C continued.

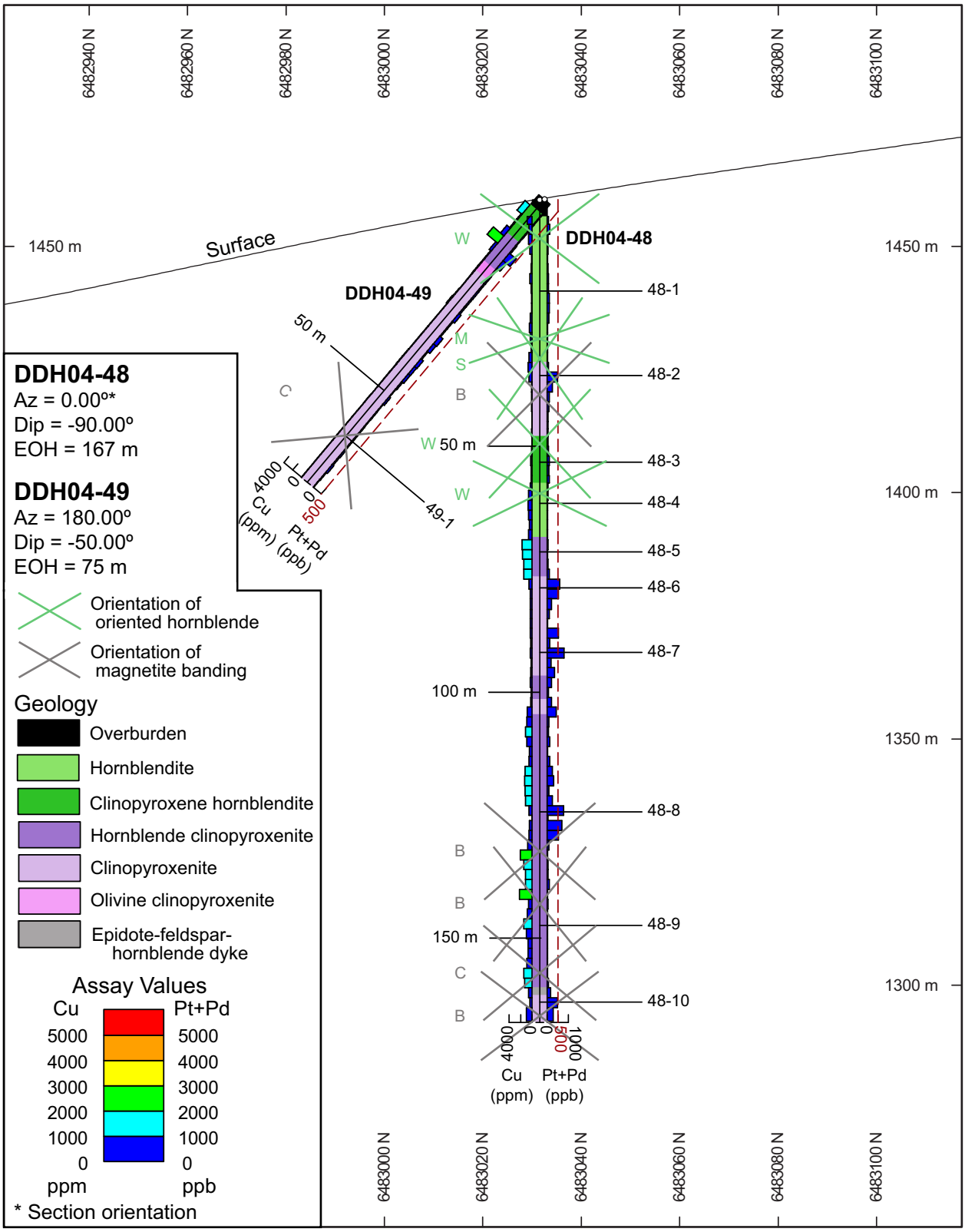

Appendix C continued.

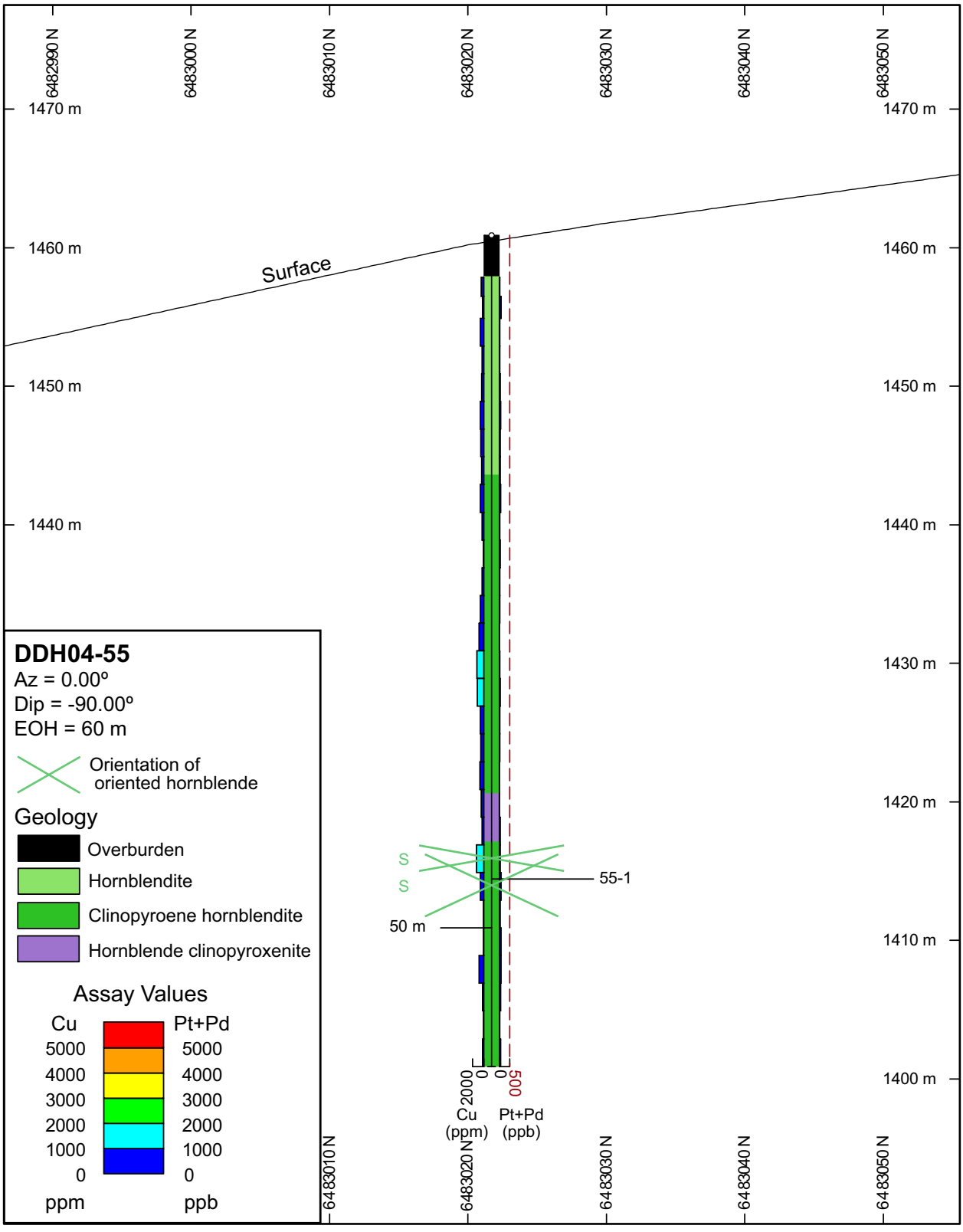

Appendix C continued.

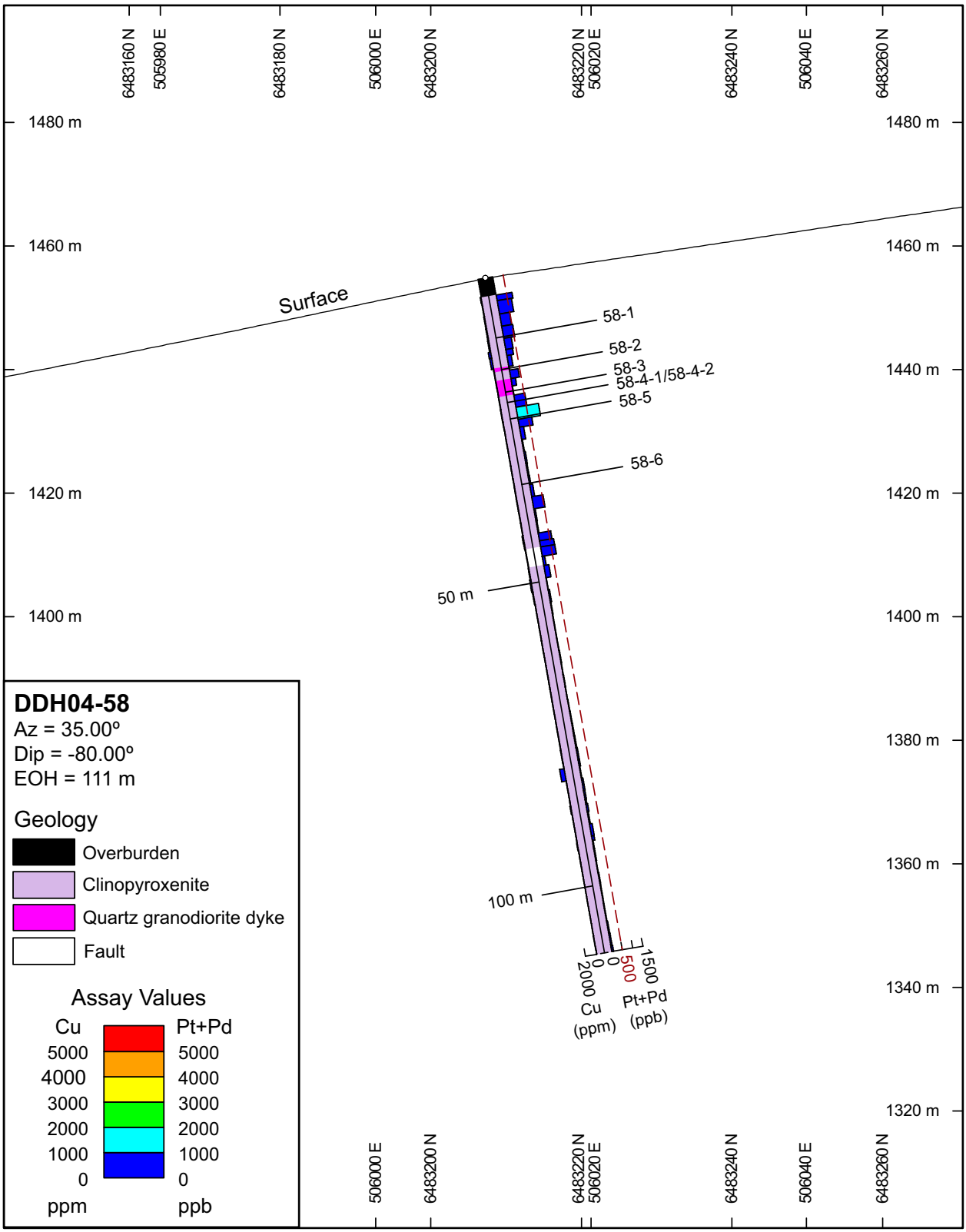

Appendix C continued.

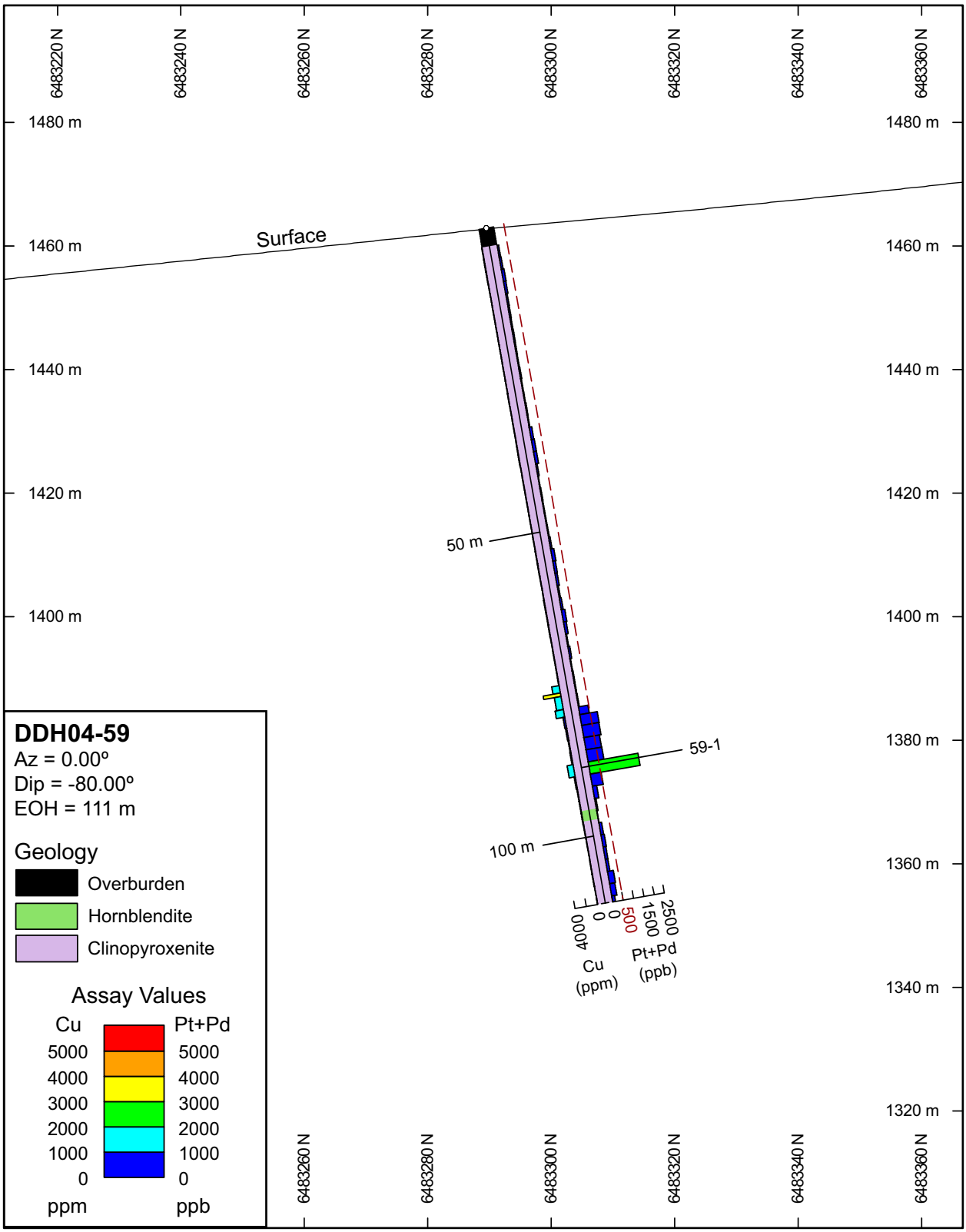

Appendix C continued.

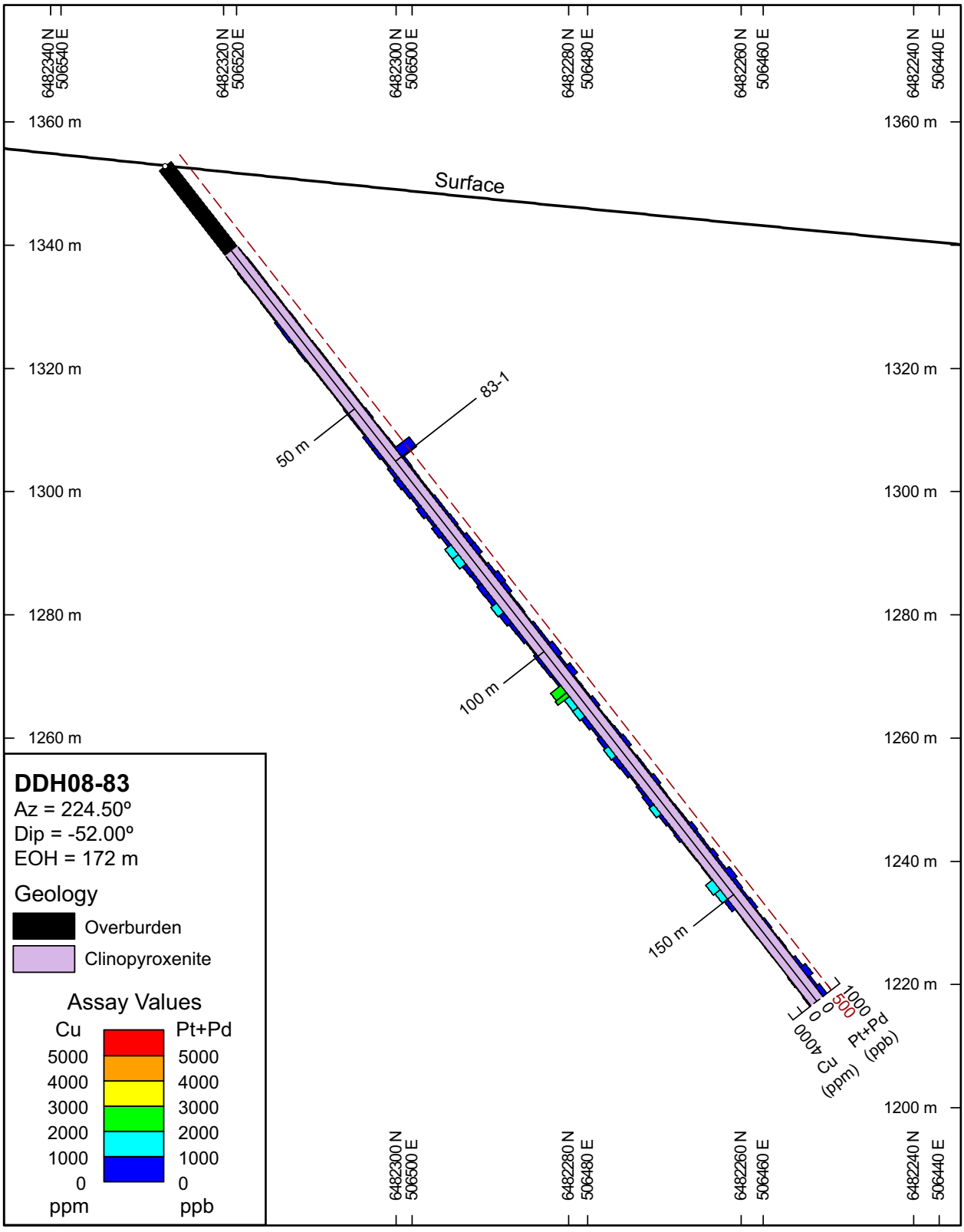

Appendix C continued.

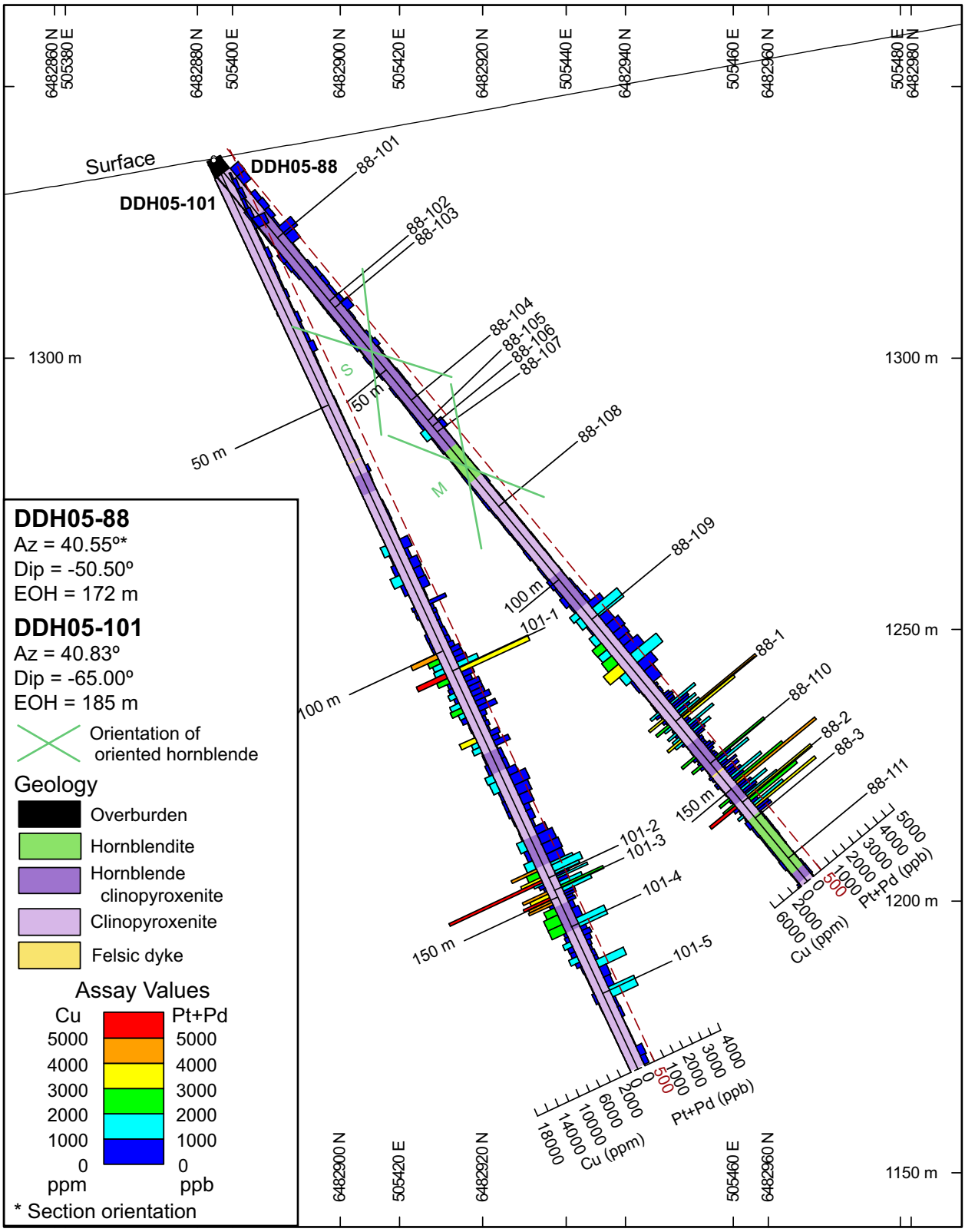

Appendix C continued.

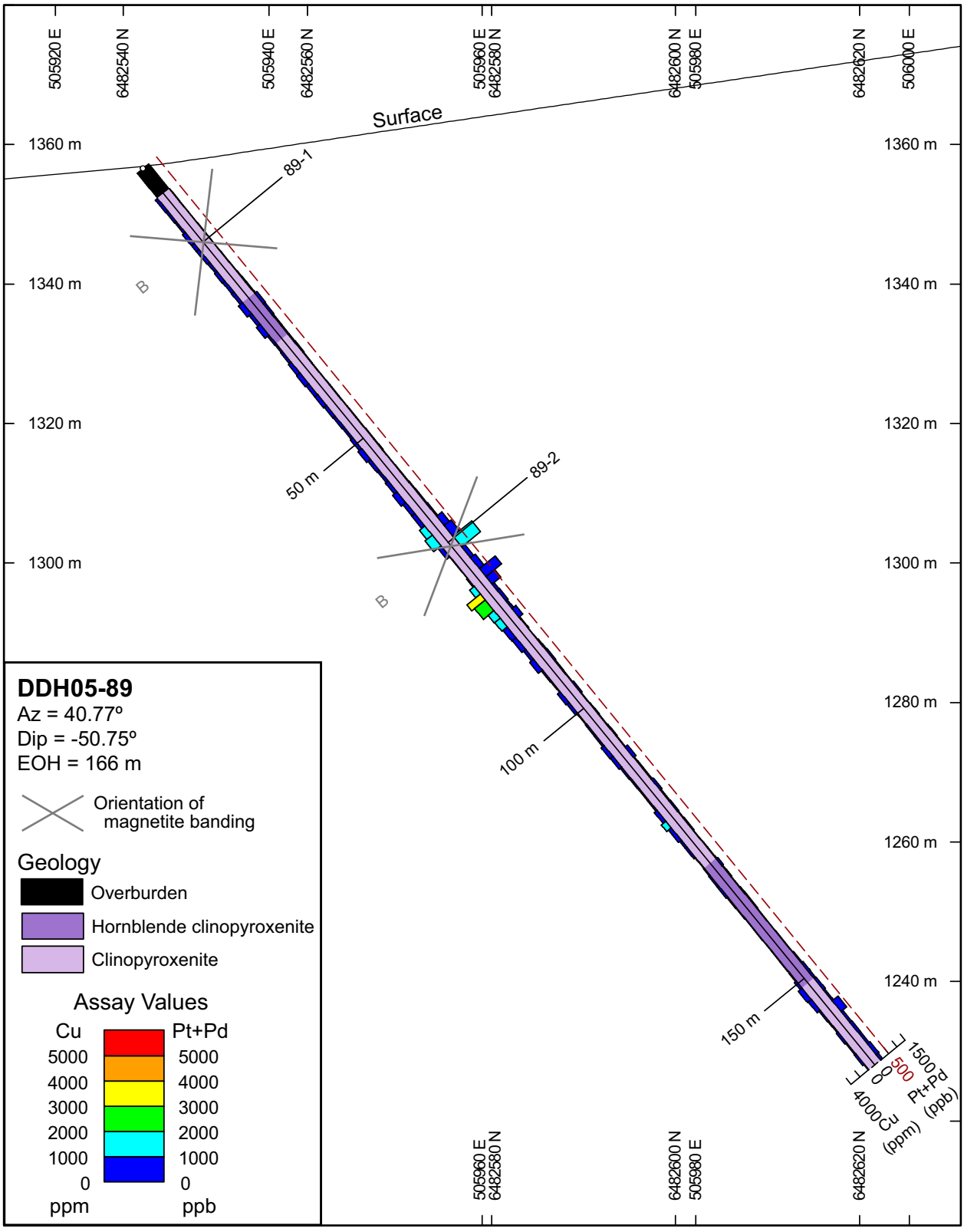

Appendix C continued.

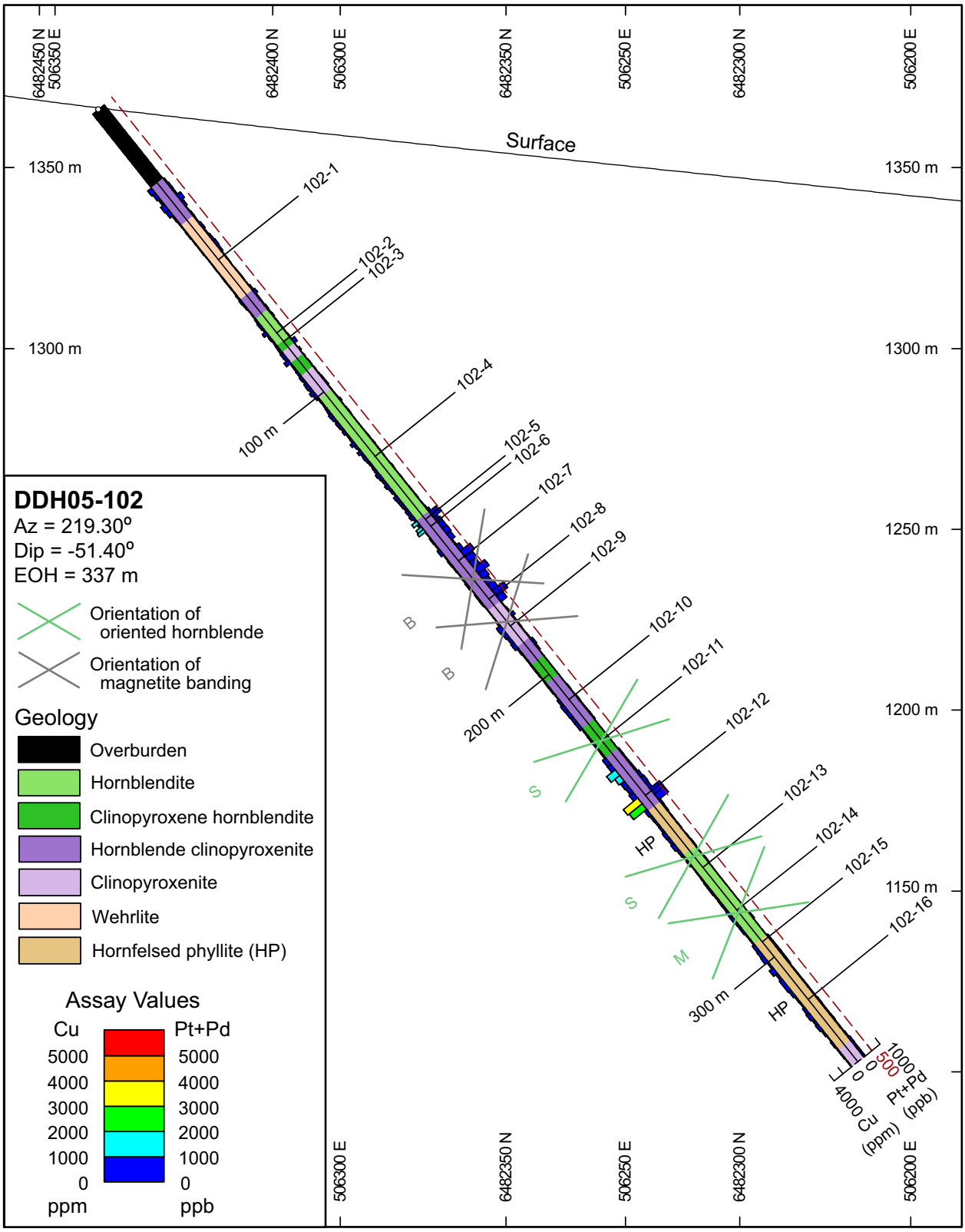

Appendix C continued.

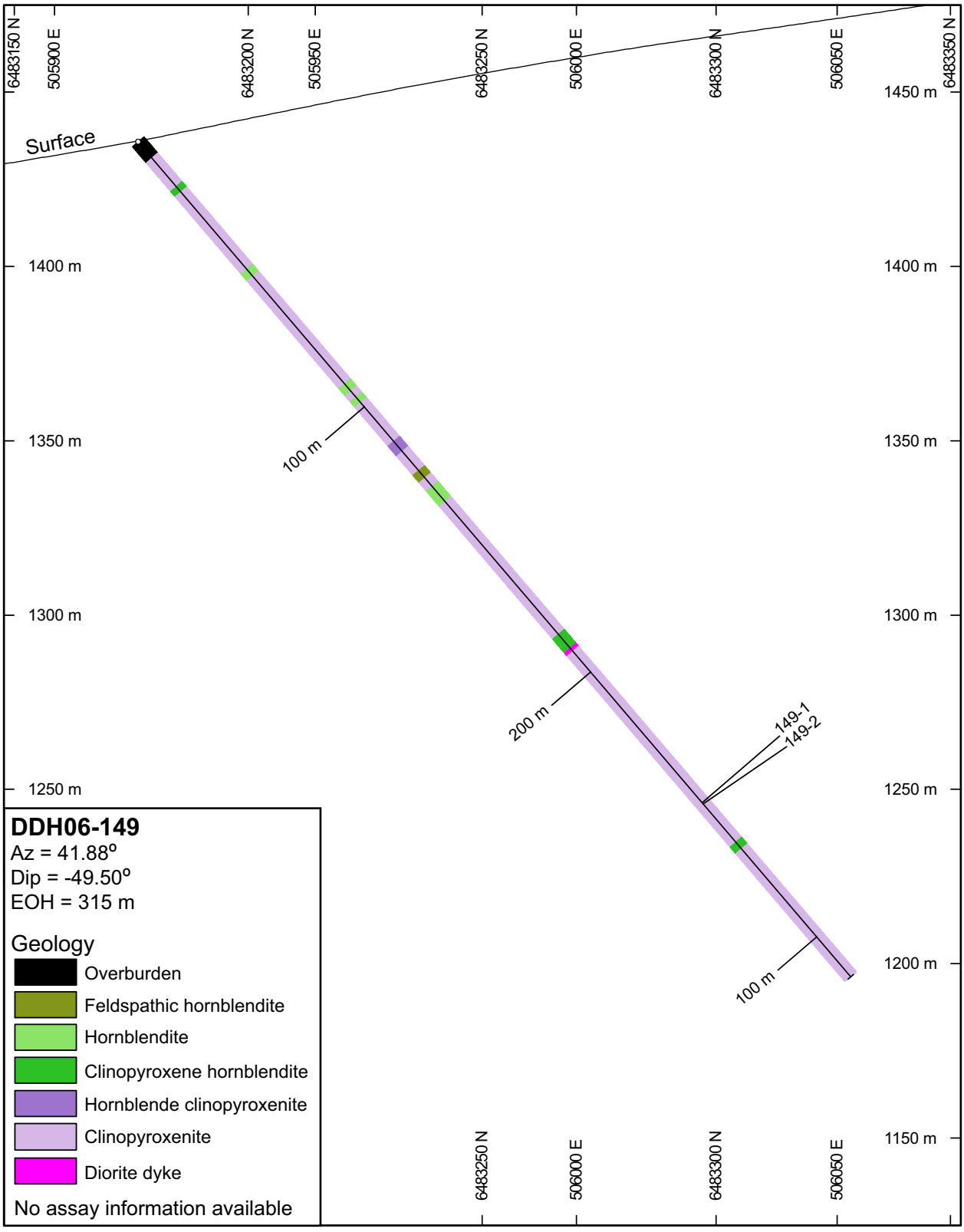

Appendix C continued.

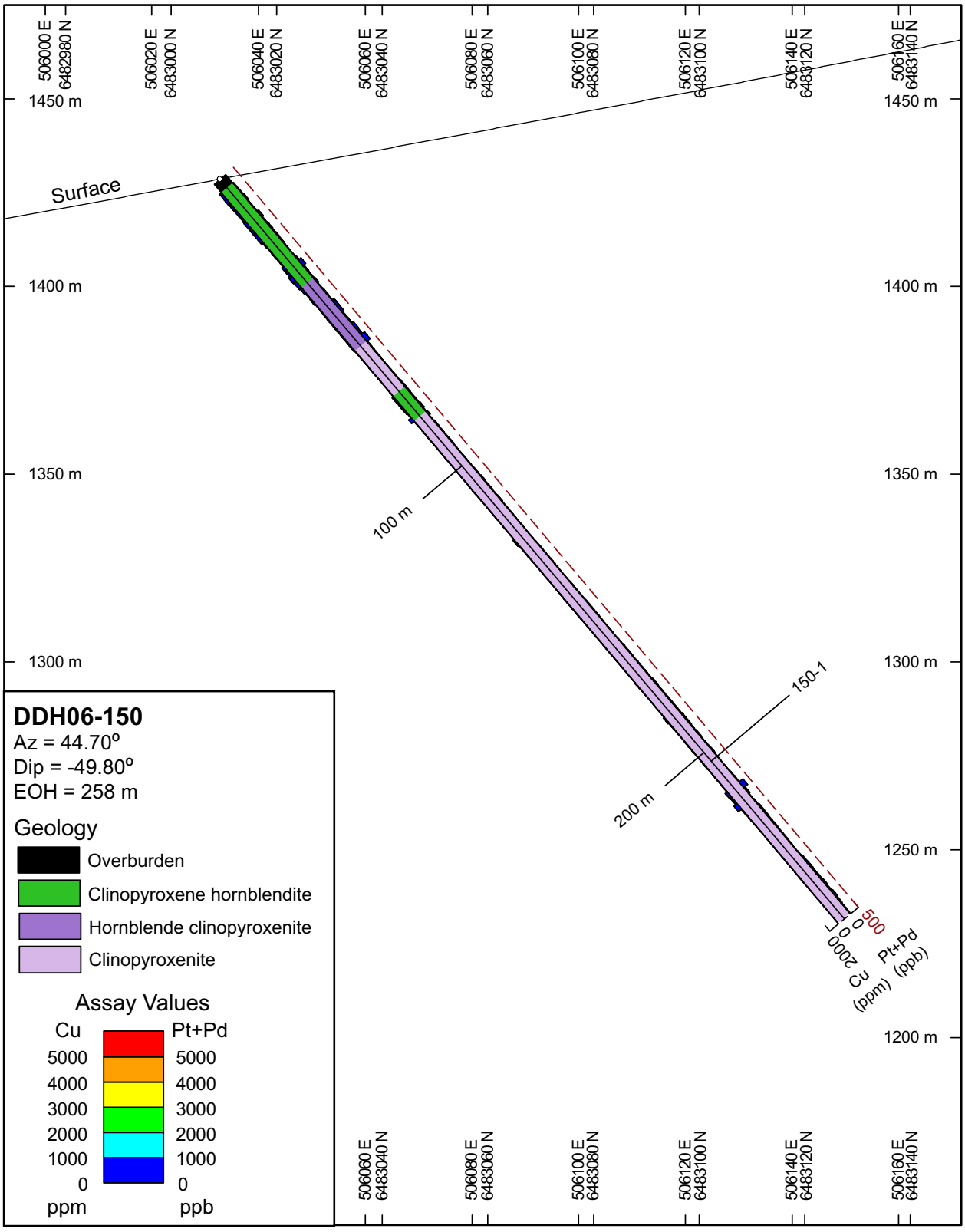

Appendix C continued.

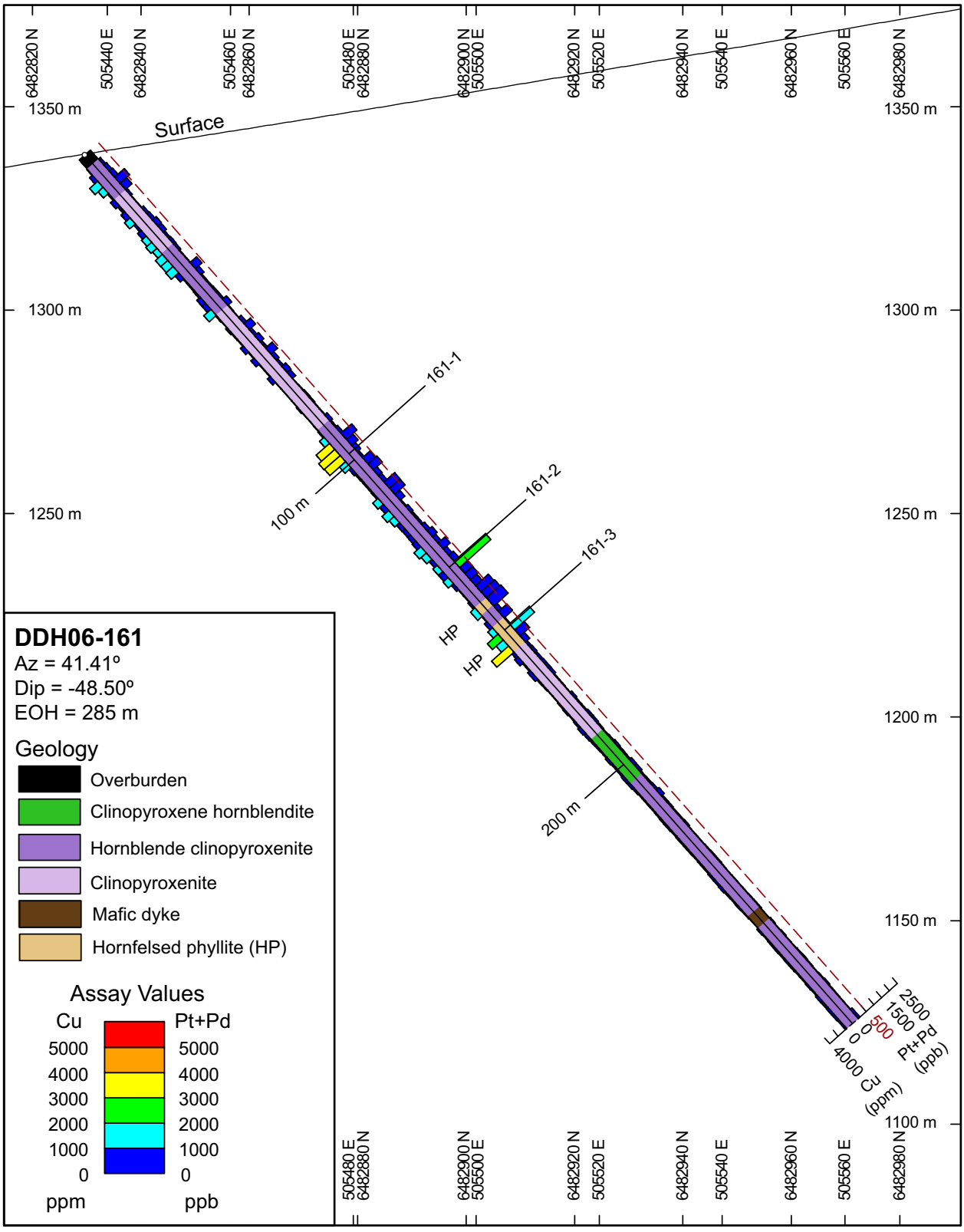

Appendix C continued.

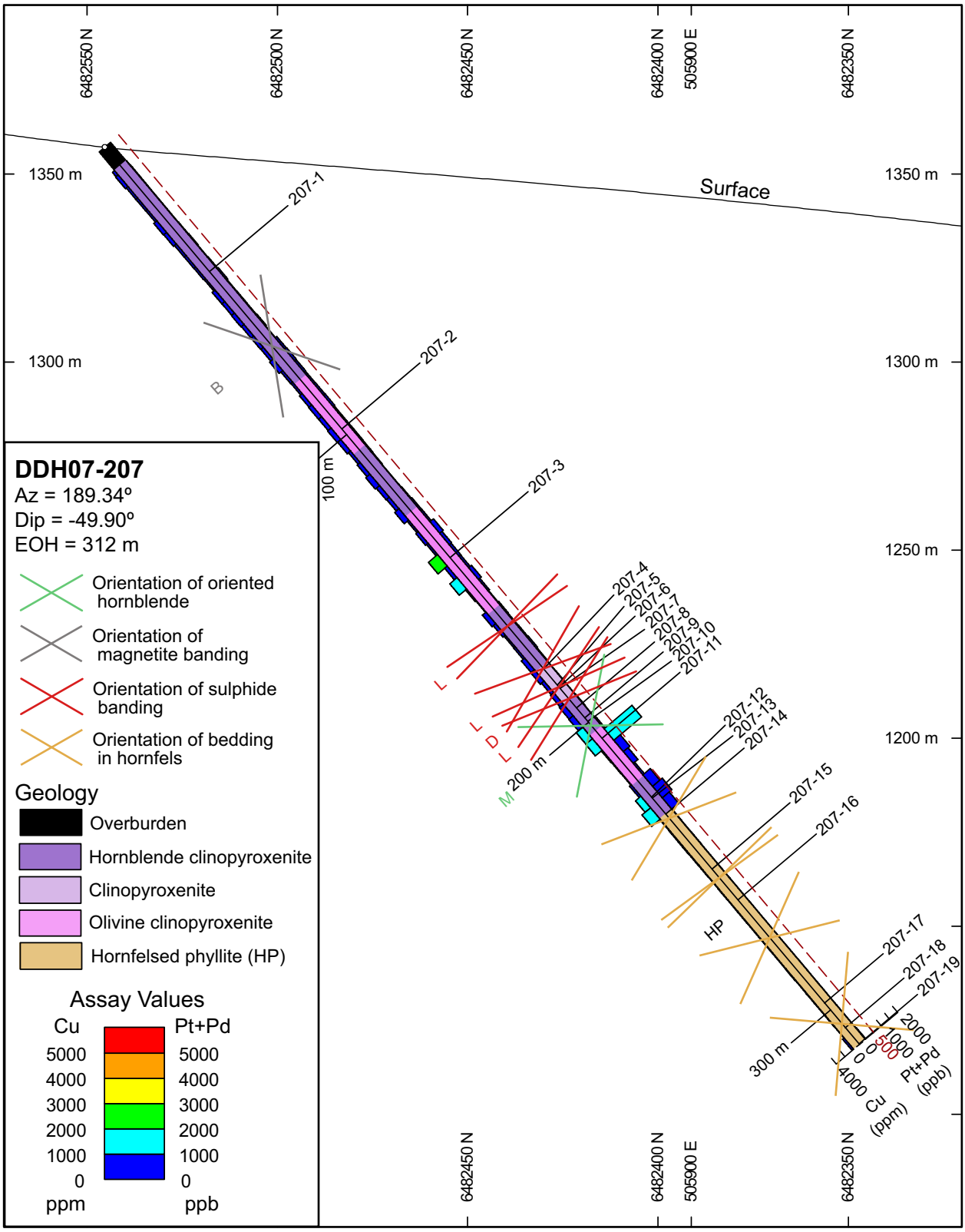

Appendix C continued.

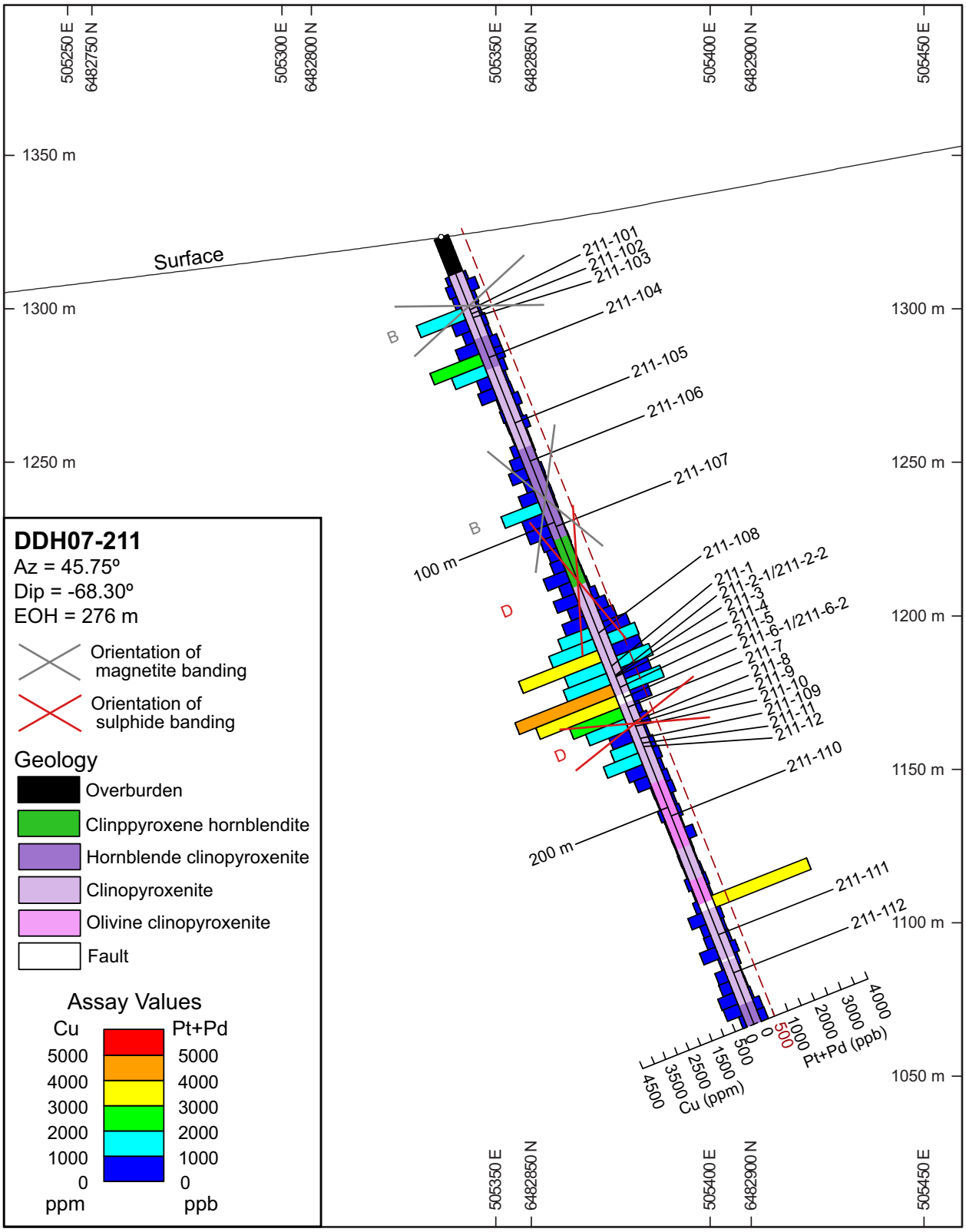

Appendix D. Photographs of drillcore and surface samples from the DJ/DB zone

Appendix D contains photographs of all samples from the DJ/DB zone, with drill collar or surface sample location (NAD83 UTM Zone 9), rock type, depth of sample (for drillcore samples), and sulphide mineralization texture. All photographs include a centimetre scale card (black band = 1 cm).

Drillhole: DDH03-07

508583.3 mE 6480856 mN, Elev: 1036.14 m

DDH03-07-1: Talc-carbonate-altered phyllite
Depth: 432.80 mv
Mineralization texture: Disseminated

Drillhole: DDH04-43

506826.2 mE 6872617 mN, Elev: 14012.58 m

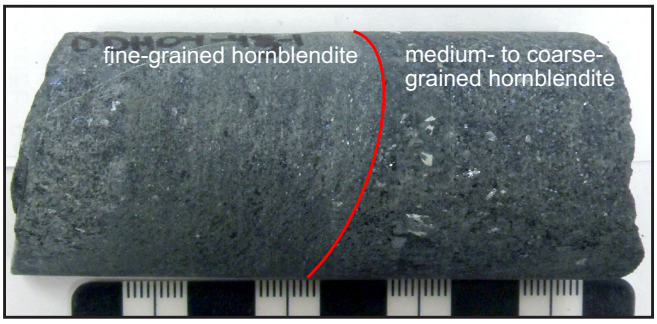

DDH04-43-1: Fine-grauned hornblendite contacting medium- to coarse-grained hornblendite
Depth: 88.10 m
Mineralization texture: Disseminated-Blebby

Drillhole: DDH04-46

506468.9 mE 6482807 mN, Elev: 1436.26 m

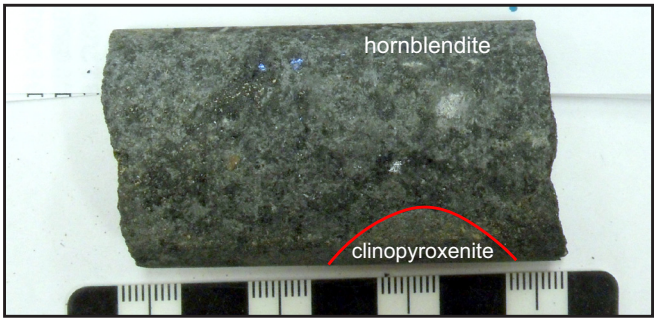

DDH04-46-1: Hornblendite with clinopyroxenite clast
Depth: 38.70 m
Mineralization texture: Disseminated

Appendix D continued.

Diamond drillhole: DDH04-48

506254.4 mE 6483032 mN, Elev: 1459.44 m

DDH04-48-1: Hornblendite
Depth: 18.50 m
Mineralization texture: Disseminated-Net textured

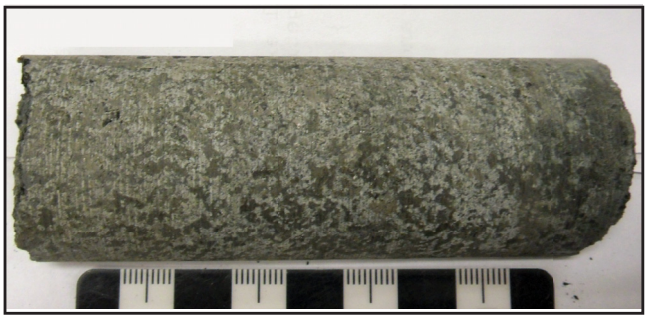

DDH04-48-2: Magnetite clinopyroxenite
Depth: 35.70 m
Mineralization texture: Disseminated

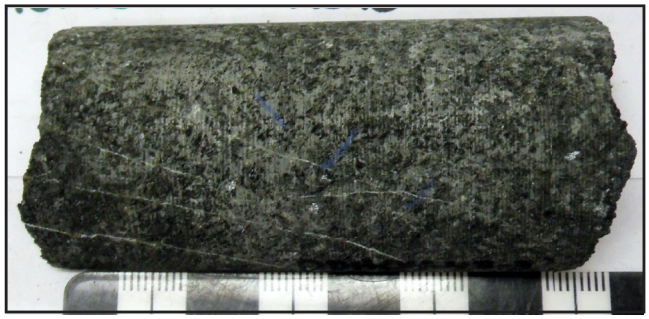

DDH04-48-3: Clinopyroxene hornblendite
Depth: 53.30 m
Mineralization texture: Disseminated

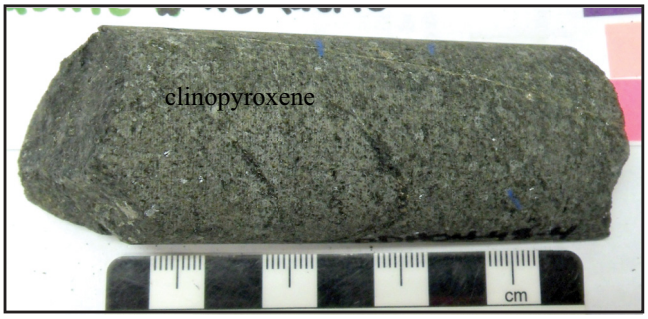

DDH04-48-4: Hornblendite
Depth: 61.63 m
Mineralization texture: Disseminated

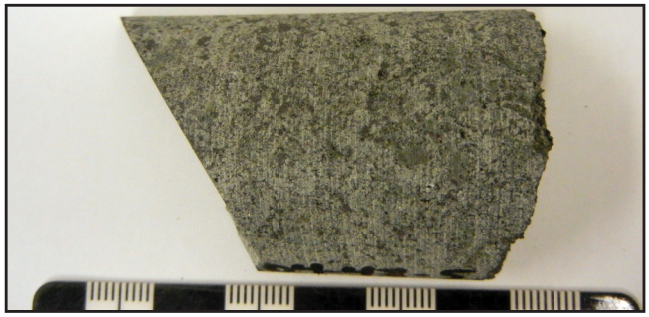

DDH04-48-5: Magnetite clinopyroxenite
Depth: 71.50 m
Mineralization texture: Disseminated

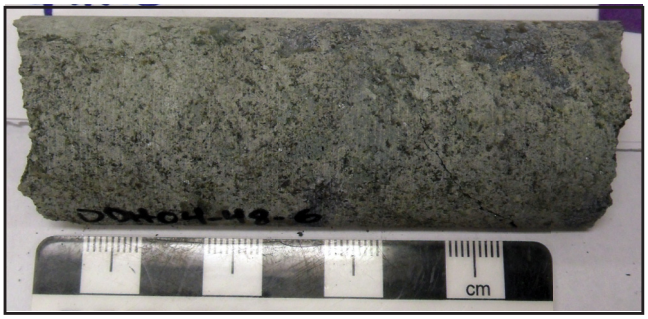

DDH04-48-6: Olivine (serpentine-magnetite) clinopyroxenite
Depth: 78.75 m
Mineralization texture: Disseminated

DDH04-48-7: Olivine (serpentine-magnetite) clinopyroxenite
Depth: 91.90 m
Mineralization texture: Disseminated

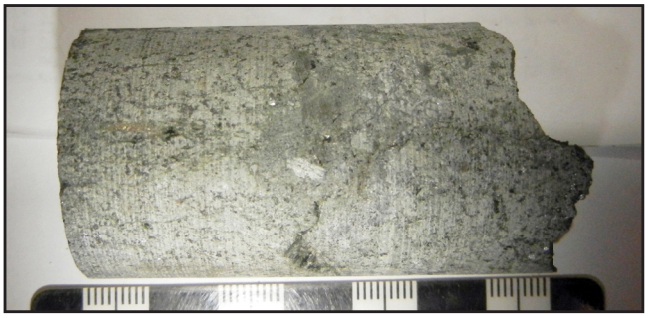

DDH04-48-8: Olivine (serpentine-magnetite) clinopyroxenite
Depth: 124.30 m
Mineralization texture: Disseminated

Appendix D continued.

Drillhole: DDH04-48

506254.4 mE 6483032 mN, Elev: 1459.44 m

DDH04-48-9: Banded magnetite clinopyroxenite contacting coarse-grained magnetite clinopyroxenite
Depth: 147.30 m
Mineralization texture: Disseminated

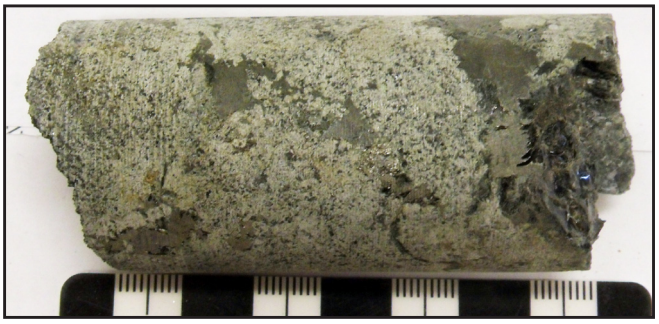

DDH04-48-10: Biotite clinopyroxenite
Depth: 162.92 m
Mineralization texture: Disseminated

Drillhole: DDH04-49

506254.4 mE 6483033 mN, Elev: 1459.44 m

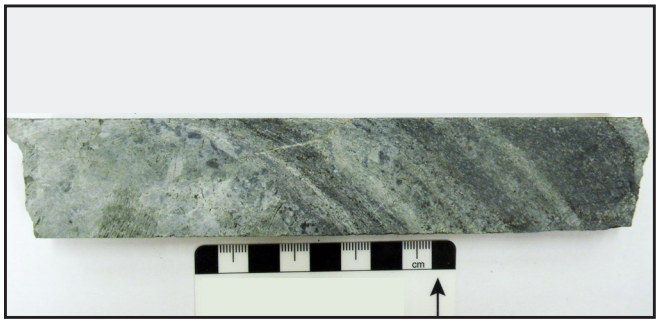

DDH04-49-1: Well banded magnetite clinopyroxenite
Depth: 62.85 m
Mineralization texture: Barren

Drillhole: DDH04-55

506280.9 mE 6483022 mN, Elev: 1462.38 m

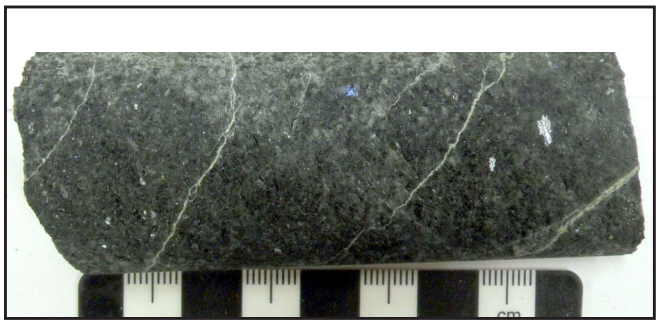

DDH04-55-1: Hornblendite with carbonate veins
Depth: 46.46 m
Mineralization texture: Disseminated

Appendix D continued.

Drillhole: DDH04-58

506010.3 mE 6483207 mN, Elev: 1454.88 m

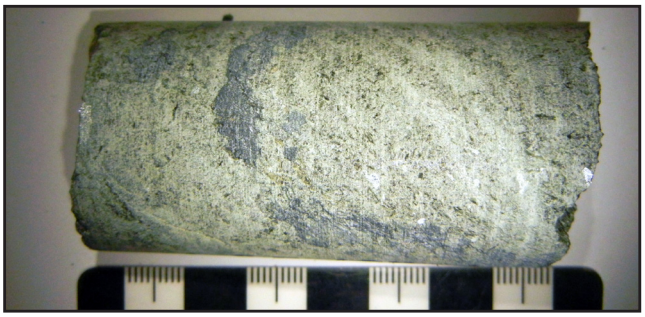

DDH04-58-1: Olivine (serpentine-magnetite) clinopyroxenite
Depth: 9.90 m
Mineralization texture: Disseminated

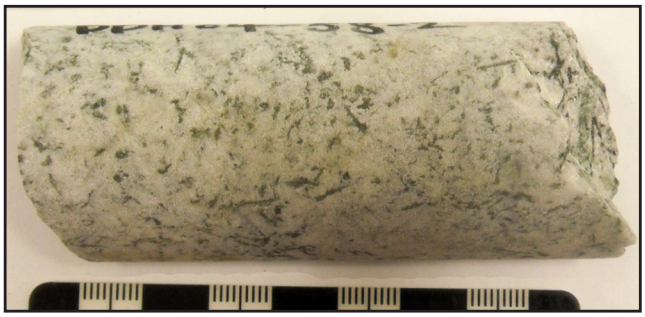

DDH04-58-2: Diorite
Depth: 15.10 m
Mineralization texture: Barren

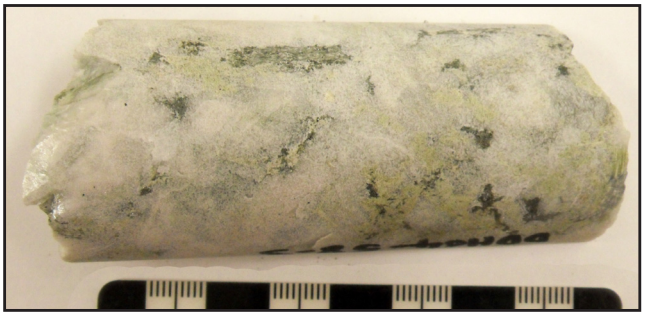

DDH04-58-3: Carbonate-sericite-altered diorite
Depth: 18.80 m
Mineralization texture: Barren

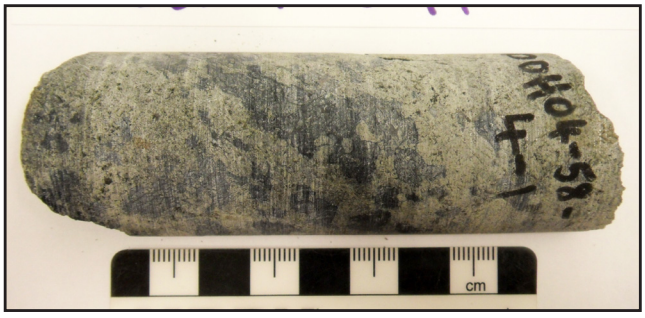

DDH04-58-4-1: Olivine (serpentine-magnetite) clinopyroxenite
Depth: 20.50 m
Mineralization texture: Barren

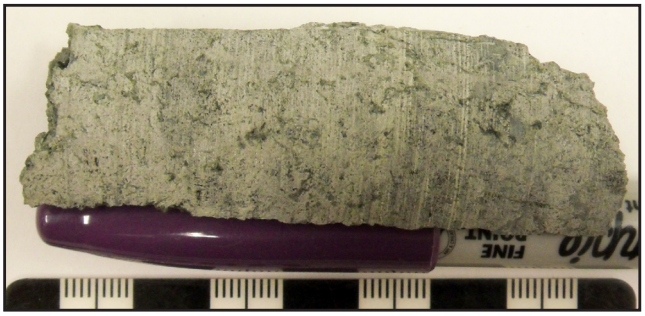

DDH04-58-4-2: Clinopyroxenite
Depth: 20.50 m
Mineralization texture: Barren

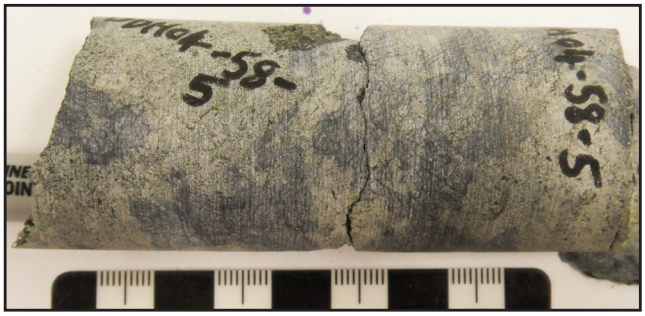

DDH04-58-5: Olivine (serpentine-magnetite) clinopyroxenite
Depth: 23.20 m
Mineralization texture: Disseminated

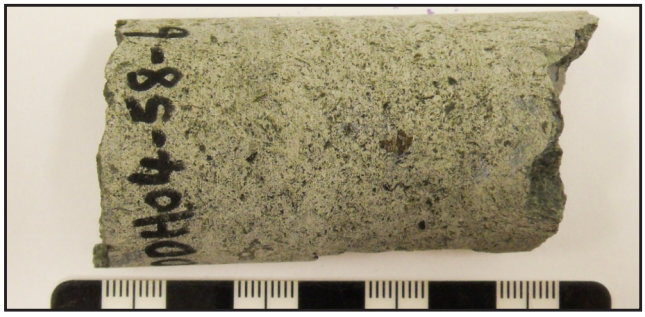

DDH04-58-6: Clinopyroxenite
Depth: 34.00 m
Mineralization texture: Barren

Appendix D continued.

Drillhole: DDH04-59

506006.9 mE 6483289 mN, Elev: 1462.93 m

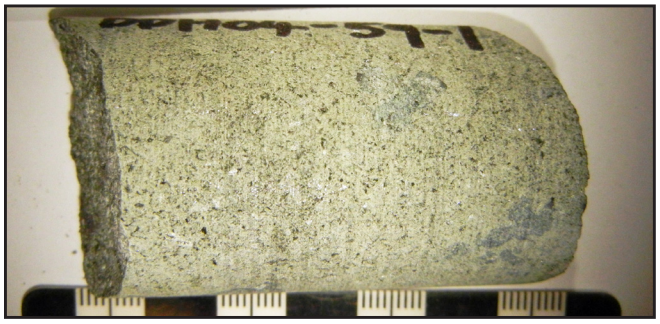

DDH04-59-1: Olivine (serpentine-magnetite) clinopyroxenite
Depth: 88.70 m
Mineralization texture: Disseminated

Drillhole: DDH05-83

506528.9 mE 6482326 mN, Elev: 1352.83 m

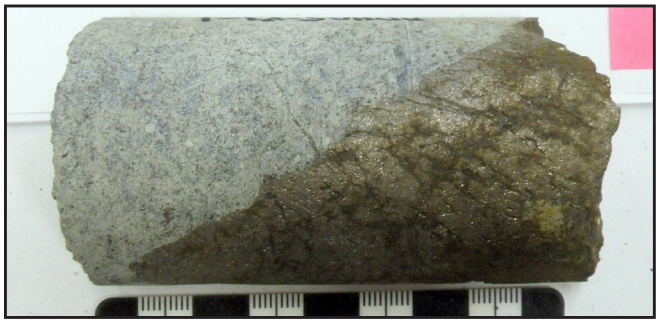

DDH04-83-1: Clinopyroxenite
Depth: 60.80 m
MineralizationTexture: Disseminated-Massive

Drillhole: DDH05-88

505395.5 mE 6482884 mN, Elev: 1336.88 m

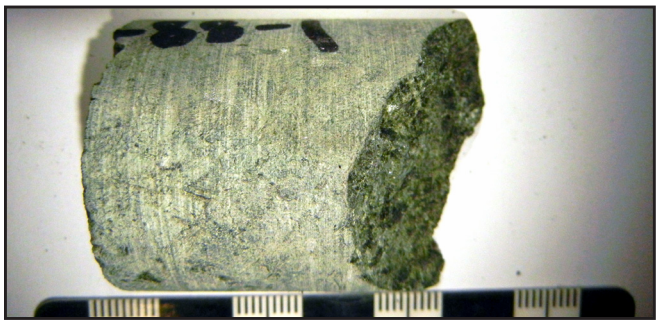

DDH05-88-1: Magnetite clinopyroxenite
Depth: 133.80 m
Mineralization texture: Disseminated

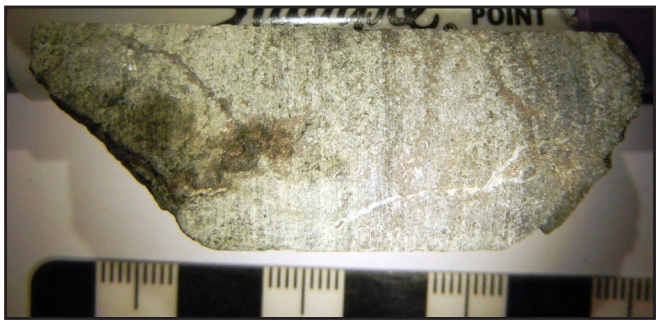

DDH05-88-2: Clinopyroxenite
Depth: 153.20 m
Mineralization texture: Disseminated-Net textured

Appendix D continued.

Drillhole: DDH05-88

505395.5 mE 6482884 mN, Elev: 1336.38 m

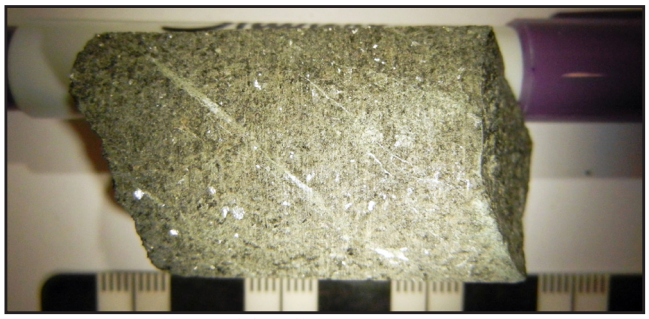

DDH05-88-3: Hornblendite
Depth: 156.90 m
Mineralization texture: Disseminated

DDH05-88-101: Hornblende clinopyroxenite
Depth: 18.42 m
Mineralization texture: Disseminated-Blebby

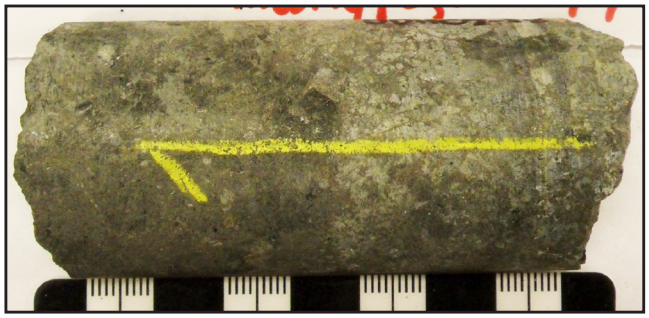

DDH05-88-102: Hornblende clinopyroxenite
Depth: 33.50 m
Mineralization texture: Disseminated-Net textured

DDH05-88-103: Hornblende clinopyroxenite
Depth: 35.10 m
Mineralization texture: Replacing magnetite

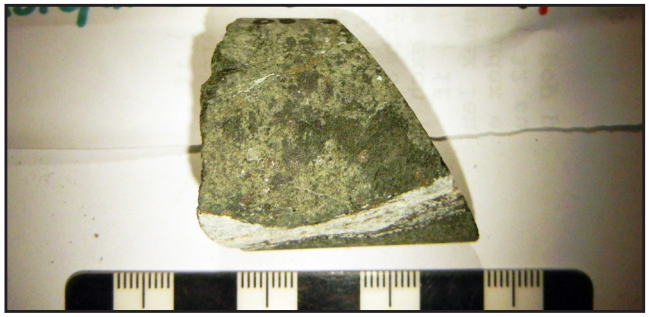

DDH05-88-104: clinopyroxenite with calcite-hornblende vein
Depth: 57.23 m
Mineralization texture: Net textured and Vein hosted

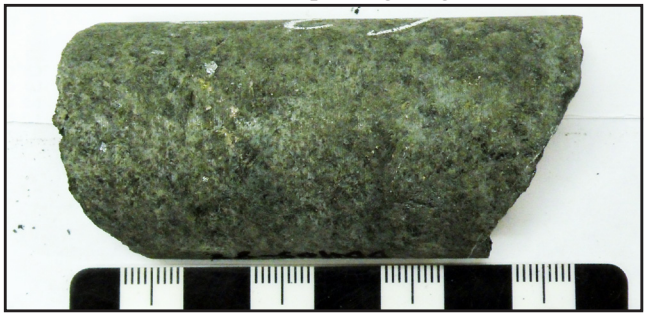

DDH05-88-105: Hornblendite
Depth: 62.12 m
Mineralization texture: Disseminated-Blebby

DDH05-88-106: Hornblendite with calcite-hornblende vein
Depth: 63.41 m
Mineralization texture: Disseminated-Net textured

DDH05-88-107: Clinopyroxene hornblendite
Depth: 64.75 m
Mineralization texture: Disseminated-Layered

Appendix D continued.

Drillhole: DDH05-88

505395.5 mE 6482884 mN, Elev: 1336.38 m

DDH05-88-108: Clinopyroxenite with carbonate veins
Depth: 82.55 m
Mineralization texture: Disseminated

DDH05-88-109: Olivine (serpentine-magnetite) clinopyroxenite
Depth: 109.53 m
Mineralization texture: Disseminated

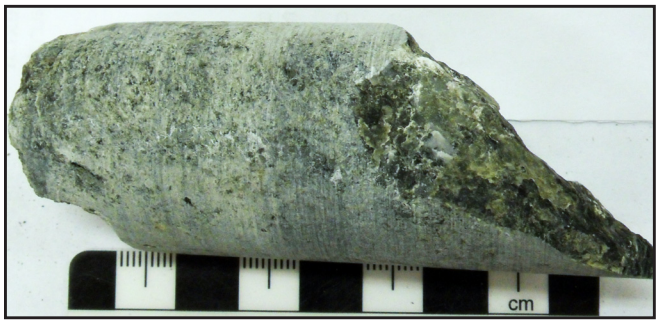

DDH05-88-110: Hornblende-magnetite clinopyroxenite
Depth: 143.87 m
Mineralization texture: Disseminated

DDH05-88-111: Hornblendite
Depth: 166.50 m
Mineralization texture: Disseminated

Drillhole: DDH05-89

505925.5 mE 6482544 mN, Elev: 1356.58 m

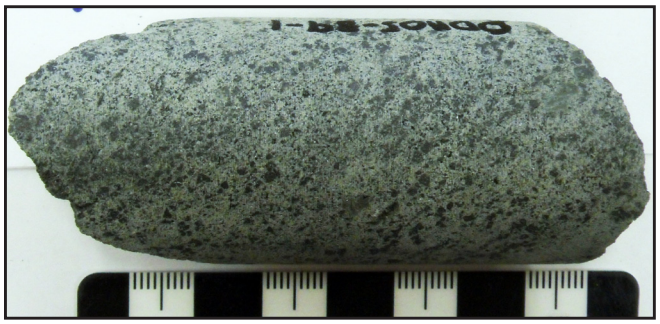

DDH05-89-1: Magnetite clinopyroxenite
Depth: 13.65 m
Mineralization texture: Disseminated

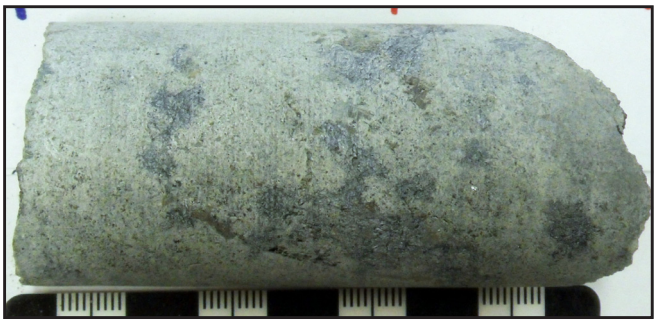

DDH05-89-2: Olivine (serpentine-magnetite) clinopyroxenite
Depth: 69.26 m
Mineralization texture: Disseminated-Blebby

Appendix D continued.

Drillhole: DDH05-101

505395.5 mE 6482884 mN, Elev: 1336.75 m

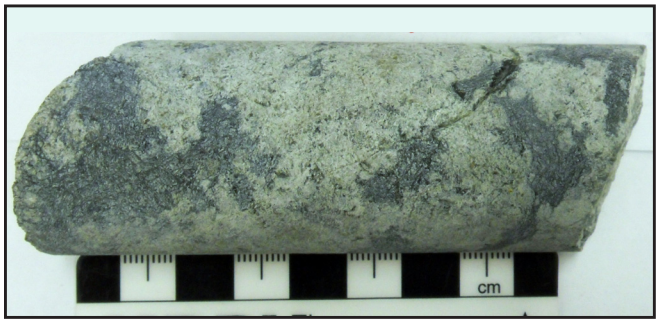

DDH05-101-1: Olivine (serpentune-magnetute) clinopyroxenite
Depth: 104.13 m
Mineralization texture: Disseminated

DDH05-101-2: Clinopyroxenite
Depth: 146.14 m
Mineralization texture: Disseminated-Semi-massive

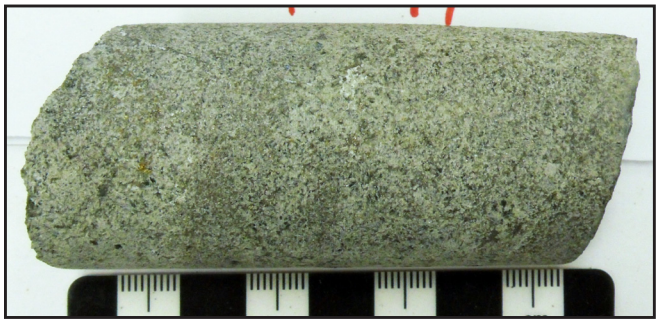

DDH05-101-3: clinopyroxenite
Depth: 148.65 m
Mineralization texture: Disseminated

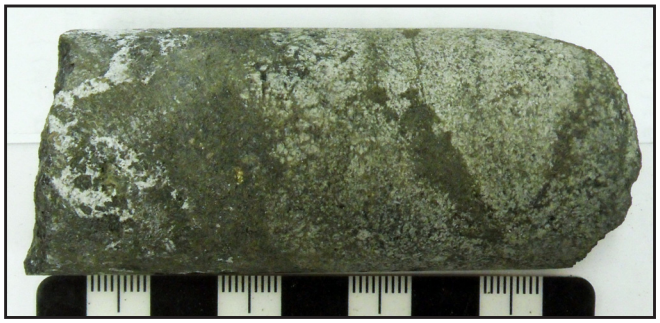

DDH05-101-4: Calcite-hornblende-chlorite vein in clinopyroxenite
Depth: 156.05 m
Mineralization texture: Disseminated-Blebby

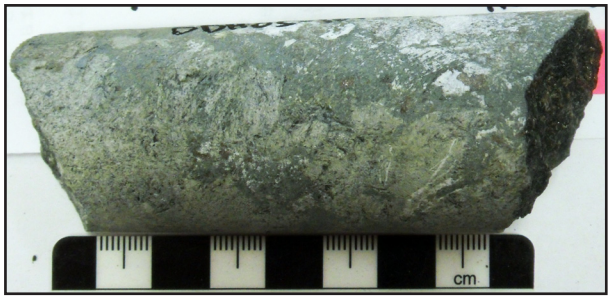

DDH05-101-5: Calcite-chlorite vein in clinopyroxenite
Depth: 169.60 m
Mineralization texture: Disseminated-Blebby

Appendix D continued.

Drillhole: DDH05-102

506346 mE 6482435 mN, Elev: 1366.17 m

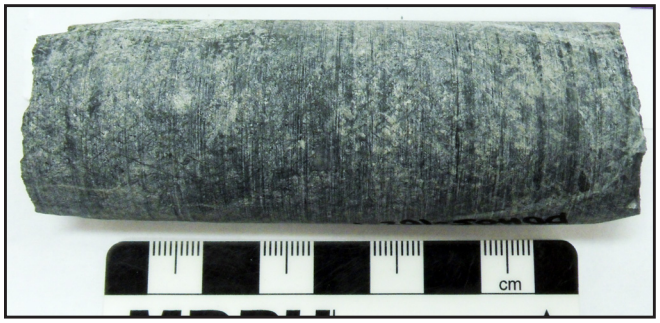

DDH05-102-1: Serpentine-altered wehrlite
Depth: 53.30 m
Mineralization texture: Blebby

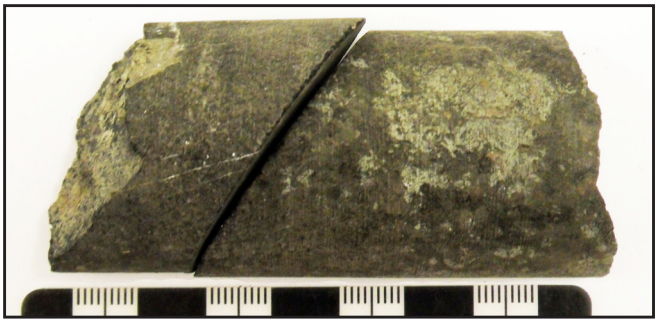

DDH05-102-2: Clinoproxene hornblendite
Depth: 79.20 m
Mineralization texture: Disseminated-Blebby

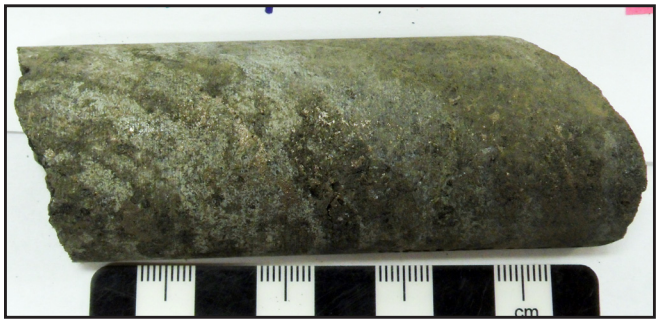

DDH05-102-3: Hornblende clinopyroxenite
Depth: 82.25 m
Mineralization texture: Net textured-Semi-massive

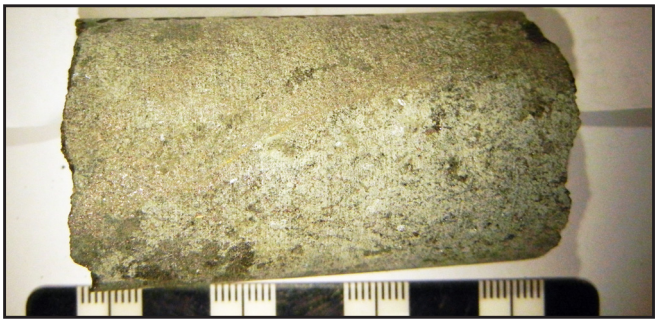

DDH05-102-4: Hornblende clinopyroxenite
Depth: 122.83 m
Mineralization texture: Disseminated-Net textured

DDH05-102-5: Clinopyroxenite
Depth: 145.15 m
Mineralization texture: Disseminated

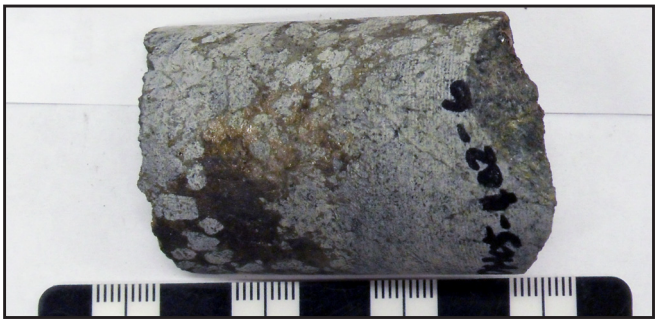

DDH05-102-6: Clinopyroxenite
Depth: 147.56 m
Mineralization texture: Net textured-Semi-massive

DDH05-102-7: Clinopyroxenite
Depth: 159.80 m
Mineralization texture: Disseminated-Net textured

DDH05-102-8: Clinopyroxenite
Depth: 173.34 m
Mineralization texture: Barren

Appendix D continued.

Drillhole: DDH05-102

506346 mE 6482435 mN, Elev: 1366.17 m

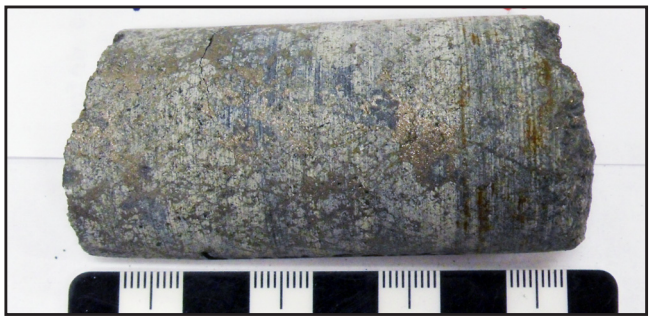

DDH05-102-9: Olivine (serpentine-magnetite) clinopyroxenite
Depth: 182.80 m
Mineralization texture: Net textured-Semi-massive

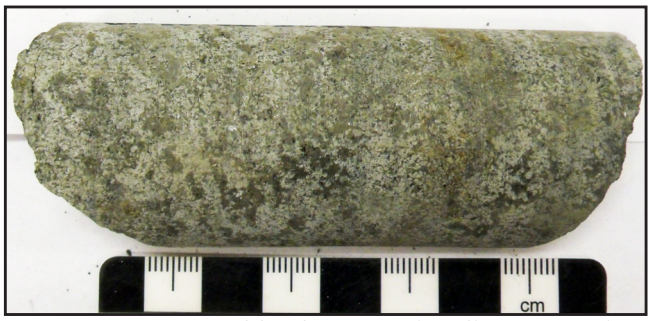

DDH05-102-10: Hornblende-magnetite clinopyroxenite
Depth: 208.80 m
Mineralization texture: Disseminated-Net textured

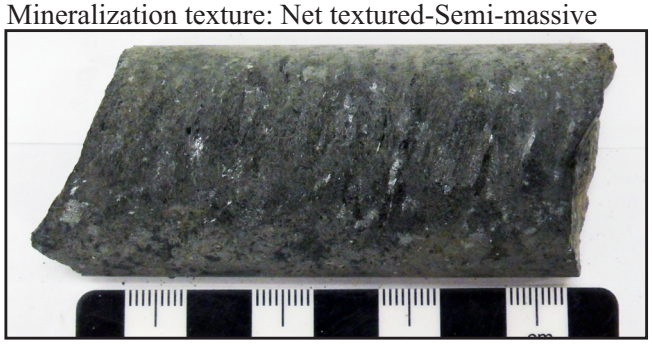

DDH05-102-11: Hornblendite
Depth: 223.27 m
Mineralization texture: Disseminated

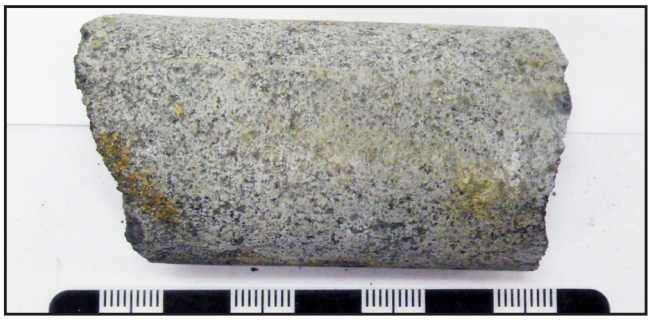

DDH05-102-12: Clinopyroxenite
Depth: 242.80 m
Mineralization texture: Disseminated-Net textured

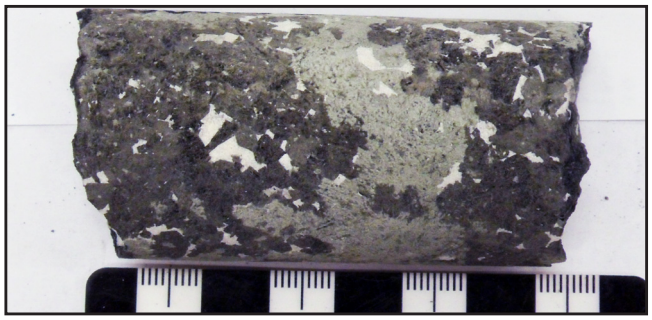

DDH05-102-13: Feldspathic hornblendite with clasts of clinopyroxenite
Depth: 268.24 m
Mineralization Texture: Barren

DDH05-102-14: Hornblendite
Depth: 283.36 m
Mineralization texture: Disseminated-Blebby

DDH05-102-15: Hornblendite
Depth: 294.62 m
Mineralization texture: Net textured-Semi-massive

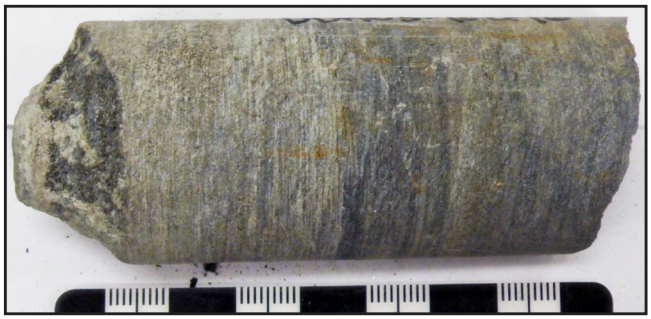

DDH05-102-16: Hornfelsed phyllite
Depth: 314.90 m
Mineralization texture: Barren

Appendix D continued.

Drillhole: DDH06-143

504769.6 mE 6483975 mN, Elev: 1402.34 m

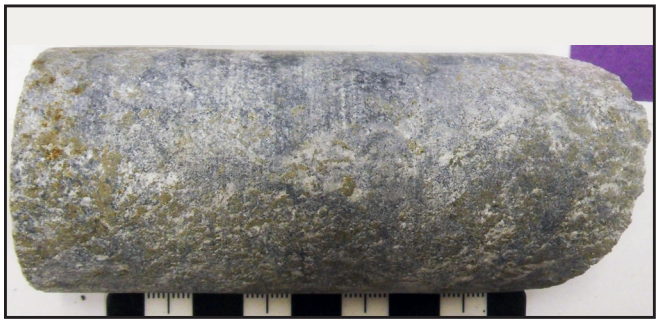

DDH06-143-1: Talc-altered dunite
Depth: 186.40 m
Mineralization texture: Blebby

Drillhole: DDH06-149

505912 mE 6483180 mN, Elev: 1435.80 m

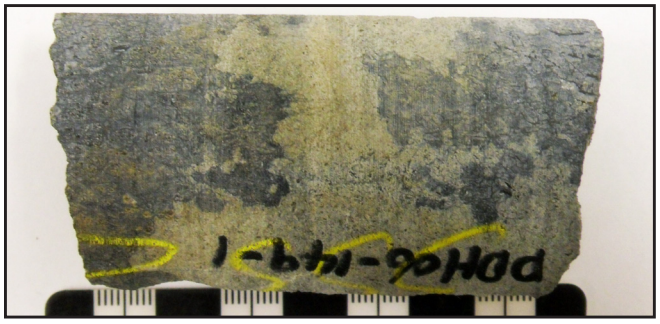

DDH06-149-1: Olivine (serpentine-magnetite) clinopyroxenite
Depth: 249.30 m
Mineralization texture: Barren

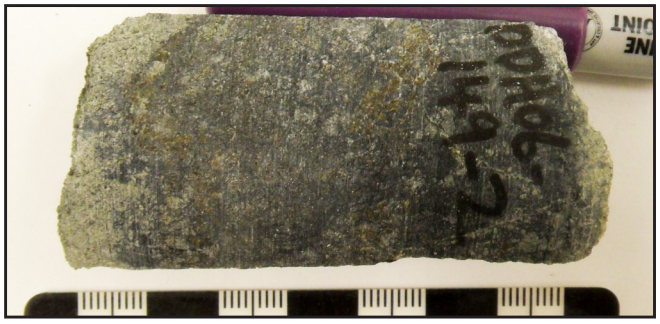

DDH06-149-2: Olivine (serpentine-magnetite) clinopyroxenite
Depth: 249.80 m
Mineralization texture: Disseminated

Drillhole: DDH06-150

506032.3 mE 6483010 mN, Elev: 1428.63 m

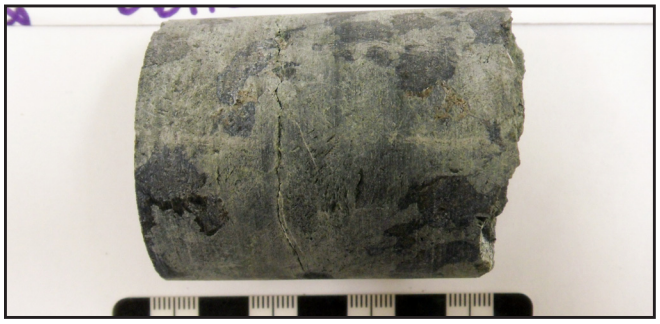

DDH06-150-1: Olivine (serpentine-magnetite) clinopyroxenite
Depth: 203.00 m
Mineralization texture: Barren

Appendix D continued.

Drillhole: DDH06-161

505431.8 mE 6482834 mN, Elev: 1338.16 m

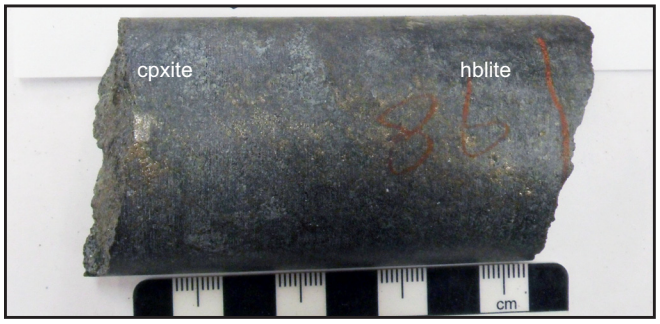

DDH06-161-1: Clinopyroxenite grading into hornblendite
Depth: 98.05 m
Mineralization texture: Net textured-Semi-massive

DDH06-161-2: Magnetite clinopyroxenite
Depth: 135.30 m
Mineralization texture: Disseminated-Net textured

DDH06-161-3: Tremolite-talc-altered clinopyroxenite
Depth: 155.90 m
Mineralization texture: Disseminated-Net textured

Drillhole: DDH07-201

508735.6 mE 6481504 mN, Elev: 1131.60 m

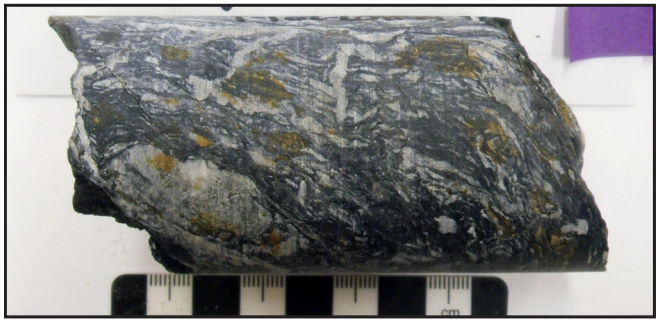

DDH07-201-1: Phyllite
Depth: 655.50 m
Mineralization texture: Blebby

Appendix D continued.

Drillhole: DDH07-207

505919.1 mE 6482546 mN, Elev: 1357.22 m

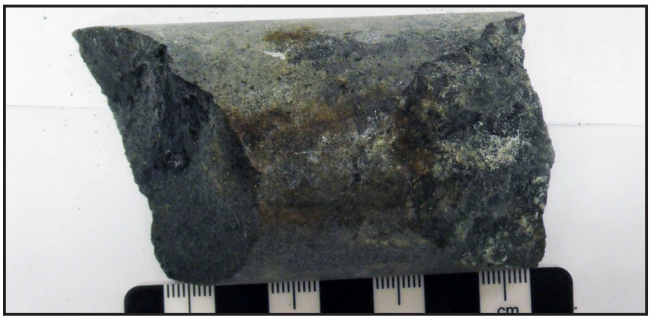

DDH07-207-1: Hornblende clinopyroxenite
Depth: 43.30 m
Mineralization texture: Disseminated

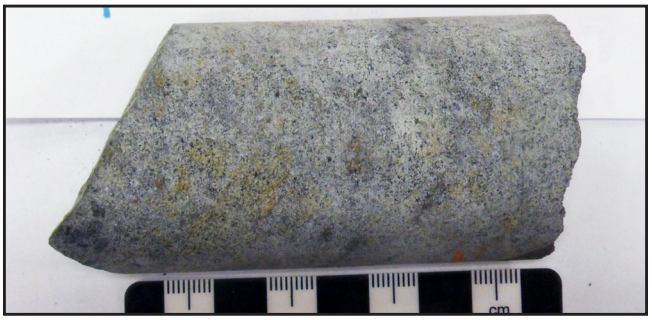

DDH07-207-2: Olivine (serpentine-magnetite) clinopyroxenite
Depth: 98.00 m
Mineralization texture: Disseminated-Net textured

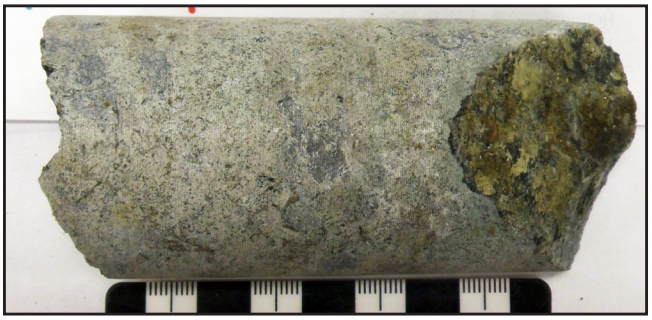

DDH07-207-3: Olivine (serpentine-magnetite) clinopyroxenite
Depth: 142.72 m
Mineralization Texture: Disseminated-Blebby

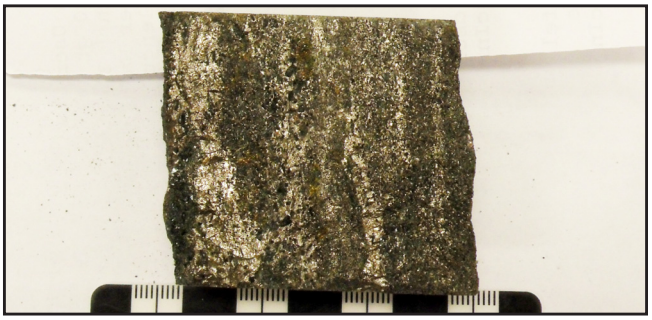

DDH07-207-4: Clinopyroxenite
Depth: 181.44 m
Mineralization texture: Net textured-Layered

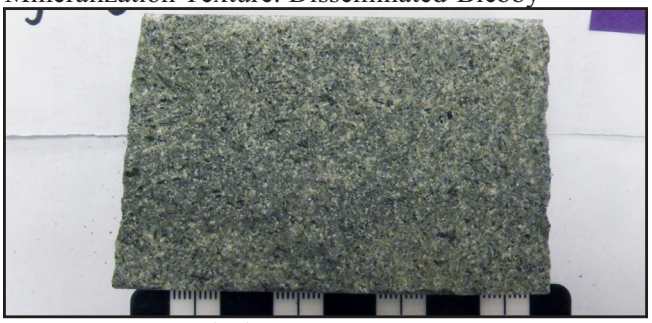

DDH07-207-5: Diorite
Depth: 187.08 m
Mineralization texture: Disseminated

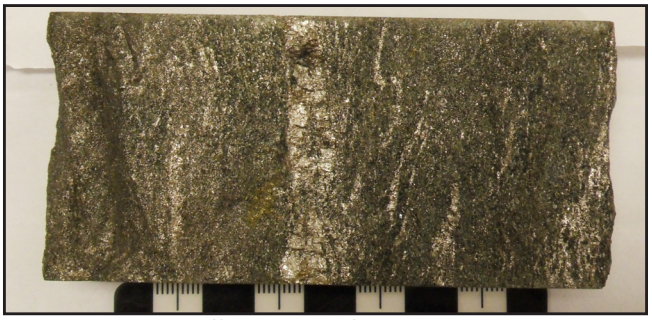

DDH07-207-6: Clinopyroxenite
Depth: 187.79 m
Mineralization texture: Net textured-Layered

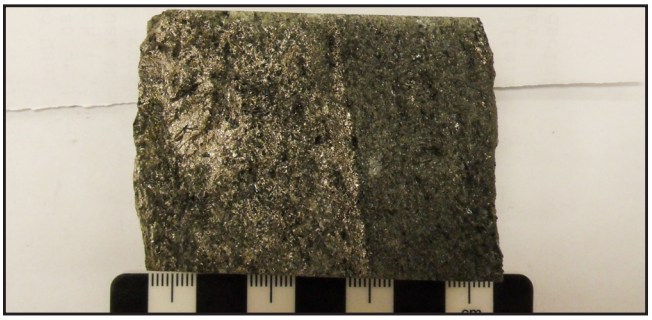

DDH07-207-7: Tremolite-altered clinopyroxenite
Depth: 188.21 m
Mineralization texture: Net textured-Layered

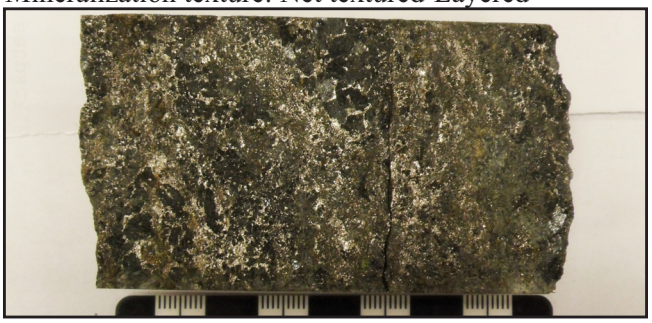

DDH07-207-8: Hornblende clinopyroxenite
Depth: 194.97 m
Mineralization texture: Net textured-Semi-massive

Appendix D continued.

Drillhole: DDH07-207

505919.1 mE 6482546 mN, Elev: 1357.22 m

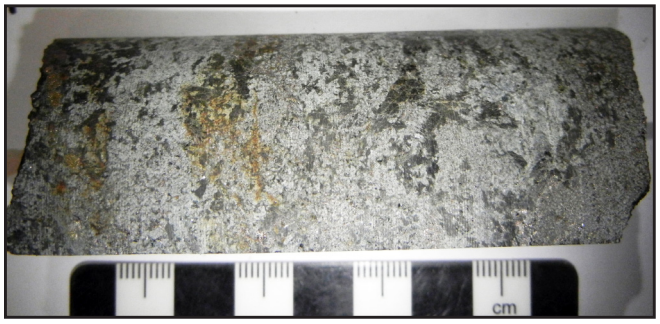

DDH07-207-9: Biotite clinopyroxenite
Depth: 198.50 m
Mineralization texture: Net textured-Semi-massive

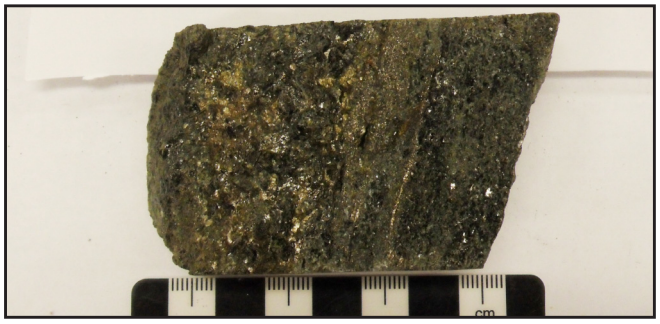

DDH07-207-10: Biotite clinopyroxenite
Depth: 199.67 m
Mineralization texture: Net textured-Layered

DDH07-207-11: Clinopyroxenite
Depth: 205.52 m
Mineralization texture: Blebby-Net textured

DDH07-207-12: Hornblende clinopyroxenite
Depth: 226.00 m
Mineralization texture: Blebby-Net textured

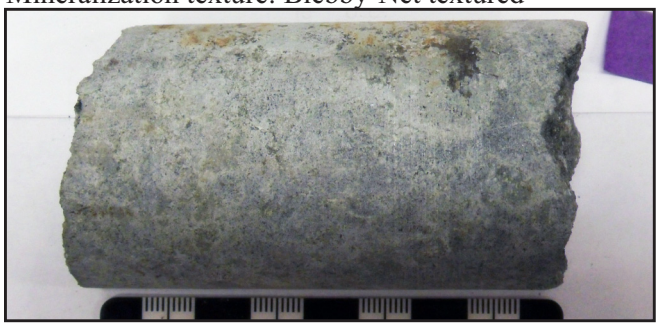

DDH07-207-13: Clinopyroxenite
Depth: 226.40 m
Mineralization texture: Disseminated-Blebby

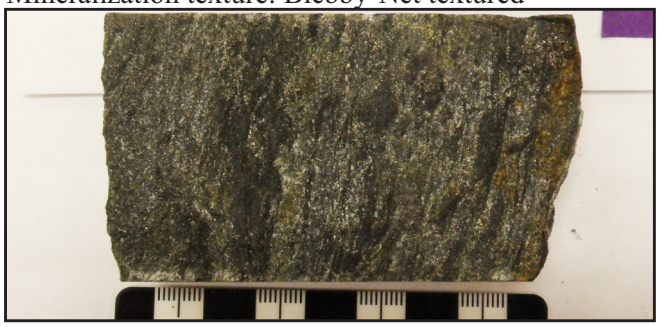

DDH07-207-14: Hornfelsed phyllite
Depth: 231.95 m
Mineralization texture: Disseminated

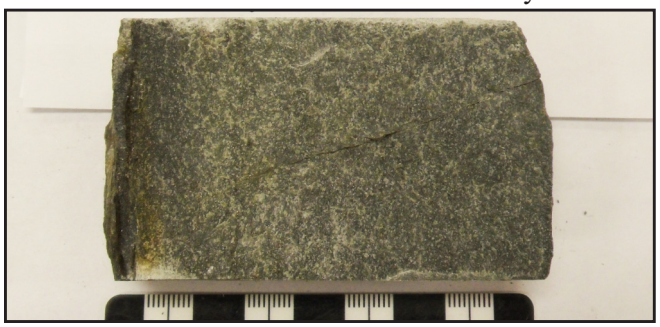

DDH07-207-15: Hornfelsed phyllite
Depth: 250.97 m
Mineralization texture: Disseminated

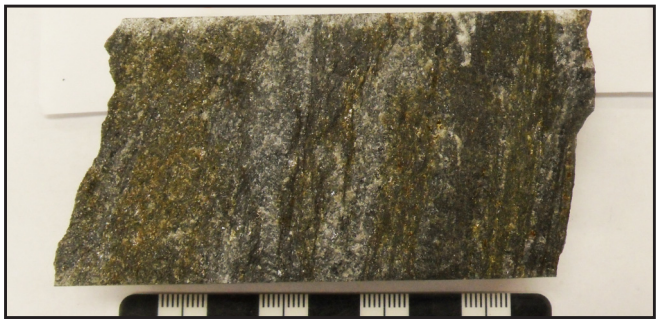

DDH07-207-16: Hornfelsed phyllite
Depth: 261.80 m
Mineralization texture: Disseminated-Blebby

Appendix D continued.

Drillhole: DDH07-207

505919.1 mE 6482546 mN, Elev: 1357.22 m

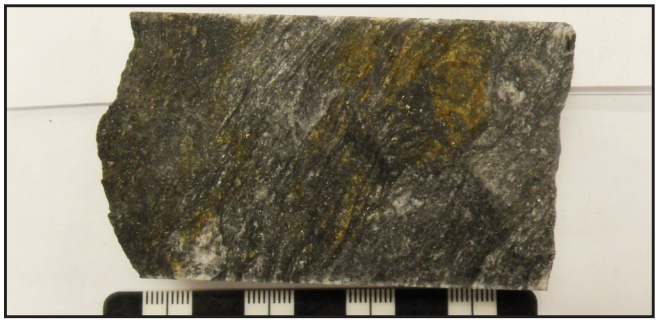

DDH07-207-17: Hornfelsed phyllite
Depth: 297.58 m
Mineralization texture: Disseminated along bedding

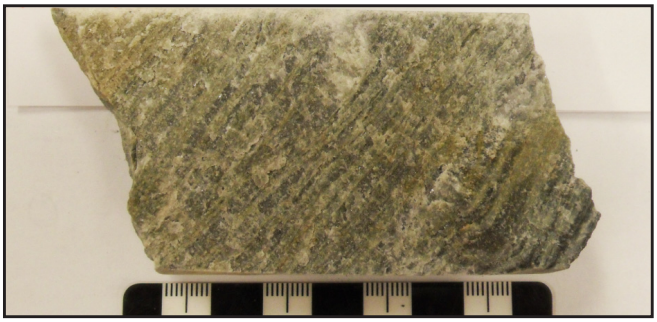

DDH07-207-18: Hornfelsed phyllite
Depth: 306.10 m
Mineralization texture: Barren

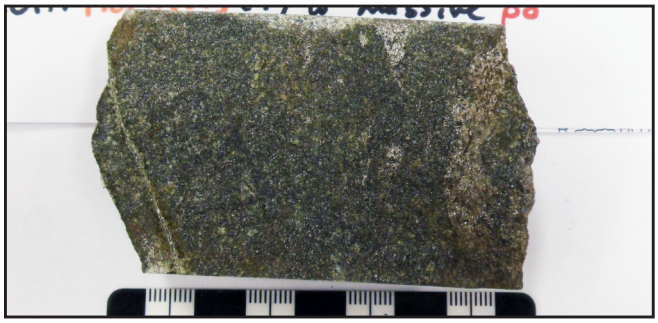

DDH07-207-19: Hornfelsed phyllite
Depth: 311.75 m
Mineralization texture: Net textured-Semi-massive

Drillhole: DDH07-211

505337.4 mE 6482829 mN, Elev: 1323.36 m

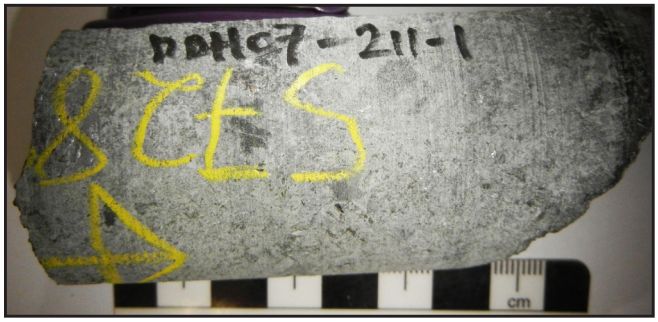

DDH07-211-1: Clinopyroxenite
Depth: 150.40 m
Mineralization texture: Disseminated-Blebby

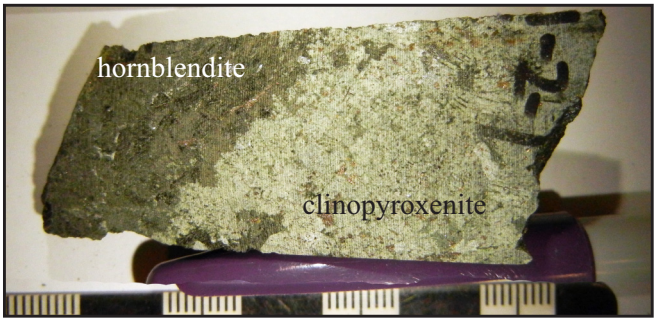

DDH07-211-2-1: Clinopyroxenite/hornblendite contact
Depth: 153.60 m
Mineralization texture: Disseminated-Blebby

Appendix D continued.

Drillhole: DDH07-211

505337.4 mE 6482829 mN, Elev: 1323.36 m

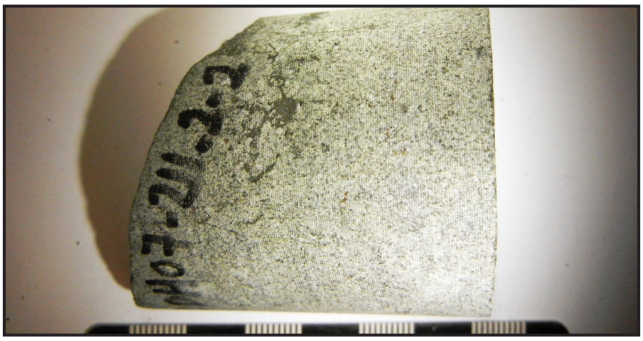

DDH07-211-2-2: Clinopyroxenite
Depth: 153.60 m
Mineralization texture: Disseminated-Blebby

DDH07-211-3: Hornblendite
Depth: 154.00 m
Mineralization texture: Disseminated-Blebby

DDH07-211-4: Hornblendite
Depth: 154.20 m
Mineralization texture: Disseminated

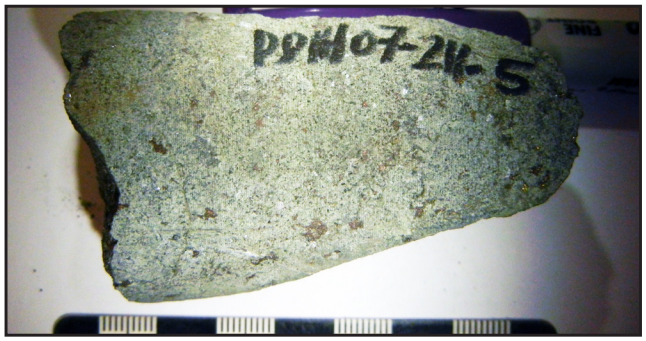

DDH07-211-5: Clinopyroxenite
Depth: 157.90 m
Mineralization texture: Disseminated-Net textured

DDH07-211-6-1/DDH07-211-6-2: Hornblendite
Depth: 161.60 m
Mineralization texture: Vein-hosted

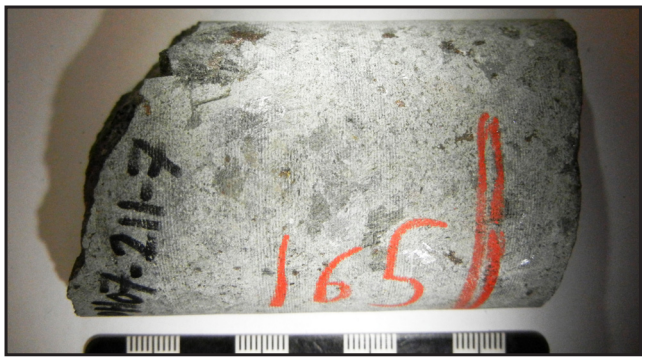

DDH07-211-7: Hornblende clinopyroxenite
Depth: 164.80 m
Mineralization texture: Disseminated-Blebby

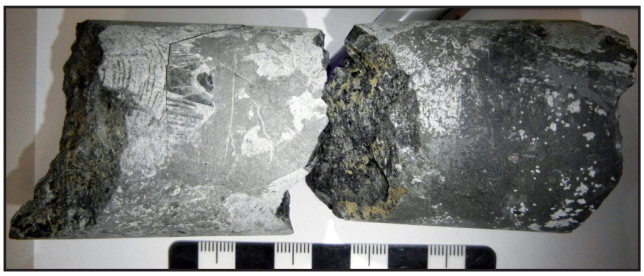

DDH07-211-8: Calcite-biotite vein in clinopyroxenite
Depth: 169.90 m
Mineralization texture: Barren

Appendix D continued.

Drillhole: DDH07-211

505337.4 mE 6482829 mN, Elev: 1323.36 m

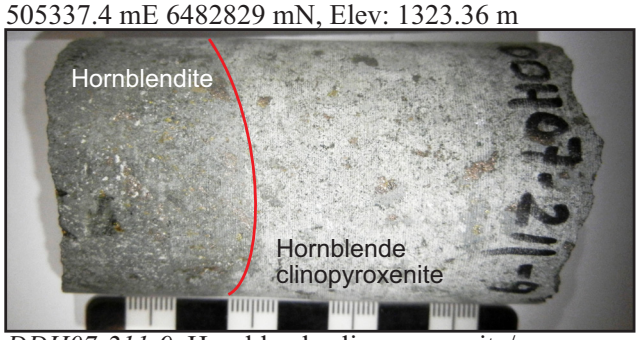

DDH07-211-9: Hornblende clinopyroxenite/ hornblendite contact
Depth: 170.60 m
Mineralization texture: Disseminated-Blebby

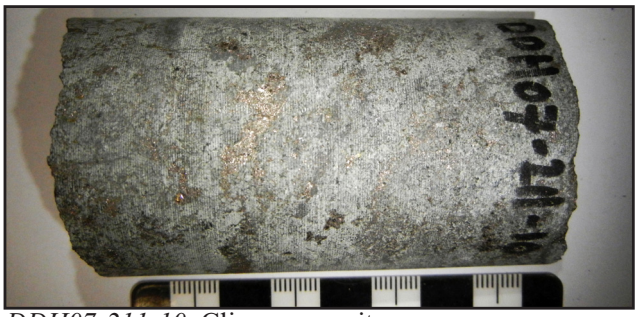

DDH07-211-10: Clinopyroxenite
Depth: 171.50 m
Mineralization texture: Disseminated-Blebby

DDH07-211-11: Olivine (serpentine-magnetite) clinopyroxenite
Depth: 177.50 m
Mineralization texture: Disseminated

DDH07-211-12: Clinopyroxenite
Depth: 178.70 m
Mineralization texture: Blebby

DDH07-211-101: Olivine (serpentine-magnetite) clinopyroxenite
Depth: 25.55 m
Mineralization texture: Disseminated

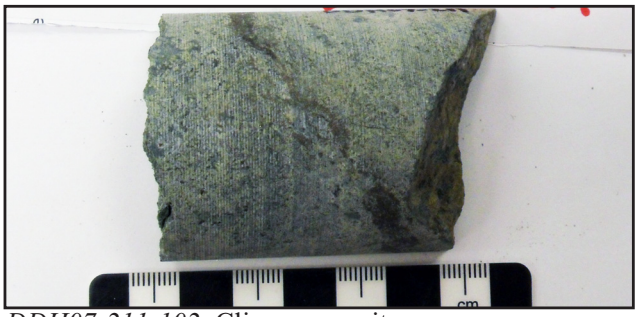

DDH07-211-102: Clinopyroxenite
Depth: 26.92 m
Mineralization texture: Disseminated-Semi-massive

DDH07-211-103: Magnetite clinopyroxenite with hornblende-calcite vein
Depth: 28.25 m
Mineralization texture: Disseminated-Blebby

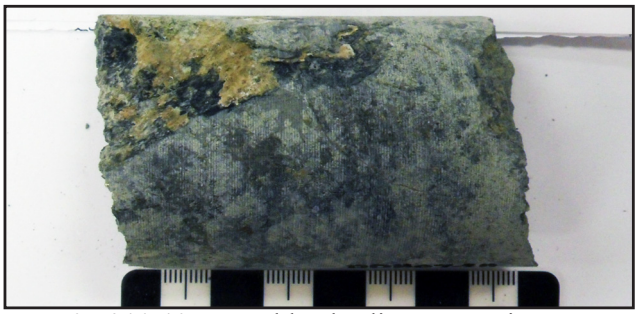

DDH07-211-104: Hornblende clinopyroxenite
Depth: 42.30 m
Mineralization texture: Disseminated

Appendix D continued.

Drillhole: DDH07-211

505337.4 mE 6482829 mN, Elev: 1323.36 m

DDH07-211-105: Clinopyroxenite
Depth: 65.16 m
Mineralization texture: Disseminated

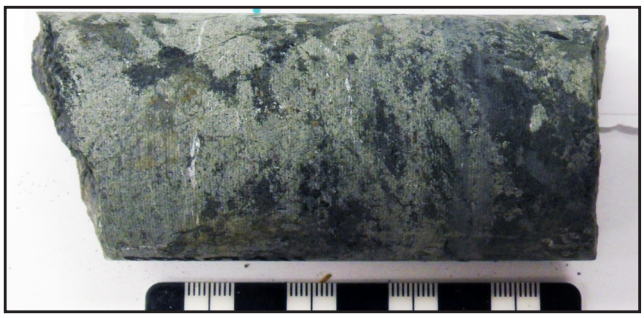

DDH07-211-106: Hornblende-magnetite clinopyroxenite
Depth: 78.59 m
Mineralization texture: Disseminated

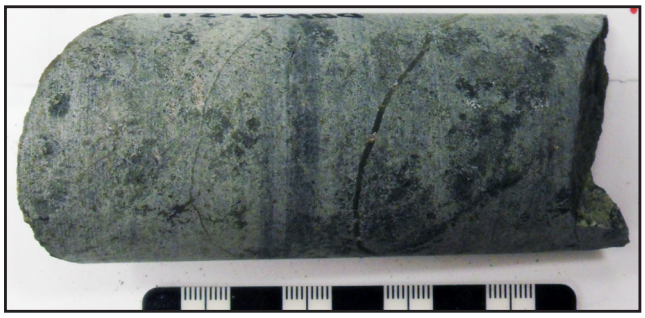

DDH07-211-107: Hornblende clinopyroxenite
Depth: 101.58 m
Mineralization texture: Blebby-Net textured

DDH07-211-108: Hornblende clinopyroxenite
Depth: 138.85 m
Mineralization texture: Disseminated-Net textured

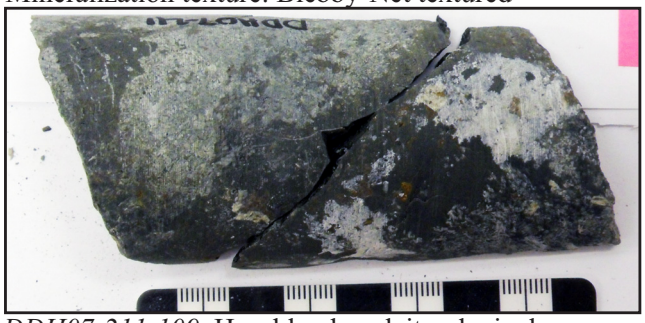

DDH07-211-109: Hornblende-calcite-plagioclase vein in clinopyroxenite
Depth: 175.75 m
Mineralization texture: Vein-hosted

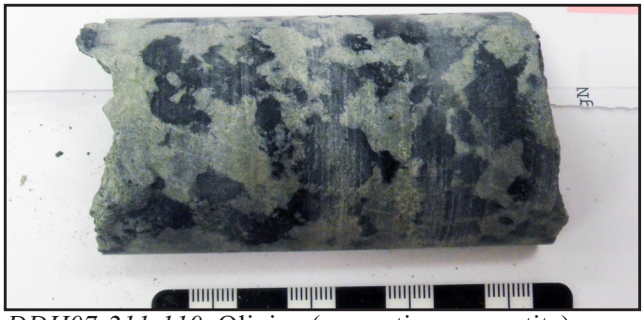

DDH07-211-110: Olivine (serpentine-magnetite) clinopyroxenite
Depth: 202.97 m
Mineralization texture: Disseminated

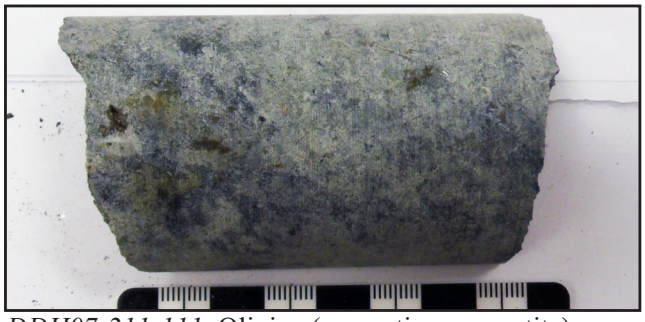

DDH07-211-111: Olivine (serpentine-magnetite) clinopyroxenite
Depth: 244.68 m
Mineralization texture: Disseminated

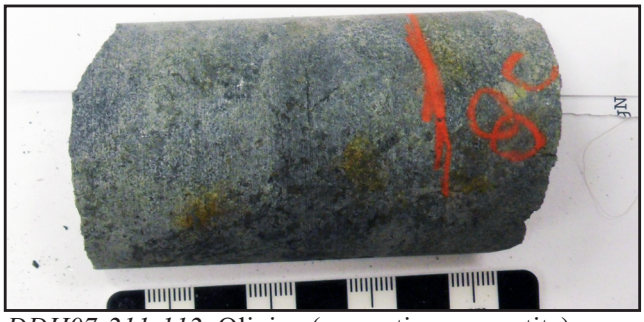

DDH07-211-112: Olivine (serpentine-magnetite) clinopyroxenite
Depth: 258.05 m
Mineralization texture: Disseminated

Appendix D continued.

Surface Samples

11GNX2-3-1: Olivine (serpentine-magnetite) clinopyroxenite
Location: 506202.0 mE, 6483195 mE
Mineralization texture: Barren

11GNX2-3-2: Olivine (serpentine-magnetite) clinopyroxenite
Location: 506202.0 mE, 6483195 mE
Mineralization texture: Barren

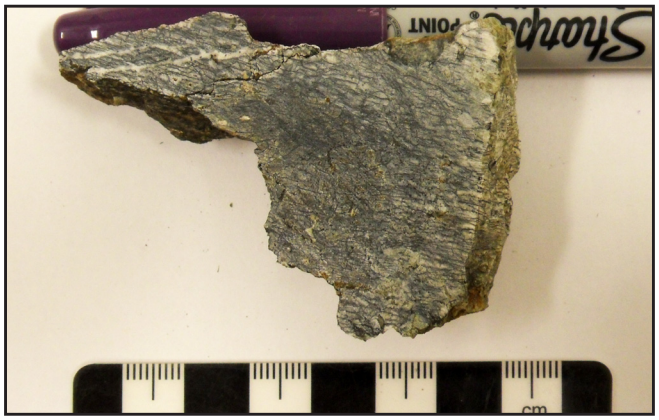

11GNX2-3-3: Olivine (serpentine-magnetite) clinopyroxenite
Location: 506202.0 mE, 6483195 mE
Mineralization texture: Barren

13-SJB-1: Diorite/hornblendite contact
Location: 506707.0 mE, 6482656 mE
Mineralization texture: Barren

13-SJB-2A: Olivine (serpentine-magnetite) clinopyroxenite
Location: 506205.0 mE, 6483201 mE
Mineralization texture: D

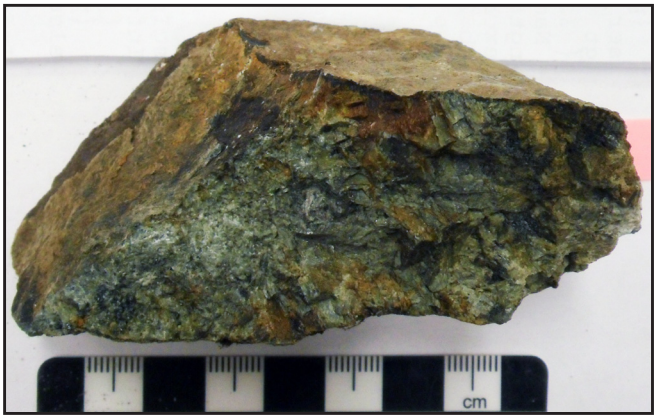

13-SJB-2B: Olivine (serpentine-magnetite) clinopyroxenite
Location: 506205.0 mE, 6483201 mE
Mineralization texture: Barren

Appendix D continued.

Surface Samples

13-SJB-3A: Hornblendite
Location: 506188.0 mE, 6482919 mE
Mineralization texture: Disseminiated

13-SJB-3B: Hornblendite
Location: 506188.0 mE, 6482919 mE
Mineralization texture: Disseminiated

13-SJB-4: Clinopyroxenite
Location: 505742.0 mE, 6482653 mE
Mineralization texture: Barren

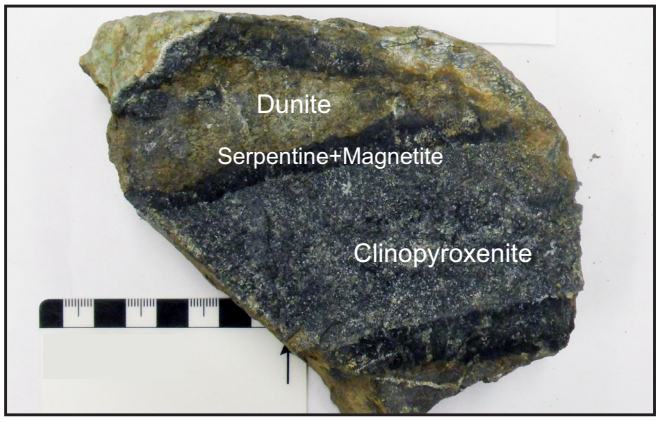

13-SJB-5A: Dunite clast with altered serpentine+ magnetite rim in clinopyroxenite
Location: 507382.0 mE, 6482274 mE
Mineralization texture: Disseminiated

13-SJB-5B: Dunite clast with altered serpentine+ magnetite rim in clinopyroxenite
Location: 507382.0 mE, 6482274 mE
Mineralization texture: Barren

13-SJB-6A: Olivine (serpentine-magnetite) clinopyroxenite
Location: 506205.0 mE, 6483201 mE
Mineralization texture: Disseminiated

Appendix D continued.

Surface Samples

13-SJB-6B: Ol ivine (serpentine-magnetite) clinopyroxenite
Location: 506205.0 mE, 6483201 mE
Mineralization texture: Disseminated

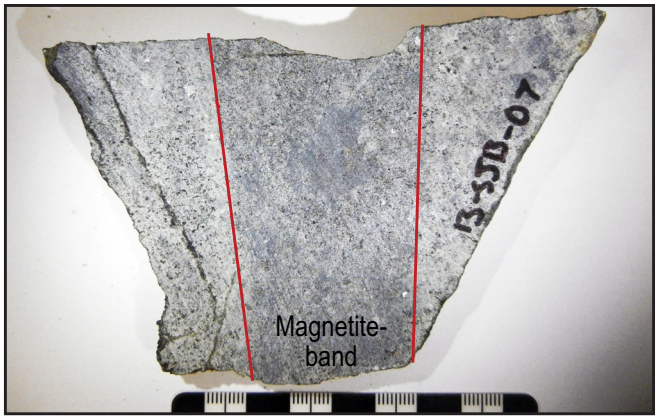

13-SJB-7: Banded magnetite clinopyroxenite
Location: 506035.0 mE, 6483078 mE
Mineralization texture: Barren

13-SJB-8: Olivine (serpentine-magnetite) clinopyroxenite
Location: DJ/DB zone
Mineralization texture: Disseminated

13-SJB-9: Banded magnetite clinopyroxenite
Location: DJ/DB zone
Mineralization texture: Disseminated

13-SJB-10: Olivine (serpentine-magnetite) clinopyroxenite
Location: DJ/DB zone
Mineralization texture: Barren

Appendix E. Scans of thin sections of samples from the DJ/DB zone in transmitted and cross-polarized light

Appendix E contains scans of all thin sections from this study from the DJ/DB zone, with drill collar or surface sample location (NAD83 UTM Zone 9; Elev = elevation), rock type, depth of sample (for drillcore samples), and sulphide mineralization texture (barren, disseminated, blebby, net-textured, semi-massive, massive, layered, or vein-hosted). Where there was a visible fabric, approximate orientation of core axis (CA) was noted. All scans are approximately 20 mm across.

Drillhole: DDH03-07

508583.3 mE 6480856 mN, Elev: 1036.14 m

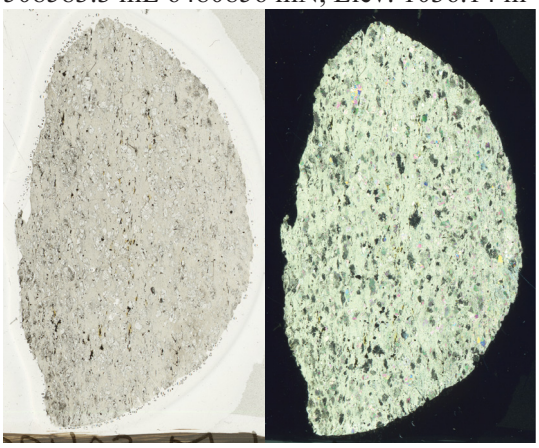

DDH03-07-1: Talc-carbonate-altered phyllite
Depth: 432.80 m
Mineralization texture: Disseminated

Drillhole: DDH04-43

506826.2 mE 6482617 mN, Elev: 1401.58 m

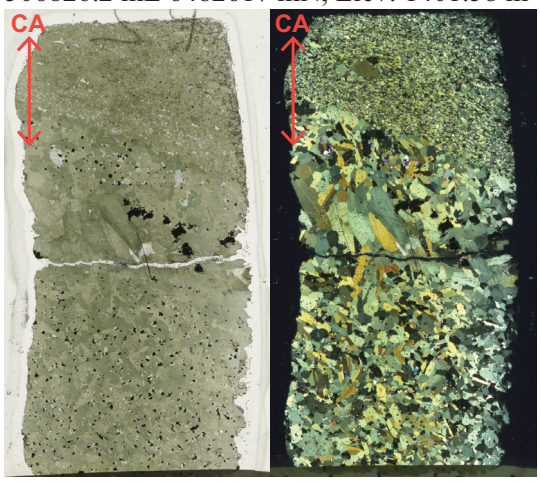

DDH04-43-1: Hornblendite
Depth: 88.10 m
Mineralization texture: Disseminated-Blebby

Drillhole: DDH04-46

506468.9 mE 6482807 mN, Elev: 1436.26 m

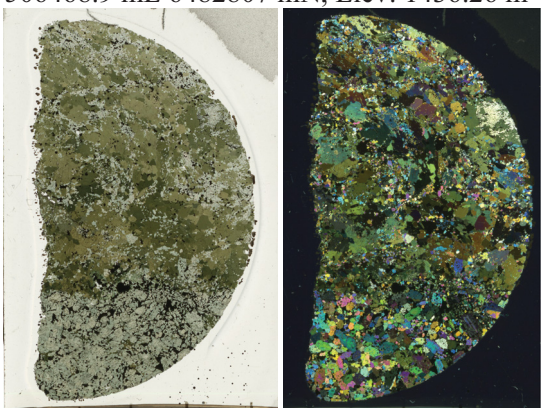

DDH04-46-1: Clinopyroxenite clast in hornblendite
Depth: 38.70 m
Mineralization texture: Disseminated

Appendix E continued.

Drillhole: DDH04-48

506254.4 mE 6483032 mN, Elev: 1459.44 m

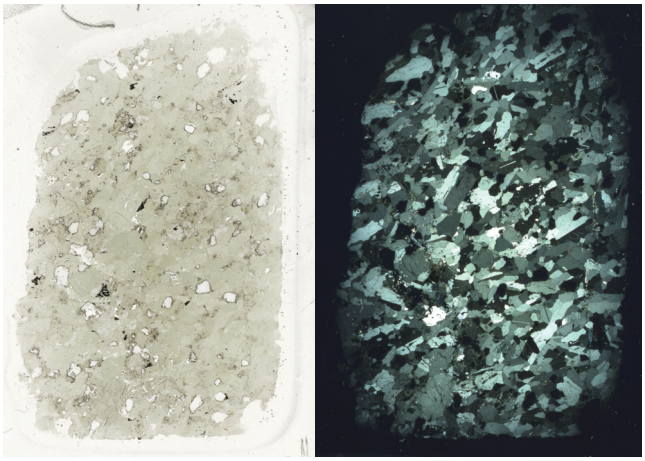

DDH04-48-3: Clinopyroxene hornblendite
Depth: 53.30 m
Mineralization texture: Disseminated

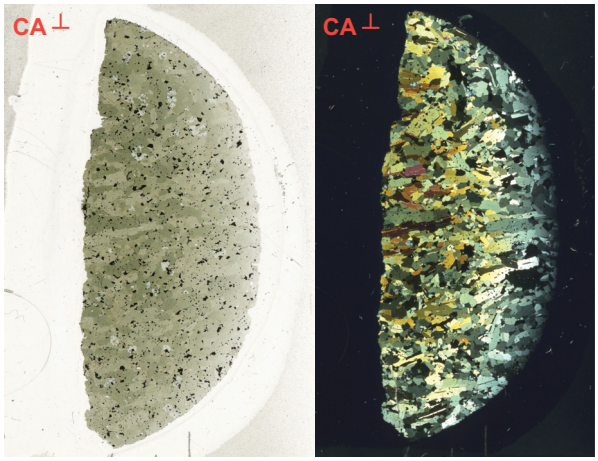

DDH04-48-4: Oriented hornblendite
Depth: 61.63 m
Mineralization texture: Disseminated

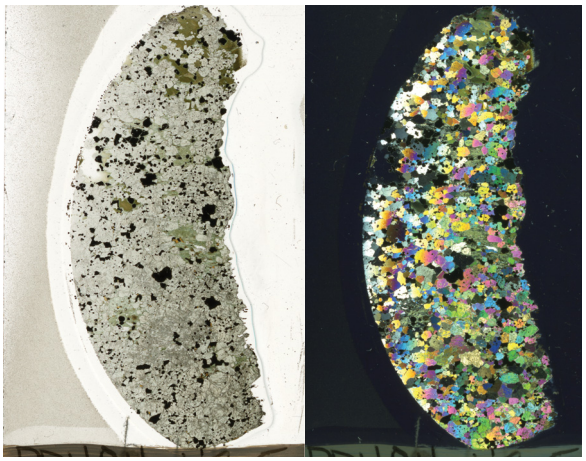

DDH04-48-5: Magnetite clinopyroxenite
Depth: 71.50 m
Mineralization texture: Disseminated

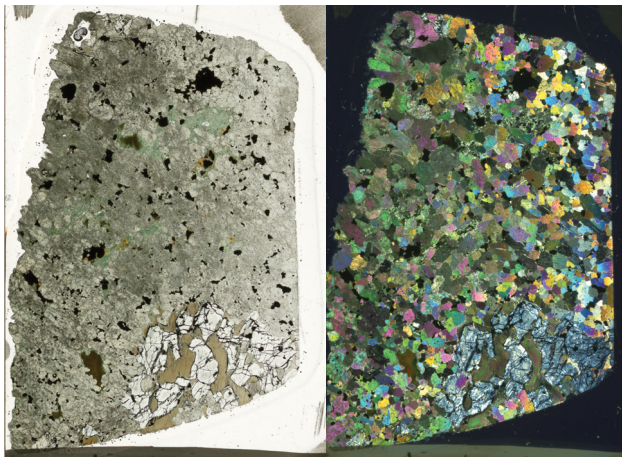

DDH04-48-6: Olivine (serpentine-magnetite) clinopyroxenite
Depth: 78.75 m
Mineralization texture: Disseminated

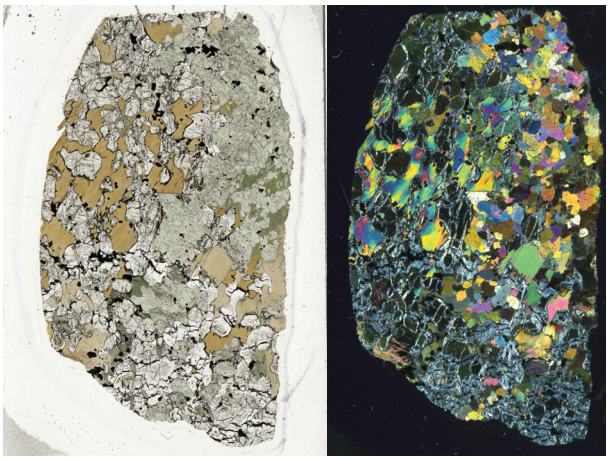

DDH04-48-7: Olivine (serpentine-magnetite) clinopyroxenite
Depth: 91.90 m
Mineralization texture: Disseminated

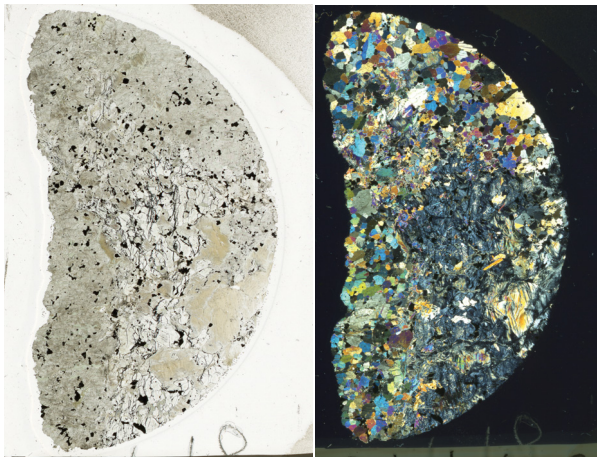

DDH04-48-8: Olivine (serpentine-magnetite) clinopyroxenite
Depth: 124.30 m
Mineralization texture: Disseminated

Appendix E continued.

Drillhole: DDH04-48

506254.4 mE 6483032 mN, Elev: 1459.44 m

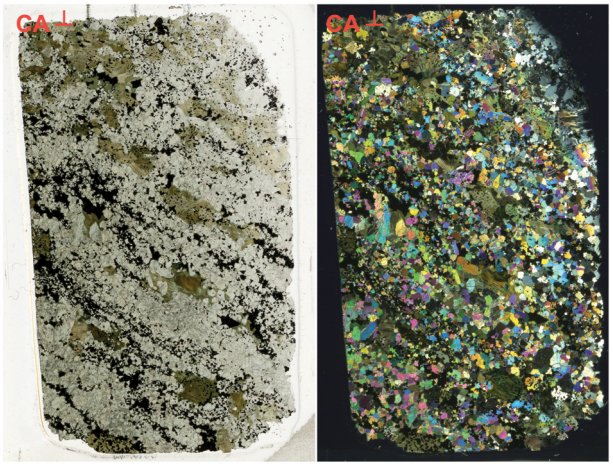

DDH04-48-9: Magnetite clinopyroxenite
Depth: 147.30 m
Mineralization texture: Disseminated

Drillhole: DDH04-55

506280.8 mE 6483022 mN, Elev: 1462.38 m

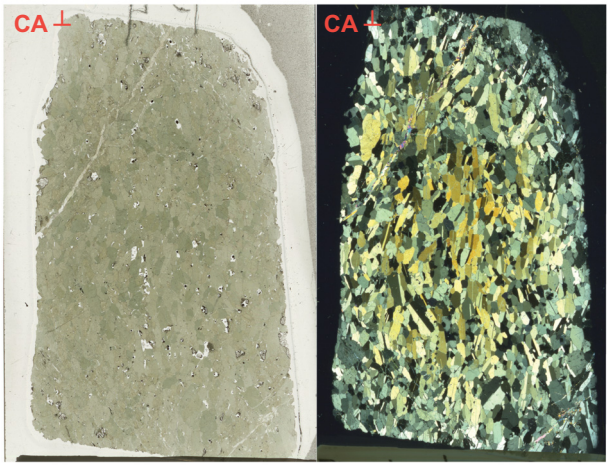

DDH04-55-1: Oriented hornblendite
Depth: 46.46 m
Mineralization texture: Disseminated

Appendix E continued.

Drillhole: DDH04-58

506010.3 mE 6483207 mN, Elev: 1454.88 m

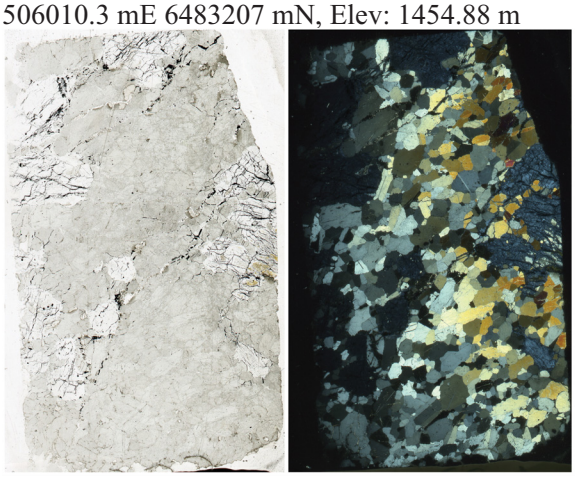

DDH04-58-1: Olivine (serpentine-magnetite) clinopyroxenite
Depth: 9.90 m
Mineralization texture: Disseminated

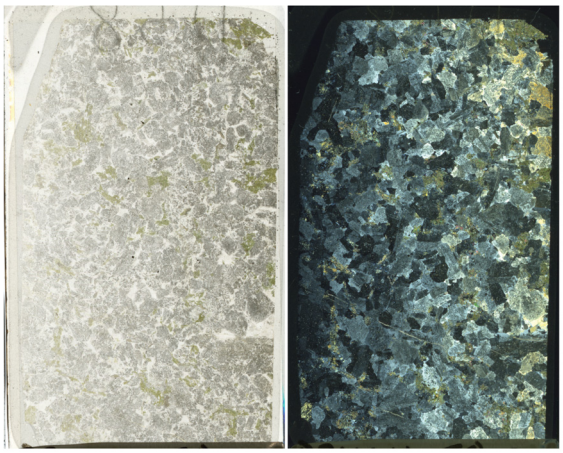

DDH04-58-2: Diorite
Depth: 15.10 m
Mineralization texture: Barren

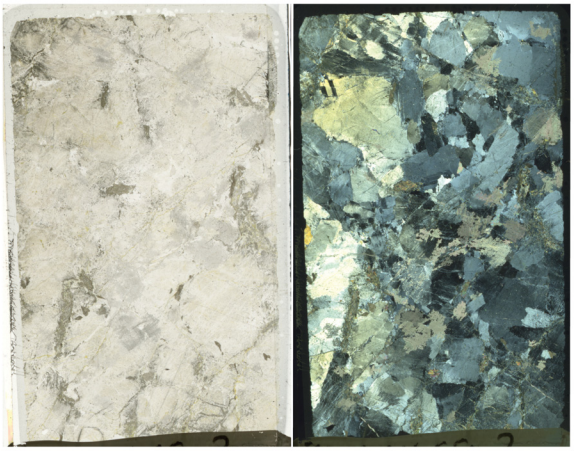

DDH04-58-3: Carbonate-serpentine-altered diorite
Depth: 18.80 m
Mineralization texture: Barren

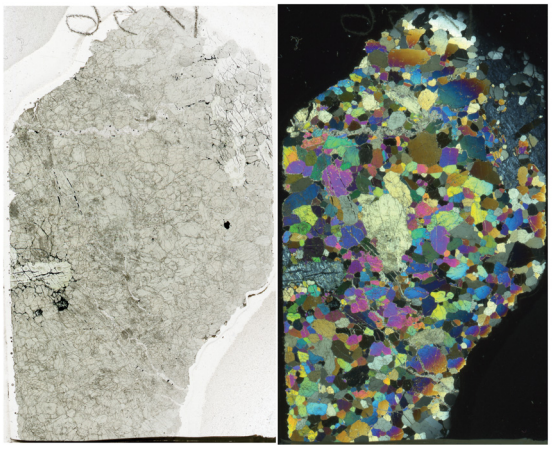

DDH04-58-4-1: Olivine (serpentine-magnetite) clinopyroxenite
Depth: 20.50 m
Mineralization texture: Barren

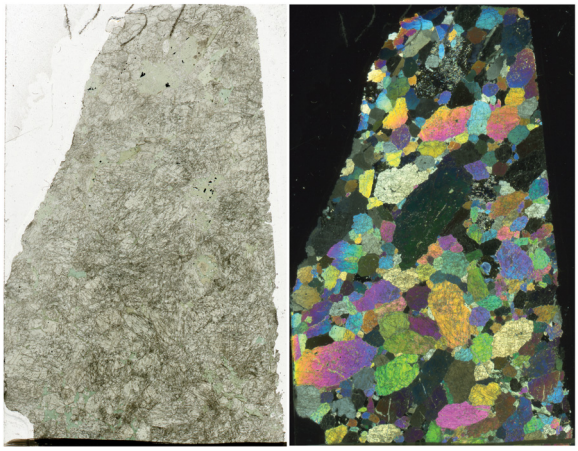

DDH04-58-4-2: Clinopyroxenite
Depth: 20.50 m
Mineralization texture: Barren

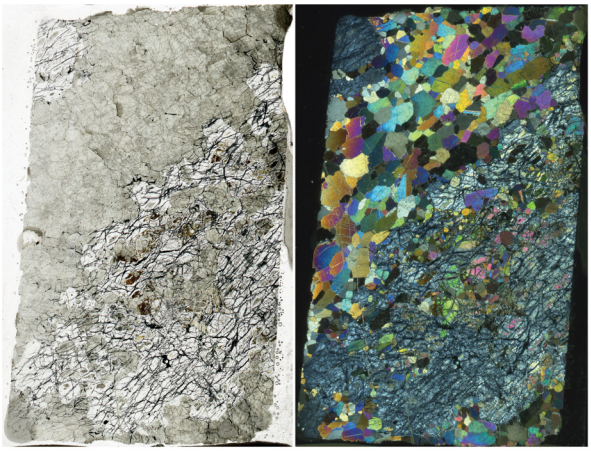

DDH04-58-5: Olivine (serpentine-magnetite) clinopyroxenite
Depth: 23.20 m
Mineralization texture: Disseminated

Appendix E continued.

Drillhole: DDH04-58

506010.3 mE 6483207 mN, Elev: 1454.88 m

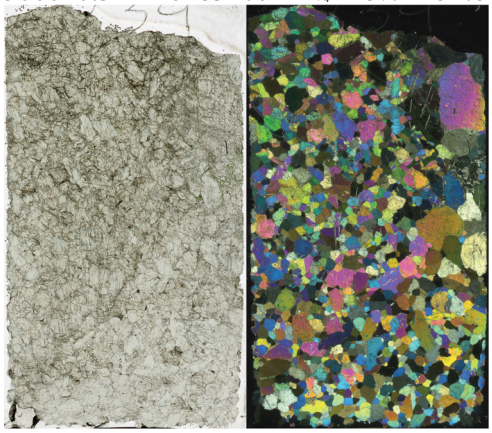

DDH04-58-6: Clinopyroxenite
Depth: 34.00 m
Mineralization texture: Barren

Drillhole: DDH04-59

506006.9 mE 6483289 mN, Elev: 1462.93 m

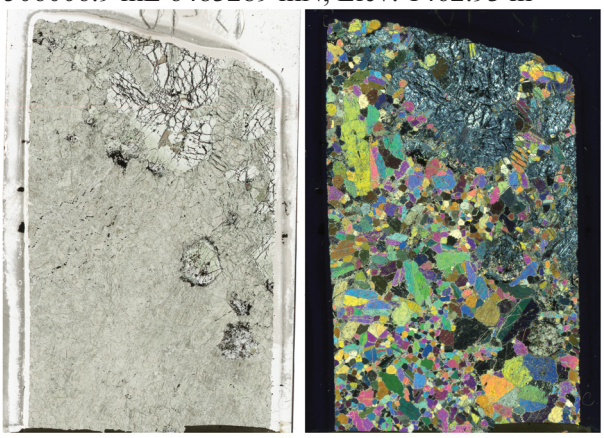

DDH04-59-1: Olivine (serpentine-magnetite) clinopyroxenite
Depth: 88.70 m
Mineralization texture: Disseminated

Drillhole: DDH05-83

506528.9 mE 6482326 mN, Elev: 1352.83 m

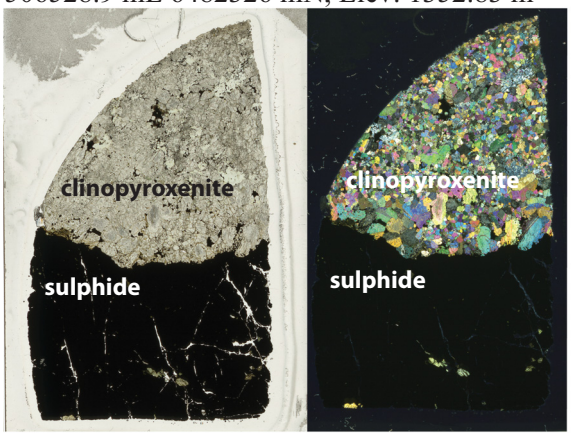

DDH05-83-1: Clinopyroxenite with massive sulphide
Depth: 60.80 m
Mineralization texture: Disseminated and Massive

Appendix E continued.

Drillhole: DDH05-88

505395.5 mE 6482884 mN, Elev: 1336.38 m

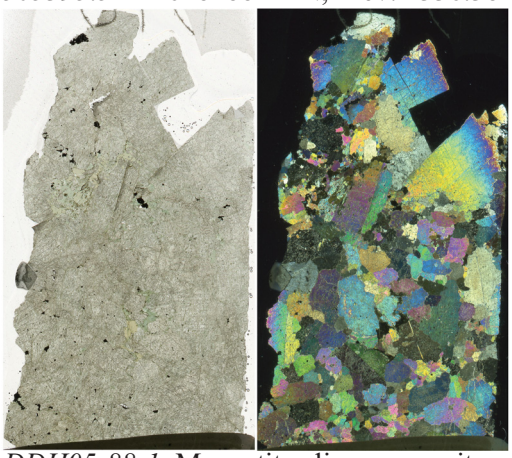

DDH05-88-1: Magnetite clinopyroxenite
Depth: 133.80 m
Mineralization texture: Disseminated

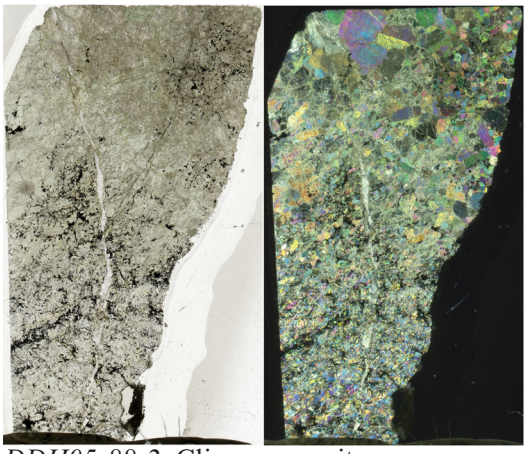

DDH05-88-2: Clinopyroxenite
Depth: 153.20 m
Mineralization texture: Disseminated-Net textured

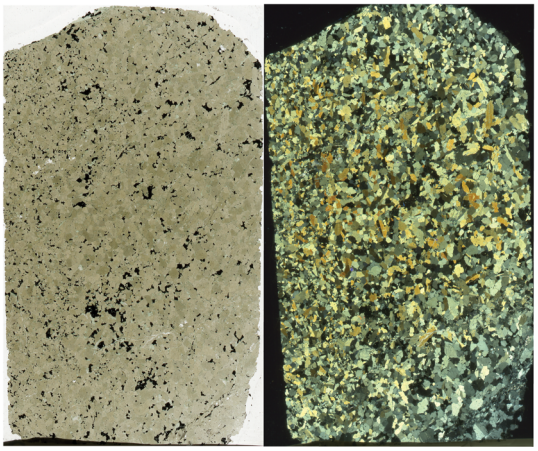

DDH05-88-3: Hornblendite
Depth: 156.90 m
Mineralization texture: Disseminated

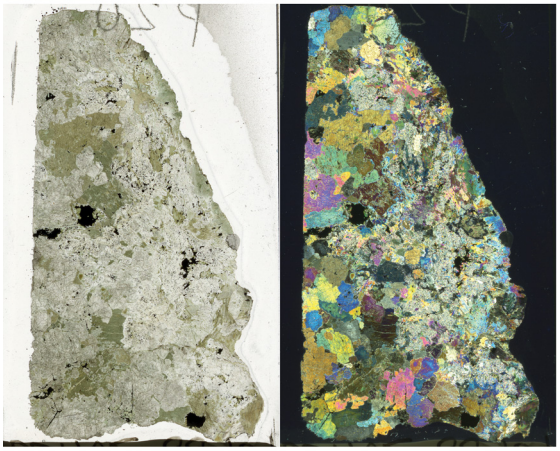

DDH05-88-101: Hornblende clinopyroxenite
Depth: 18.42 m
Mineralization texture: Disseminated-Blebby

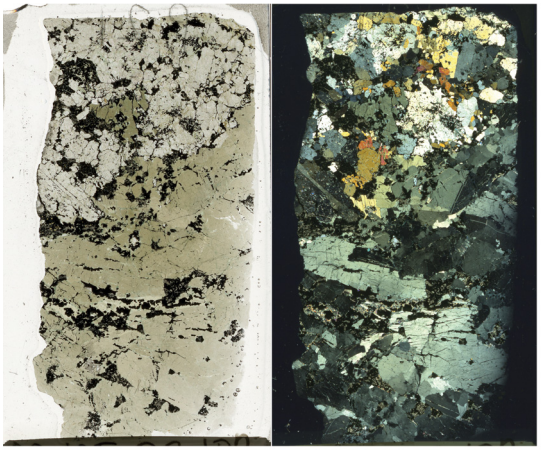

DDH05-88-102: Hornblende clinopyroxenite
Depth: 33.50 m
Mineralization texture: Disseminated-Net textured

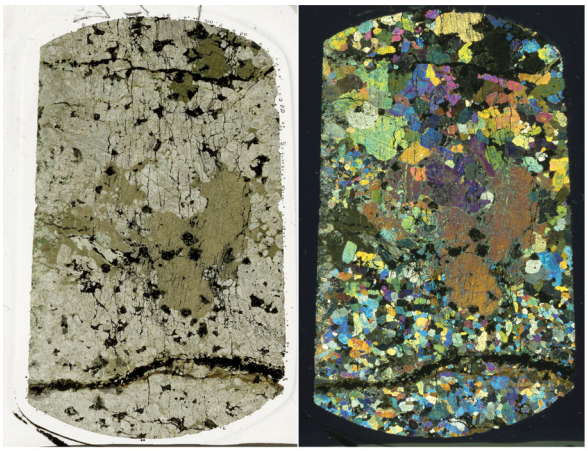

DDH05-88-103: Hornblende clinopyroxenite
Depth: 35.10 m
Mineralization texture: Replacing magnetite

Appendix E continued.

Drillhole: DDH05-88

505395.5 mE 6482884 mN, Elev: 1336.38 m

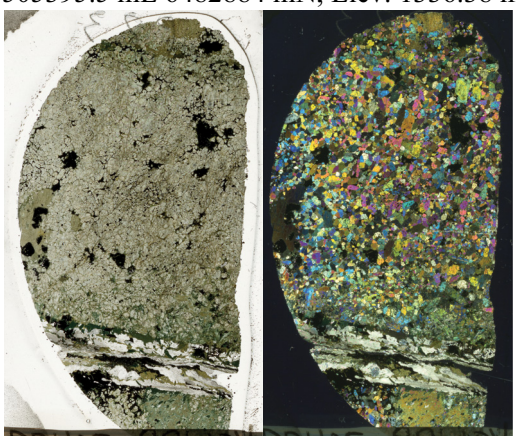

DDH05-88-104: clinopyroxenite with calcite -hornblende vein
Depth: 57.23 m
Mineralization texture: Net textured and Vein-hosted

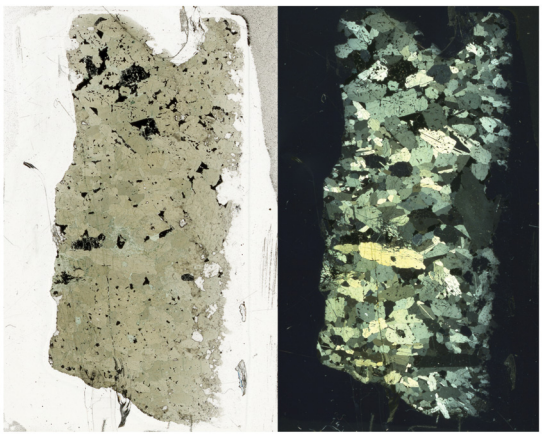

DDH05-88-105: Hornblendite
Depth: 62.12 m
Mineralization texture: Disseminated-Blebby

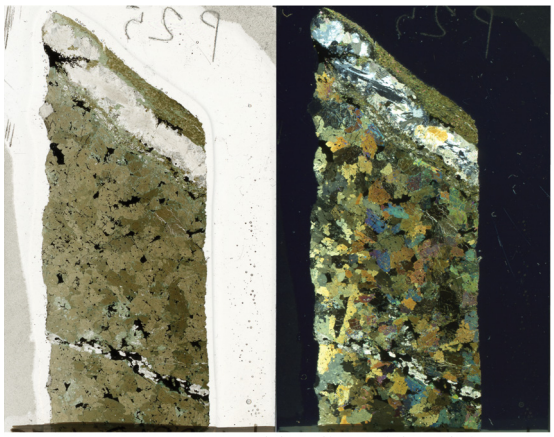

DDH05-88-106: Hornblendite with calcite-plagioclase vein
Depth: 63.41 m
Mineralization texture: Disseminated-Net textured and Vein-hosted

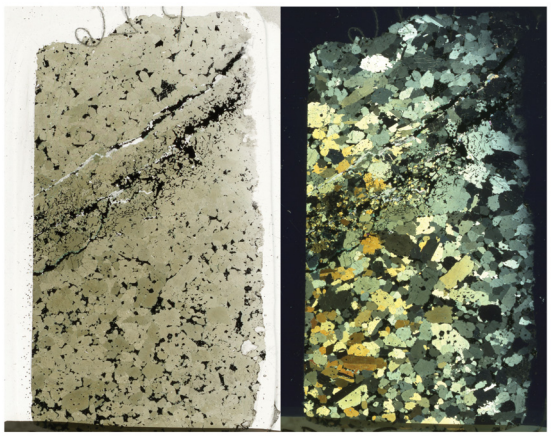

DDH05-88-107: Clinopyroxene hornblendite
Depth: 64.75 m
Mineralization texture: Disseminated-Layered

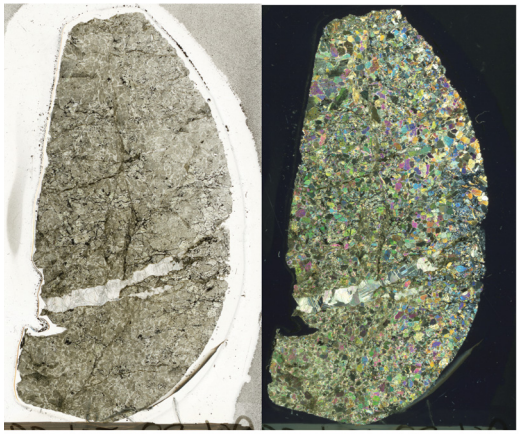

DDH05-88-109: Olivine (serpentine-magnetite) clinopyroxenite
Depth: 109.53 m
Mineralization texture: Disseminated

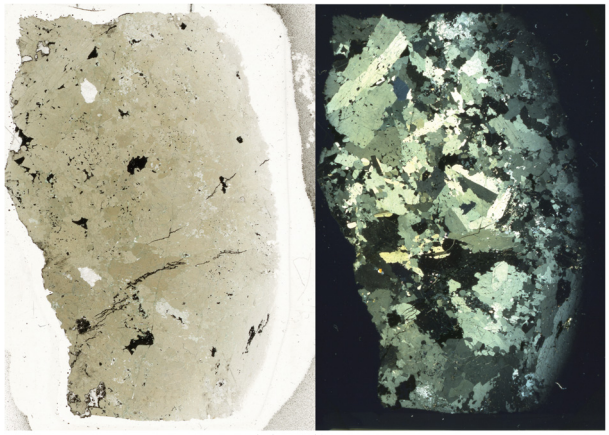

DDH05-88-111: Hornblendite
Depth: 166.50 m
Mineralization texture: Disseminated

Appendix E continued.

Drillhole: DDH05-89

505925.5 mE 6482544 mN, Elev: 1356.58 m

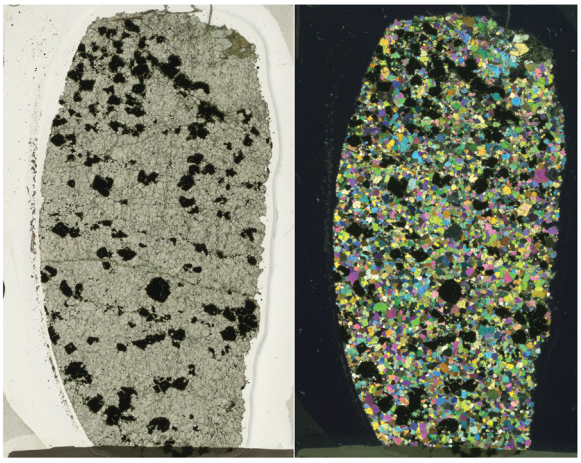

DDH05-89-1: Magnetite clinopyroxenite
Depth: 13.65 m
Mineralization texture: Disseminated

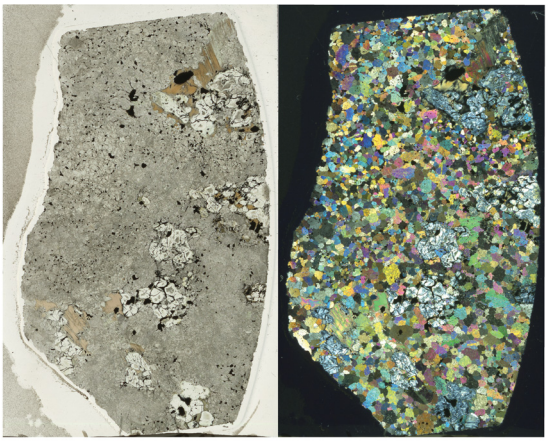

DDH05-89-2: Olivine (serpentine-magnetite) clinopyroxenite
Depth: 69.26 m
Mineralization texture: Disseminated-Blebby

Appendix E continued.

Drillhole: DDH05-101

505395.5 mE 6482884 mN, Elev: 1336.75 m

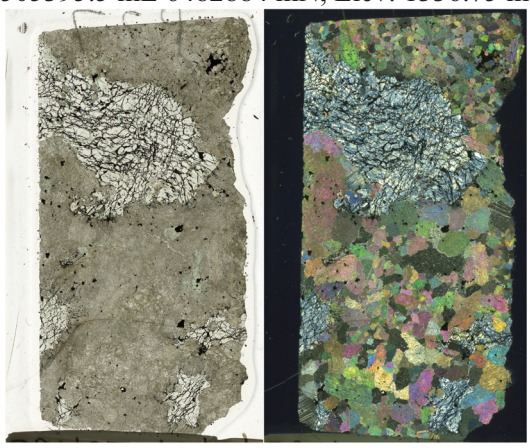

DDH05-101-1: Olivine (serpentine-magnetite) clinopyroxenite
Depth: 104.13 m
Mineralization texture: Disseminated

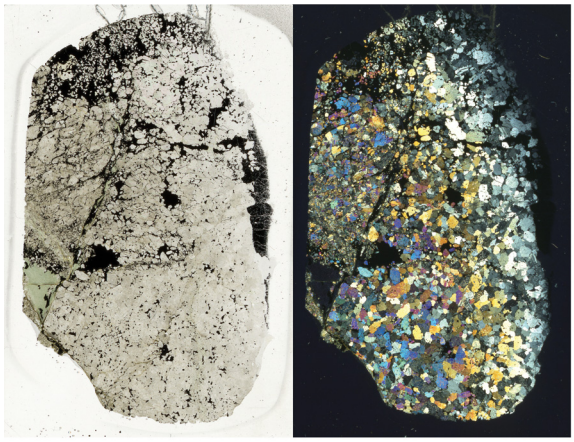

DDH05-101-2: Clinopyroxenite
Depth: 146.14 m
Mineralization texture: Disseminated-Semi-massive

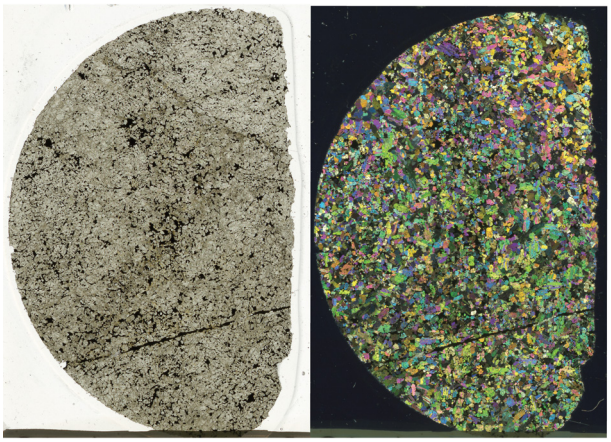

DDH05-101-3: Clinopyroxenite
Depth: 148.65 m
Mineralization texture: Disseminated

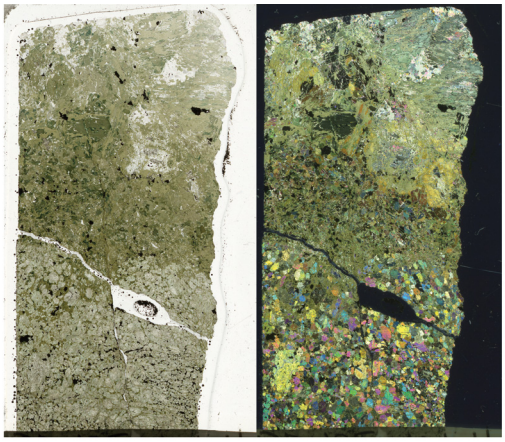

DDH05-101-4: Calcite-hornblende-chlorite vein in clinopyroxenite
Depth: 156.05 m
Mineralization Texture: Disseminated-Blebby and Vein-hosted

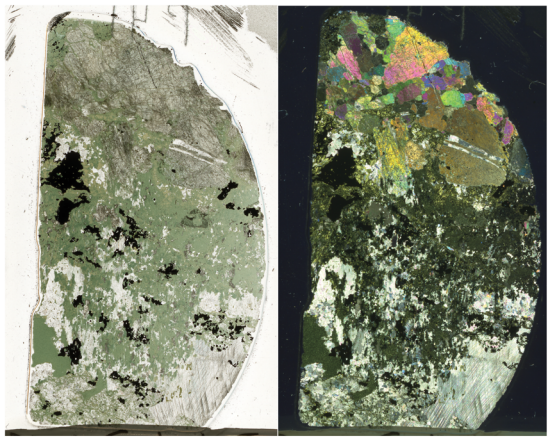

DDH05-101-5: Calcite-chlorite vein in clinopyroxenite
Depth: 169.60 m
Mineralization Texture: Disseminated-Blebby and Vein-hosted

Appendix E continued.

Drillhole: DDH05-102

506346.0 mE 6482435 mN, Elev: 1366.17 m

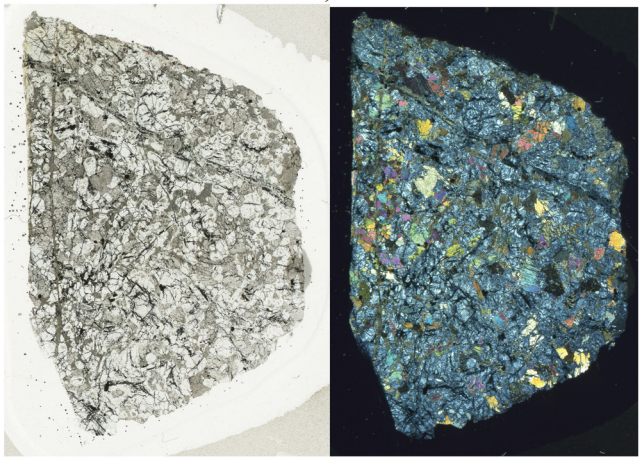

DDH05-102-1: Serpentine-altered wehrlite
Depth: 53.30 m
Mineralization texture: Blebby

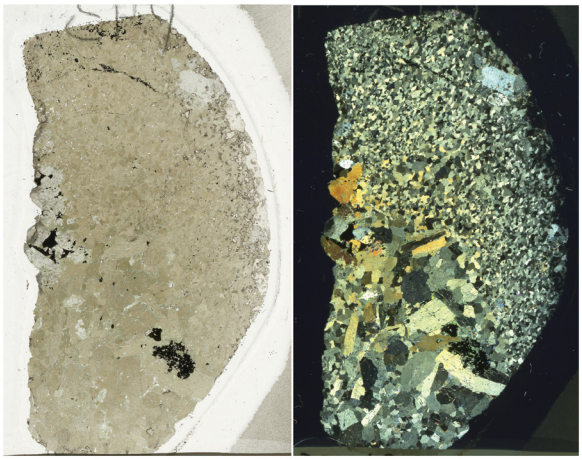

DDH05-102-2: Clinopyroxene hornblendite
Depth: 79.20 m
Mineralization texture: Disseminated-Blebby

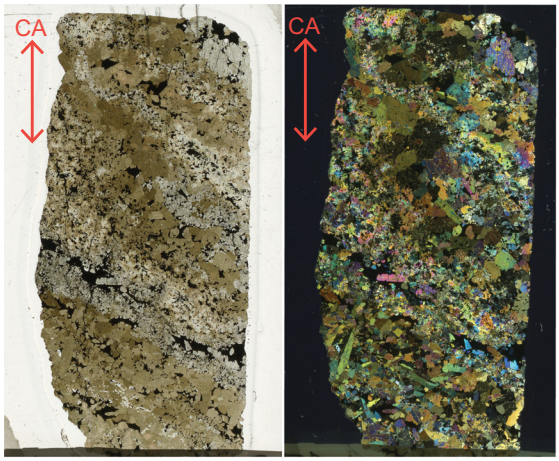

DDH05-102-3: Hornblende clinopyroxenite
Depth: 82.25 m
Mineralization texture: Net textured-Semi-massive

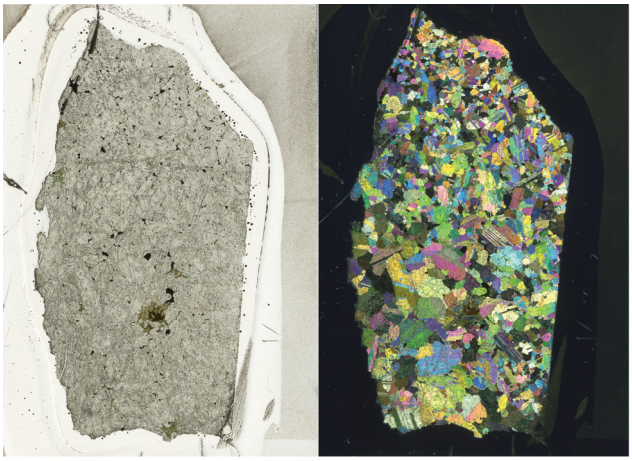

DDH05-102-5: Clinopyroxenite
Depth: 145.15 m
Mineralization texture: Disseminated

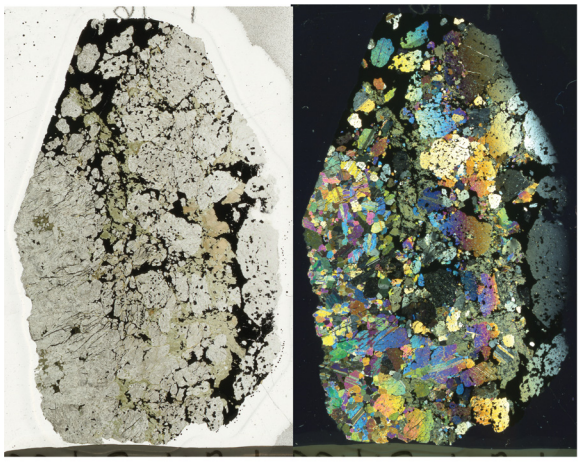

DDH05-102-6: Clinopyroxenite
Depth: 147.56 m
Mineralization texture: Net textured-Semi-massive

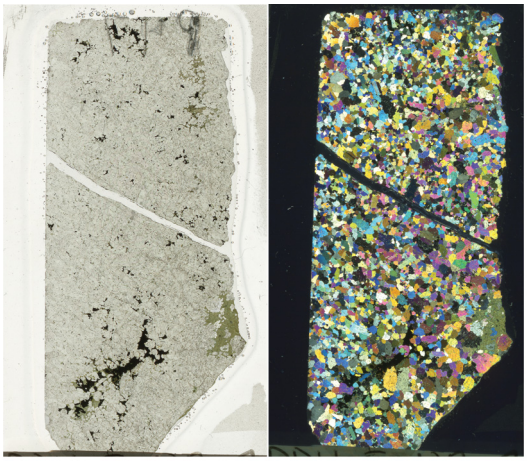

DDH05-102-7: Clinopyroxenite
Depth: 159.80 m
Mineralization texture: Disseminated-Net textured